ASSESSMENT OF THE RUN OF THE RIVER HYDROPOWER POTENTIAL AT THE DOWN STREAM OF KOKA DAM AND FORECASTING THE LEVEL OF FLOODING AT SELECTED SITE (CASE STUDY OF AWASH RIVER BASIN, ETHIOPIA)

M.Sc. Thesis

By

ASHENAFI AYZA ASELE

HAWASSA UNIVERSITY, ETHIOPIA

AUGUST, 2023

ASSESSMENT OF THE RUN OF THE RIVER HYDROPOWER POTENTIAL AT THE DOWN STREAM OF KOKA DAM AND FORECASTING THE LEVEL OF FLOODING AT SELECTED SITE (CASE STUDY OF AWASH RIVER BASIN, ETHIOPIA)

ASHENAFI AYZA ASELE

A THESIS SUBMITTED TO THE

SCHOOL OF BIOSYSTEMS AND WATER RESOURCES ENGINEERING

INSTITUTE OF TECHNOLOGY, SCHOOL OF GRADUATE STUDIES

HAWASSA UNIVERSITY

HAWASSA, ETHIOPIA

IN PARTIAL FULFILLMENT OF THE REQUIREMENTS FOR THE DEGREE OF THE MASTER OF SCIENCE IN WATER RESOURCES ENGINEERING AND MANAGEMENT

Major advisor: Abebe Tadesse (PhD)

Co-advisor: Lemma Tufa (Msc)

HAWASSA UNIVERSITY, ETHIOPIA

AUGUST, 2023

ADVISORS' APPROVAL SHEET

SCHOOL OF GRADUATE STUDIES

HAWASSA UNIVERSITY ADVISORS' APPROVAL SHEET

This is to certify that the thesis/dissertation entitled ''**ASSESSMENT OF THE RUN OF THE RIVER HYDROPOWER POTENTIAL AT THE DOWN STREAM OF KOKA DAM AND FORECASTING THE LEVEL OF FLOODING AT SELECTED SITE,**'' **(CASE STUDY OF AWASH RIVER BASIN, ETHIOPIA)** submitted in partial fulfillment of the requirements for the degree of master (MSc) with specialization in hydraulic engineering, the Graduate program of the department/school of Hydraulic and Water Resources Engineering Department, and has been carried out by **Ashenafi Ayza Asele ID.No. GPHYdrR/0003/13**, under my/our supervision. Therefore, I/we recommended that the student has fulfilled the requirements and hence hereby can submit the dissertation to the department.

_____	_____	_____
Name of major advisor	Signature	Date

_____	_____	_____
Name of co-advisor	Signature	Date

EXAMINER'S APPROVAL SHEET

SCHOOL OF GRADUATE STUDIES

HAWASSA UNIVERSITY EXAMINERS' APPROVAL SHEET

We, the undersigned, members of the Board of Examiners of the final open defense by **ASHENAFI AYZA ASELE** have read and evaluated his/her thesis/dissertation entitled ''**ASSESSMENT OF THE RUN OF THE RIVER HYDROPOWER POTENTIAL AT THE DOWN STREAM OF KOKA DAM AND FORECASTING THE LEVEL OF FLOODING AT SELECTED SITE,**'' **(CASE STUDY OF AWASH RIVER BASIN, ETHIOPIA)**, and examined the candidate. This is, therefore, to certify that the thesis/dissertation has been accepted in partial fulfillment of the requirements for the Degree of masters (MSc).

_____	_____	_____
Name of Major Advisor	Signature	Date
_____	_____	_____
Name of Internal Examiner	Signature	Date
_____	_____	_____
Name of Chairperson	Signature	Date
_____	_____	_____
Name of External examiner	Signature	Date
_____	_____	_____
SGS Approval	Signature	Date

DEDICATION

This research dedicated to my mother Almaz Chiljo

ACKNOWLEDGEMENTS

I first and foremost thank God, the Almighty for His unconditional love and impeccable support, guidance, protection and blessings. Words cannot express my gratitude for all He has done to me.

I would like to acknowledge my major advisor, Dr. Abebe Tadesse for his constructive and professional advice in guiding to select well-defined topic of the thesis. And I wish to give my truly praise to my co-adviser Lemma Tufa (M.Sc) for giving the direction to follow the guidline suggested by university (HUSGS) and general advice spatially during the begging of the study.

My special gratitude goes to Dr. Shemelies Asseffa for his proofreading and competent comment to shape and direct document according to the science of the research. And I appreciate my friend Gemechu Shiferaw (M.Sc) who lend me a hand when I got in trouble and gives essential material that helps for the study.

I would also express my deepest love and respect to my wife Betelhem Mesfin and Sister Mitike Ayza for their persistent support throughout my school time.

Finally, it is not possible to mention everybody who helped me in one way or another to successfully finish this work. I am indebted to you for your help. I thank you all.

DECLARATION

I hereby declare that this Master of Science thesis is my original work and has not been presented for a degree in any other university, and all sources of material used for this thesis have been appropriately admitted.

Full Name _____

Signature _____

LIST OF ACRONYMS AND SYMBOLS

1D/2D	One/two Dimensional
AHP	Analytic Hierarchy Process
ASTER	Advanced Space borne Thermal Emission and Reflection Radiometer
DEM	Digital Elevation Model
EELPA	Ethiopian Electric Light and Power Authority
EEPCO	Ethiopian Electric Power Corporation
FAO	Food and Agriculture Organization
FDC	Flow Duration Curve
GE	Google earth
GEORAS	Geographical river analysis system
GIS	Geographical Information System
HEC	Hydrological Engineering Center
HEC-RAS	Hydrologic Engineering Center for River Analysis System
ICTZ	Inter-Tropical Convergence Zone
IDW	Inverse Distance Weighted
LULC	Land use land cover
MCDA	Multi criteria Decision Analysis
MoWIE	Ministry of Water, Irrigation and Electricity
MoWR	Ministry Of Water Resource
NSE	Nash-Sutcliffe Efficiency
PBIAS	Percent of bias

PDC	Power Duration Curve
R	Correlation Coefficient
RMSE	Root Mean Square Error
RoR	Run of River
RS	River station
SRTM	Shuttle Radar Topography Mission
TIN	Triangular Irregular Network
USACE	United State Army Crops Engineers
USGS	United State Geological Survey
UTM	Universal Traverse Mercator
WGS	World Geodetic System
WMO	World Metrological Organization
WS	Water surface profile

TABLE OF CONTENTS

LIST OF TABLES

LIST OF FIGURES

ABSTRACT

Energy demand is increasing exponentially. This is because of rapid population growth, urbanization, the higher standards of living, industrial and agricultural expansion. Nevertheless, the available energy supply is not reliable due to sedimentation problem. So, it is advisable to use the nearby available natural resources (i.e. river and suitable topography) for potential assessments without adverse effect to cope with increasing and diversified energy demands. This study aims to investigate the assessment of river run of hydropower potential at 50km downstream of Koka Dam. To achieve the goal, Stream flow data were collected from 1991-2016 and height information was quantified from contour map and 3D spatial analyst tool in ArcGIS. Initially, the study was identified three possible potential sites and from these sites; site one was selected as the most prioritized site using MCDA method. The study included the Flood level forecasting at mostly prioritized site for further precaution using HEC-GeoRAS for preprocessing of geometric data and HEC-RAS for post processing of hydraulic modeling. Following the aforementioned model, methods and data the study computed the theoretical power at site one was (8981kw and 4197kw), technical power was (6960kw and 3253kw) and the annual energy output was (60.9GWh/year and 28GWh/year) are the maximum and minimum power at Q_{30} and Q_{95} respectively. The most preferred site had dependable flow of 19.71m3/s and is occur 95% of the year and the design flow was 42.17m3/s and is occur 30% of the year. The flood inundation area and the maximum flood depth at mostly prioritized river station 1100 where the study starts head measurement (i.e. upstream full reservoir level) and around 1km upstream of R.S. 1100 (i.e. at R.S.2050) were (145.79m^2, 4.96m) and (204.09m^2, 5.62m) respectively for 100 year return period. The validation of spatial information for site one tested were 0.71 for RMSE and hydraulic model performance for R.S.1100 and R.S.2050 were (0.7, -8.29 and 0.97) and (0.83, 5.92 and 0.96) for ENS, PBIAS and R for return period of 100 year and show the applicability of the model was good. To encapsulate we can get the site at 50km downstream of Koka Dam that have the capacity to produce annual energy of 60.9GWh/year. Consequently, it is possible to minimize the problem of highly increased and diversified electric demands at the target area. Hence, it is recommended that the government at national as well as local level or any other agency should look over it in detail and finding to implement thorough investigation of the area.

Keywords: ArcGIS, HEC-GeoRAS, HEC-RAS, MCDA, hydropower, assessment, downstream, power, Koka dam, site, stream flow, head, flood forecasting and energy.

1. INTRODUCTION

1.1. Background

Energy crisis has emerged as a serious issue all over the world due to rapid increase of the population, socio economic development, living standards with the fast growing of industry. In addition, urbanization has put enormous pressure on natural resource in the world. Today the progresses of development of nation are described by their per capita energy consumptions, which mean that nations have highly used their resources for their development. On the other hand, the extensive production and use of energy may adversely affect the surrounding environment. A situation may be reached by utilizing renewable energy source to produce sufficient energy to meeting the expanding demand without degrading of the environment (Kumar and Schei, 2009).

In the study area the system maximum demand on the interconnected system has increased from 9.7 MW in 1959 to 25.5 MW in 1963, and is expected to reach 85.0 MW in 1971. The actual increase per annum during l959-l963 has averaged 30.7% and the average increase per annum forecast to 1971 is 16.3% (EELPA, 1964). This is due to intensive urbanization and agricultural development in the area. The current demand increase about 13%-14% annually (EELPA, 2022). The electricity loss in Ethiopia is about 20%, which is much higher than the international average, 12-13%. Most of the loss happens during distribution from the national grid to end users (http://www.et.emb-japan.go.jp/oda_e.htm, 2008). Among the other things nowadays the government has been selling the electric power to the neighborhoods countries such as Sudan, Djubouty, Kenya and on the process to sell to Somalia and Tanzania and South Sudan (EELPA, 2023) to support the economy.

Furthermore, in the study area in a long while, Koka Dam has been losing its purpose. The total sediment deposited in the Koka reservoir in the period 1961-1981 has been estimated at 0.34km3, yielding an average of 17Mm^3/year. A certain sediment prediction formula yielded 0.362km3 and 18Mm3/year, respectively (Imru, 1992). Primarily, Koka Dam was built for hydropower generation, but now works as a multi-purpose dam. In addition to electricity it is used for downstream irrigation demand supply and flood control operated by Ethiopian Electric Power Utility (EEPU). Most of the sediment load brought in by the river inflow to

the Koka reservoir being deposited there, the capacity of the reservoir has gradually been reduced over the more than forty years of its existence. At this time estimates are that the reservoir volume, having lost more than 40% of its capacity, does not have a remaining capacity of more than about1 bill m3 (WMO/GWP, 2003). Herein, two things happen side by side, one is attenuation of the power supply and the other is exacerbation of the downstream due to flooding.

The purpose of this investigation is to assess the nearby available natural resources in the area (i.e. river and suitable topography) for potential assessments of Run off river hydropower without adverse effect to cope with increasing demands resulting from expected rapid increase of population, industry and commercial demands. So, assessing the potential sites at the downstream of Koka Dam is really important to indicate the total available power that the areas endowed to tackle the unbalanced energy demands and to minimize what is lost by koka Hydroelectric Dam expected work.

RoR power plants have several desirable advantages over their reservoir fed counterparts that make them suitable for energy production. For instance, RoR power plants have a much lower impact on the local ecosystem (construction), their design is less complex and they. RoR plants are also much better amenable to smaller water heads, and their construction time is much shorter than that of reservoir fed counterparts. What is more, RoR plants offer the possibility of decentralized electrification at a relatively low operational and maintenance cost. Thus, RoR plants are generally considered to be environmental friendly, flexible to operate, and ideally suited for localized energy production (Yildiz and Veysel, 2015). By using the available nearby potential power of study area, the cost of installing electrification material and the electric loss from the grid to the end user highly minimized.

Choosing the most feasible site from topographical, geological, hydrological point of view and identifying the possible flood event for further precaution before implementation of water resource projects are critical issues that must be seen thoroughly in planning and designing stage. So that to tackle the problem the study used stream flow from the department of Ministry of Water and Energy (MoWIE) for flow analysis and hydraulic modeling using HEC-RAS 6.3 coupling with HEC-GeoRAS 10.41 for post processing flow data and pre-processing of river geometry and Arc-GIS 10.41 for spatial analysis using Aloss Palsar DEM and MCDA method to select most prioritized site.

1.2. Statement of the problem

Awash basin is known by population density and intensively utilized river basin in Ethiopia due to its strategic location, access roads, and available land and water resources (Zemede, 2011). The first stage development in Awash River is the Koka scheme which was completed in 1960. Storage of the Koka Reservoir is estimated to be decreasing due to irrigation expansion in addition to sedimentation (Berhanu, 2008). This leads to decreasing the capacity of the dam to produce electricity. Due to this reason the current power plant is not dependable to satisfy the intensive demand from population growth, urbanization, industry expansion and the need to live with safe environment.

Another critical problem in the study area is downstream flooding during heavy rainy season. Since Wonji is located only about 20 km downstream of Koka hydroelectric dam, Awash River flow at Wonji is directly related to water release from the Koka hydroelectric dam reservoir. In its normal operation the Koka hydroelectric dam regulates the Awash River flow downstream. However, in exceptional cases of high water inflow into Koka hydroelectric dam reservoir, water level in the reservoir exceeds the design water level and flood gates of the dam need to be opened to avoid a rather catastrophic phenomena of dam failure. High-water level in the reservoir usually occurs following days-long heavy rainfall in the upstream catchment (Yohannis and Peter, 2022). Besides, the Koka hydroelectric dam reservoir has lost much of its capacity to sedimentation (Abebe, 2001; SHAHIN, 1993). This leads to higher water levels in the reservoir even if the inflow into the reservoir and the outflow from the reservoir are unchanged. Opening of flood gates during high-water levels in Koka hydroelectric dam reservoir results in flood flows in Awash River downstream of Koka hydroelectric dam. These and other issues trigger to see other option to minimize the current uncontrolled needs as well as the future endless energy demand to get environmental friendly, flexible to operate, and ideally suited for localized energy production.

So, it is advisable to use the nearby available natural resources (i.e. river and suitable topography) to minimize the project cost and time for potential assessment without adverse effect to cope with increasing energy demands resulting from the expected rapid increase in population, industry, agricultural and commercial demands. The power potential assessment provides the basis for the planning of layout and design of the scheme and estimation of cost and evaluation of the financial aspect of the scheme. (Sanoj, 2014-2015). To address the above problem the study used Arc-GIS 10.4.1 for spatial analysis and stream flow taken from Ministry of Water and Energy (MoWIE) for flow analysis and in addition to this, for further

precaution and protection of the study area from the consequence high flooding event, especially during rainy season HecRAS 6.3 and Hec-GeoRAS 10.4.1 for hydraulic and geometry modeling software were used for flood level forecasting.

1.3. Research questions

Based on the stated objectives, the following questions have been used to guide the research process and finally answered from the findings of the study.

- ✓ What looks like the fluctuation of potential power with flow condition?
- ✓ What will be the variability of flow in proposed hydropower sites?
- ✓ What is the flood level of the most prioritized location?

1.4. Objectives

The main objective of this research is to assess the hydropower potential site and forecast the level of flooding at the selected site of Awash River at 50km downstream of Koka dam.

1.4.1. Specific Objectives

- ✓ To develop (FDC) and power duration curve (PDC) of the selected locations.
- ✓ To prioritize and rank the best suitable site using Multi criteria decision analysis.
- ✓ Assess the maximum flood depth and flow area (inundation) at the most selected location using HEC-GeoRAS and HEC-RAS.

1.5. Hypothesis

Choosing the most feasible site from hydrological, topographical, soil and geological point of view and identifying the possible flood event before implementation of water resource development are critical issues that must be seen thoroughly in planning and designing stage.

1.6. Scope and Limitation of the study

The study area coverage bounded at 50km from downstream of Koka Hydroelectric Power Plant (i.e. the dominant basin between Koka reservoir and upstream of metehara stations that drain all drainage network). The study is limited in using Arc-GIS for spatial analysis and HEC-GeoRAS for pre-processing of geometric data and HEC-RAS for further flood level analysis. In addition, the study focuses to assess the potential site at the downstream of Koka Dam, specifically below 29.12km from Awash II and 26.97km from Awash III. Finally, due to time, cost and essential instrument constraint the study investigate about site one, site two and site three located along 31.83km downstream of Awash Melkasa.

1.7. Significance of the study

This study provides a piece of information for national and regional policy makers especially ministry of water, energy and electricity and water resource implementing agency on available potential power of feasible site. The significance of this study could be;

1. To know where to focus to get high potential area to solve the diversified energy demand.
2. Used as benchmark for further detail investigation of the hydropower potential of the area.
3. To initiate decision makers to establish hydropower development program.
4. Improving socioeconomic living standard of end users.
5. To use the nearby available natural resources (i.e. river and suitable topography).
6. Reduce the cost and gap of time from planning stage to implementation of the project.

2. LITRETURE REVIEW

2.1. General Description of Hydropower

Hydropower, hydraulic power or water power is power that is derived from the force or energy of moving water, which may be harnessed for useful purposes. Hydropower is available in a broad range of project scales and types. Projects can be designed to suit particular needs and specific site conditions. As hydropower does not consume or pollute the water it uses to generate power, it leaves this vital resource available for other uses. At the same time, the revenues generated through electricity sales finance other infrastructure essential for human welfare. This can include drinking water supply systems, irrigation schemes for food production, infrastructures enhancing navigation, recreational facilities and ecotourism (Yuksel, 2008).

2.2. The Hydropower Development in Ethiopia

Ethiopia is located in East Africa with total area of 1.1 million km and population more than100 million and is endowed with enormous renewable energy resources that include 45000MW hydropower, 10000MW geothermal power, 135000 MW wind and massive solar and biomass potential. Biomass covers 90% of the total energy consumption, mainly used for cooking in the household. Hydropower contributes significantly for electric generation; the current installed electrical capacity reached 2268 MW and two big hydropower projects with capacity 1870 MW (Gilge l & Gibe lll) and 6250 MW (Grand Renaissance dam) are under construction. The installed capacity is expected to jump to about 8000 to 10000 MW by the end of growth and transformation plan (REEEP, 2014).

Considering the substantial hydropower resources, Ethiopia has one of the lowest levels of per capita electricity consumption in the world. The standard of living is reflected by the per capita power consumption and as such Ethiopia ranks 174 in the human development index. Ethiopian per capita consumption of electric was estimated to be 28KWh equivalents to about 1% of the world average only 17% of the population has access to electricity. Most of energy consumption of the country is met from biomass related products. The traditional source of energy cannot supply the increase and diversified demand of the community. Ethiopia needs energy to increase agricultural productivity and food distribution, deliver basic education, medical service, and establish adequate water supply and sanitation facilities as well as to build and power newly job creation industries. So that formulation must be required to reduce the traditional source of power as much as possible (Hall, 2009).

Generally, background infrastructural development in Ethiopia radically limits the pace of economic growth. Particularly the rural communities are adversely affected. This has a negative impact on the overall economy of the nation as the rural communities are the basis for agricultural development of the amount of financial requirement and insufficient financial source. The small-scale hydropower development in developing countries with its low investment cost, short construction period and environmentally friendly in nature (Zuo et al., 2015). The agencies of the responsible for electric power in Ethiopia have the Ethiopian Electric Light and power that responsibility for the investigation, development and subsequent construction of power generation schemes. It is responsible for the transmission and distribution of electric energy. It is responsible for the transmission and distribution of electric energy (Hamisi, 2013). Energy access is increasingly seen as a vital catalyst to wider social and economic development, enabling education, health and sustainable agriculture as well as creating jobs. By 2025 electrify access is expected to reach 100% in both rural and urban areas of Ethiopia. To attain this, electrification enables the provision of affordable electricity to poor households who are forced to use fuel wood to meet their energy needs, over 85% of which is used for cooking and heating (EELPA).

Ethiopia's hydropower potential estimated at up to 45000MW and is the second highest in Africa. Hydropower based development provides a gate way to economic transformation through industrialization, urbanization as well as through the provision of access to modern energy to rural areas. The current electricity installed capacity of 4284 MW is 97% renewable of which effective hydropower installed capacity is 3810 MW. Furthermore, 8864 MW of hydropower development under construction (Trade and Forum, 2015). Since 2009, the country has commissioned five hydro dams with total capacity of 3147 MW. The last commissioned in the Gibe III Dam with an installed capacity of 1870 MW with the largest roller compacted concrete dam technology in the world. Among the dams under construction, the Grand Ethiopian Renaissance dam (GERD), with an expected installed capacity of 6450 MW on completion, will be the largest hydropower dam station in Africa. It is also important to note that Ethiopia has about 17 identified sites ranging from 60 MW to 2000 MW in the pipeline and expected to be largely developed by the private sector as independent power producers (Ministry of Water Irrigation and Electricity Federal Democratic Republic of Ethiopia, 2017).

2.3. Types of Hydropower Plant

Hydropower technology utilizes the potential energy possessed by water body between two elevation levels, which is proportional to the rate of flow of water and elevation difference, referred to as the head. Therefore, hydropower planning and design are focused towards increasing these two parameters by selecting proper sites and construction measures. Various types of hydropower plants have been developed depending upon the availability of head and control of discharge (Wien, 2015). They are as follows: Run-of-river (ROR), Peak Run-of-river (PROR) hydropower plants, Storage hydropower plants and Pumped storage plants.

2.3.1. Run-of-river (ROR) hydropower plant

The ROR hydropower plants have very little or no control of the natural flow of water and therefore, generates electricity as and when the water is available in the stream. When the flow in the river recedes, the power produced by the plant also decreases. It has almost constant head and is usually operated as a base load plant. These plants are normally designed to utilize the flows in the river during the dry season and the installed capacity shall be based on the dependable flow available in the river throughout the year (Wien, 2015). However, in rivers with large and rapid flow fluctuations, which is typically the case in smaller unregulated rivers, such strategies can lead to a large number of changes in the production, the cost of which cannot be neglected; for example, starting and stopping the turbines induces wear and tear on the machines and may also require intervention from personnel. Moreover, each start and stop involves a risk which can be considered a cost (Marcus et al., 2021). To give an example, the major breakdown in the Akkats hydropower plant (Lule river, Sweden) 2002 was caused by a turbine being stopped too quickly, resulting in rushing water destroying the foundation of both the turbine and the generator (Yang 2010; Yang et al. 2018). Therefore, the need for consistent flow with manageable fluctuation is mandatory for reliability of ROR.

ROR plants are designed with discharge at certain percentile of available flow in the river. Abarrage or weir is constructed to divert the water to the conveyance which delivers the water to the powerhouse through the penstock pipe. The ROR plants can have various possible layouts: I) ROR plant with the canal system, II) ROR plants with pipe system and III) ROR plants with tunnel system and IV) ROR plants with waterways.

2.3.2. Peak Run-of-river (PROR) hydropower plants

PROR hydropower plants are similar to the ROR plants, but with some control over the discharge. A small pondage is constructed to collect the daily flow available in the river so that some regulation is possible during peak hours to generate more power during dry season when the flow in the river recedes below the design flow. During the rainy season, when the river discharge exceeds the design flow, the plant operates like a ROR plant (Wien, 2015).

2.3.3. Storage hydropower plants

The storage power plants are constructed with a high dam across a river to create a reservoir and therefore, flow regulation is possible according to the power demand. In such power plant, the gross head is not constant, but varies according to the immediate past power generation, volume of reservoir and natural water inflow (Buehring et al., 1984). The main components of the storage plants are dam to store water, spillway, headrace tunnel, surge tanks, penstock and powerhouse. Based on the layout, the storage plant may be two types: I) Storage plant with powerhouse at dam toe and II) Storage plant with powerhouse at a certain distance from the dam. In the first type of storage plant, powerhouse is constructed at the toe of the dam. This type of plant layout is preferred for the location where there is a wide river at dam axis. In the second type of storage plant, powerhouse is constructed at a certain distance downstream from the dam (Wien, 2015).

2.3.4. Pumped storage plants

The pumped storage plants generally employ two reservoirs located at different elevations. The lower reservoir is usually an existing reservoir or natural lake. Water is pumped from a lower reservoir to the higher reservoir using low cost off-peak electric power. During the periods of high power demand, the stored water is released through the turbine to generate electric power. The same turbine acts as a pump as well as the turbine. The economy of pumped storage plant is achieved by selling electricity during peak hours when the price of electricity is high. Pumped storage plants provide a speedy response to the large variation in load and surplus electricity can be used to pump the water to the higher reservoir (Wien, 2015).

2.4. GIS APPLICATION

Study conducted by (Asrat et al., 2020) in the Gumara and Ribb rivers in the Guna-Tana landscape using information at the local level and a GIS-based tool to assess the hydroelectric potential indicates that the maximum hydroelectric potential reaches the sites in the rivers.

In GIS, location data and their map representations are dynamically linked so that any changes made in the databases are reflected immediately on its map presentation. This linkage makes GIS a powerful tool for spatial data visualization and analysis (Ian, 2010). GIS provides an efficient framework for geo-referencing information enabling expedited and accurate decision making based on location and innate relationships hence reducing the costs associated with extensive fieldwork and manual office work (Gerald, 2016).

The collection and analysis of accurate information on topography, land use pattern, river morphology and geology is easier in the GIS environment than by conventional field survey, as GIS can manage all variables with reference to location, and can provide a clear picture about the hydropower project area and its impact zone (Pathak, 2008).

Likewise GIS, SWAT model can be used to perform spatial information. But the main weakness of SWAT model is a non-spatial representation of the hydrological response unit inside each sub catchment. In addition threats may adversely impact the model performance and use, if they are not addressed in the process of building a model several adjustments of the parameters need to be made in order to improve simulations. Adjustments are usually not measurable and are made using the modelers' experience, best knowledge and subjective assessment of the study area. This can have important implications on overall performance and outcome of the model and its suitability for certain case studies which are difficult to quantify (Matjaž and Marina, 2012). This research used GIS due to its capacity and performance of analyzing spatial information of study area.

2.5. Digital Elevation Model (DEM)

Digital elevation models (DEMs) provide an important topographic product that is fundamental for many scientific and commercial applications (Rizzoli et al., 2017; Uysal et al., 2015). However, traditional methods to acquire information for DEM generation are often expensive and time-consuming due to land surveying necessity (Uysal et al., 2015). On the other hand, several DEM products from many sources have been made freely available to geo-information users in the last decade, so it is important to investigate their possible applications by assessing their accuracy (Moura et al., 2014). DEM products accuracy has been regularly investigated to evaluate their applicative potentialities, thus improving mapping methods (Polidori et al., 2014). Most of these experiments are performed by comparing the extracted data from DEMs to a set of reference data, i.e., control points, through accuracy statistical indicators, such as mean difference, standard deviation, or root

mean square error (Polidori et al., 2014). According to (Zuleid and Pedro, 2022) study in Balsas River Watershed with the area of 12352.50km2 to assess the vertical accuracy of ALOS PALSAR, GMTED 2010, SRTM and Topo Data DEMs, it is noticed that a very strong correlation coefficient between the altitudes of the reference points from the Brazilian official network and the altitude extracted from the assessed DEMs (i.e. R^2=0.99). Furthermore, regarding the statistical indicators, it is observed that ALOS PALSAR and SRTM demonstrated the best performance since ALOS PALSAR has the lowest ME and MAE, while the SRTM showed the lowest RMSE and the small error range.

2.5.1. Triangulated Irregular Network (TIN)

In Digital Terrain Modeling, the Triangulated Irregular Network (TIN) is a representation of a surface derived from irregularly spaced sample points and break line features. Due to its simplicity and economy TIN Model is a significant alternative to regular raster or grid (Hanjianga et al., 2008). It is suitable for regular and irregular distributed data points both, but grid model is only suitable for regular distributed data points. Mostly, the data points acquired from the field work are not distributed regularly. TIN model is a more flexible model than the grid model. The earth's surface is rarely completely flat; the density of data is changing with the complexity of different terrain. In grid model regular square meshes are used to represent the earth's surface, while in TIN model, the irregular triangle meshes are used. TIN model can reduce the redundant data of Grid model and especially excel at the regions where the terrain is complicated and changes sharply. TIN model have higher precision than any other models while representing the terrain. It gives better precision and efficiency of calculating the elevation than contours model.

2.6. Hec-RAS Model

Developed by the U.S. Army Corps of Engineers, HEC-RAS allows users to perform one dimensional steady and unsteady flow calculations (HEC, 2002). In a HEC-RAS steady state simulation, water surface profiles are computed from one cross-section to the next by solving the standard step iterative procedure to solve the energy equation. The energy equation is intended to calculate water surface profiles for steady gradually varied flow and the equation is shown below for two adjacent cross-sections XS1 and XS2 (Figure 1).

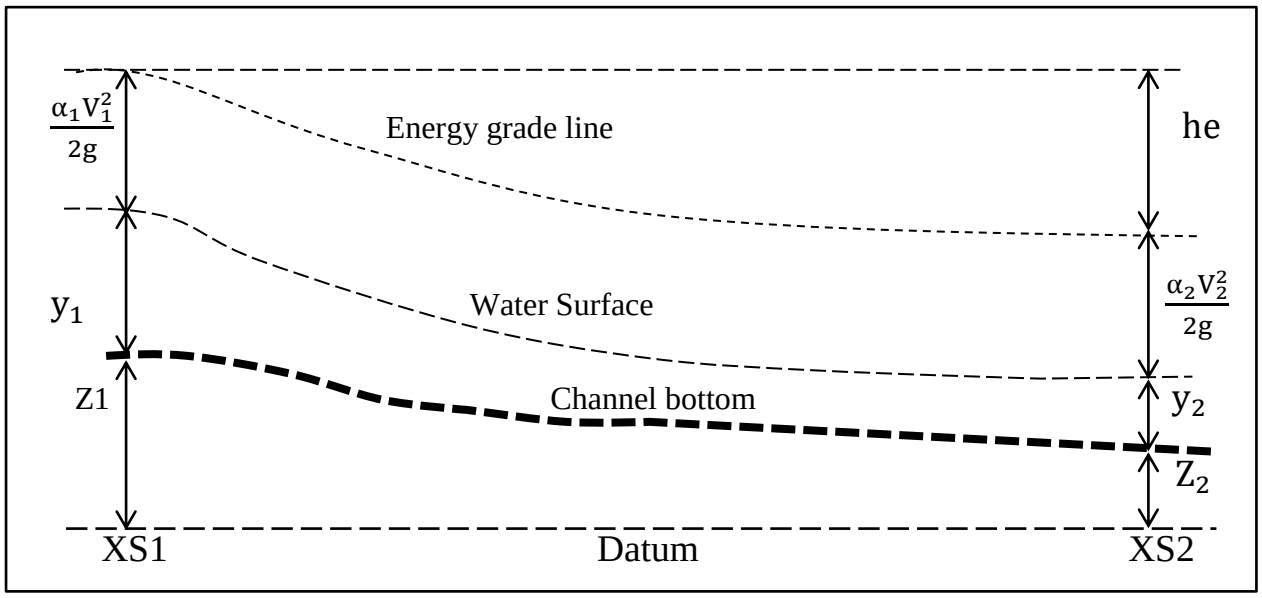

Figure 1: Representation of terms in the energy equation

$$y_1 + Z_1 + \frac{\alpha_1 V_1^2}{2g} = y_2 + Z_2 + \frac{\alpha_2 V_2^2}{2g} + he \ldots\ldots\ldots\ldots\ldots\ldots\ldots\ldots\ldots\ldots\ldots\ldots\ldots\ldots\ldots\ldots 2.1$$

Where y_1 and y_2 are depths of water at adjacent XS1 and XS2, Z_1 and Z_2 are elevations of the main channel inverts, V_1 and V_2 are average velocities (total discharge/ total flow area), α1 and α2 are velocity weighting coefficients, g is the gravitational acceleration, he is energy head loss. The energy head loss term is defined in equation 2.2

$$h_e = LS_f + c\left[\frac{\alpha_2 V_2^2}{2g} - \frac{\alpha_1 V_1^2}{2g}\right] \ldots\ldots\ldots\ldots\ldots\ldots\ldots\ldots\ldots\ldots\ldots\ldots\ldots\ldots\ldots\ldots 2.2$$

Where L is discharge weighted reach length, S_f is representative friction slope between XS1 and XS2, and C is an expansion or contraction loss coefficient. The representative friction slope using the average conveyance equation and the distance weighted reach length are defined in equations 2.3 and 2.4, respectively.

$$S_f = \left(\frac{Q_2 - Q_1}{K_2 - K_1}\right)^2 \ldots\ldots\ldots\ldots\ldots\ldots\ldots\ldots\ldots\ldots\ldots\ldots\ldots\ldots\ldots\ldots\ldots\ldots 2.3$$

$$L = \frac{L_{LOB}Q_{LOB} + L_{ch}Q_{ch} + L_{ROB}Q_{ROB}}{Q_{LOB} + Q_{ch} + Q_{ROB}} \ldots\ldots\ldots\ldots\ldots\ldots\ldots\ldots\ldots\ldots\ldots\ldots\ldots\ldots\ldots 2.4$$

Where: K is conveyance (it is a measure of the carrying capacity of the channel section) and L_{LOB}, L_{ch}, L_{ROB}, Cross section reach lengths specified for flow in the left over bank, main channel, and right over bank, respectively, Q_{LOB}, Q_{ch}, Q_{ROB}, Arithmetic average of the flows between sections for the left overbank, main channel, and right over bank, respectively.

To determine total conveyance and the velocity coefficient for a cross-section, HEC-RAS subdivides flow in the main channel from the over-banks. Conveyance is calculated for each subdivision using equations 2.5 and 2.6.

$$Q = KS_f^{1/2} \quad \text{.....2.5}$$

$$K = \frac{1.486}{n} AR^{2/3} \quad \text{.....2.6}$$

Where K is conveyance for the subdivision, n is Manning's roughness coefficient for the subdivision, A is flow area for the subdivision, and R is hydraulic radius for each subdivision. The total conveyance for each subdivision is calculated as the sum of the conveyance from the left over-bank, main channel, and right over-bank. Flow in the main channel is subdivided only when the Manning's roughness coefficient changes within the channel area.

The study selected the roughness coefficient by considering the most important factors that affect the selection of channel n values are (1) the type and size of the materials that compose the bed and banks of the channel and (2) the shape of the channel. Cowan (1956) developed a procedure for estimating the effects of these factors to determine the value of n for a channel. The value of n could be computed as:

$$n = (n_b + n_1 + n_2 + n_3 + n_4)m \quad \text{.....2.7}$$

where, n_b= a base value of n for a straight, uniform, smooth channel in natural materials, ,n_1= a correction factor for the effect of surface irregularities, n_2= a value for variations in shape and size of the channel cross section, n_3 =a value for obstructions, n_4 =a value for vegetation and flow conditions, and m =a correction factor for meandering of the channel.

Limitations in the HEC-RAS steady flow simulation include the assumptions that the flow is steady, the flow is gradually varied, the flow is one-dimensional, and the river channels have small slopes.

2.6.1. Case studies using 1D hydraulic models

Case studies have been performed using one-dimensional models to show the capabilities of the model being used. Some of these case studies have been performed to calibrate hydraulic models or validate results; but the main focus of these studies has been to analyze the effect of topographic data on the hydraulic model.

Case studies using one-dimensional models such as HEC-RAS (Brandt, 2005; Omer, 2003; and Casas, 2006), HEC-2 (Mohammed, 2006), and HEC-6 (Sinnakaudan, 2002) have been performed. In each of these studies, the goal has been to show how the effect of changes in topography will impact the floodplain. A one-dimensional model is often selected for this process because it represents the most basic approach to floodplain modeling. In each of the three studies listed above, the one-dimensional model used was successful in showing how a change in topography would affect the model. In the case study of the Linggi River in Seremban Town, Malaysia, HEC-2 was used to calibrate and validate the results. It was shown that the absolute error in predicted water surface levels was within 5% of the observed levels (Mohammed, 2006).

2.6.2. Case studies comparing 1D and 2D hydraulic models

In flood inundation modeling, a distinction must be made between one- and two dimensional hydraulic models. One-dimensional models treat flow through both the channel and floodplain as only in the longitudinal direction. The equations for modeling one-dimensional flow are derived from the conservation of mass and conservation of momentum equations between adjacent cross-sections (Bates et al., 2005). Two dimensional hydraulic models are based on integration over the flow depth to obtain depth averaged velocity values and are solved using an appropriate numerical approach such as a finite element model (Aaron, 2008).

A study of a 6 kilometer reach of the River Wharf, UK compared inundation extent from HEC-RAS with a two-dimensional diffusion wave model (Tayefi et al., 2007). The DEM for this study was created using a combination of 58 GPS surveyed cross-sections for the main channel and remotely sensed LiDAR for the floodplains. The results from this study show that, in qualitative terms, the two-dimensional model produces the best results although the one-dimensional model could be calibrated to produce accurate results.

Similarly, a study conducted for flood inundation area analysis on Brazos river and strouds creeks using FESWMS and Hec-RAS (Aaron, 2008) depicts that the one-dimensional HEC-

RAS model linearly interpolates the floodplain boundary between cross-sections, and then defines the floodplain by subtracting the topographic data from the water surface elevations. This process often results in a discontinuous floodplain. The advantage of using the one-dimensional floodplain mapping process is that is easy to use and produces results quickly. In a HEC-RAS simulation, the Manning's n value is often used as the lone calibrating parameter, and can change results significantly (HEC, 2002). Where the HEC-RAS simulation takes a matter of seconds to complete, the FESWMS simulation can take multiple hours. The advantage of the two dimensional model is that it produces a continuous floodplain as it represents the topography as a series of mesh elements and can model flow in both the lateral and longitudinal directions resulting in a more accurate representation of the floodplain. For a FESWMS simulation, two calibrating parameters, Manning's n and eddy viscosity, can be used as calibrating parameters and may have an affect of the results of the hydraulic simulations (FESWMS, 2002). The experience of the modeler can have an affect on the resulting floodplain due to the calibrating parameters in both the one and two dimensional model and the meshing type in the two-dimensional model.

2.7. Data requirements for the HEC-RAS model

2.7.1. Geometry Data

Cross section data represent the geometric boundary of the stream. Cross sections are located at relatively short intervals along the stream to characterize the flow carrying capacity of the stream and its adjacent floodplain. Even though it is not a must, it is advisable to take cross section at constant interval. Cross sections are required at representative locations throughout the stream and at locations where changes occur in discharge, slope, shape, roughness; at locations where levees begin and end; and at hydraulic structures (bridges, culverts, and weirs) (Gary, 2016; Elias, 2018).

The required information for a cross section consists of: the river, reach and river station identifiers; a description; X & Y coordinates (station and elevation points); downstream reach lengths; Manning's roughness coefficients; main channel bank stations; and contraction and expansion coefficients (Gary, 2016; Elias, 2018).

2.7.2. Flow Data

Once the geometric data is entered, the necessary flow data can be entered. Steady flow data consist of: the number of profiles to be computed; the flow data; and the river system

boundary conditions (Elias, 2018). The study was used forecasted flow data for 2, 5, 10, 25, 50, 100 and 200year profiles.

2.7.3. Plan data

Usually the first step in performing a simulation is to put together a Plan. The Plan defines which geometry and flow data are to be used, as well as provide a description and short identifier for the run. If the geometry and flow data do not exist, then this action is performed after their creation. Also included in the plan information are the selected flow regime and the simulation options (Gary, 2016; Cited by Elias, 2018).

2.8. HEC-Geo RAS Extension

HEC-GeoRAS is an ArcView GIS extension, cooperatively developed by the HEC and the Environmental System Research Institute, Inc. (ESRI), specifically designed to process geospatial data for use with HEC-RAS (HEC, 2010). The HEC-GeoRAS is a GIS extension with a set of procedures, tools, and utilities for the preparation of river geometry GIS data to import into HECRAS and it is used to generate the final inundation map. The input data required for the River geometry preparation using the HEC-GeoRAS model are Triangular Irregular Network (TIN), DEM, and land use. The HEC-GeoRAS or HEC-RAS has been used worldwide for inundation mapping, such as in Europe (Dragan and slobodan, 2009; Gkiokas et.al , 2013) in the USA (Brunner, 2013; kamal , 2011; Liu et. al , 2008) in Africa (Botes and Smith , 2010) and in Asia (Hasanpour et . al ,2013 ; karim and Suleiman ,2009).

HEC-GeoRAS is used to create the boundary of the flood extent and the depth of water at each location within the boundary. HEC-GeoRAS creates water depths and floodplain boundaries by subtracting topographic data from water surface elevations imported from HEC-RAS. An area where the water depth is greater than zero is considered to be in the flood boundary. To analyze the data, two variables are taken into consideration. The first being the area of the flood extent and the second being the width of flood along each cross-section in the original HEC-RAS project file (Aaron, 2008).

2.9. Estimation of flow to un-gauged sites

The flow data at any required location is necessary for further flow analysis. To determine flow data at ungauged site the study discusses about drainage area ratio method and Hydrologic modeling routing method (channel routing) using Muskingum routing to select the best one.

2.9.1. Drainage area ratio (DAR)

The applicability of the DAR method is closely related to the hydrological similarity (similar drainage area, climate, and geographical conditions) between two stations. DAR method is commonly used when the stations are located on the same stream and the ratio between the drainage areas of the donor station and the target station $\left(\frac{A_{target}}{A_{donor}}\right)$ is between 0.5 and 1.5 (Hortness, 2006).

2.9.2. Hydrologic routing

HEC-HMS is a numerical and semi-distributed hydrologic model developed by the United States Army Corps of Engineers (USACE 2010). Muskingum method is one of hydrologic routing method in channel routing to determine outflow hydrograph at the downstream location using inflow hydrograph at the upstream (i.e. used to determine flow data at ungauged site at any required location using gauged inflow data at the upstream location).

Study made by Tewolde (2005) on three sub catchments in the Thukela catchment in KwaZulu-Natal, South Africa were selected for analyses, with river lengths of 4, 21 and 54 km to determine flow data at ungauged site using Muskingum method with empirically estimated parameter methods produced acceptable results with errors of less than 20% for most statistics considered.

Similarly study conducted in china (Xiao et al., 2011) in the Louzigou Basin in Henan Province of China, in a tributary basin of the Huaihe Basin, with a drainage area of 1244 km^2 using Muskingum method for hydrologic routing in HEC-HMS model and simulation of the ungauged basin shows high simulation accuracy to demonstrate that the method is a reliable for flow estimation in ungauged basins.

2.10. Frequency Analysis

The estimation of the frequencies of flood is essential for the quantitative assessment of the flood problem. The proper choice of a statistical distribution which best fits the annual maximum flow (AMF) data is necessary to analyze flood frequency for a particular area. According to Chow (1988), there are a number of distributions in hydrology used to analyze the probability of occurrence of a stream flow. Some of these are Normal distribution, lognormal distribution, Pearson type III distribution, Log-Pearson type III distribution, Exponential distribution, Extreme value distribution and Gamma distribution. UK Natural Environment Research Council (1975) found that three parameter distributions such as the

log Pearson type III and the general extreme value distribution (GEV) were found to fit data from 35 annual flood series better than the two parameter distribution functions. The log Pearson type III (LP III) distribution has extensively been used in flood frequency analysis since its favorable recommendation by the Water Resources Council in 1976. The frequent use of the LP III attracted a number of detailed mathematical and statistical studies regarding its role in flood frequency analysis. Various alternative fitting techniques for the log Pearson type III distribution have been suggested by Matalas and Wallis (1973) and Condie (1977).

Study conducted by Yaynshet (2020) in Ethiopia Zeway-Shala sub basin on regional flood frequency analysis on 10 stations selected for the analysis based on continuity and the length of record period. The study used Gen-extreme value (Gumbel-distribution), log-pearson type 3, log-normal type 3, gamma (3p), gamma and log-normal. Among the fitted distribution Generalized Extreme Value distribution is selected for region one and Log Pearson Type III distribution is selected for region two based on statistical value, simple to apply and widely acceptance.

In a similar study performed by Mengistu (2008) in Ethiopia upper awash sub-basin (i.e. upstream of koka Dam) on regional frequency analysis of 10 selected gauging station consisting of stream flow record varying from 12 to 37 years, out of which 6 stations are found in the upper region and 4 of the stations are found in the lower region. An Extreme value EV1, GEV and Lognormal LN2, LN3 distributions are selected as the best fit distribution for the stations in the sub-basin. Among the selected distributions; LN2 and EV1 with MOM method of parameter estimation for stations in the upper region and LN3 and GEV with PWM method of parameter estimation for stations in the lower region of the sub-basin by using goodness fit test.

In another study on Regional Flood Frequency Analysis on Upper Wabi-Shebelle River Basin of Ethiopia by Alemgena (2019) showed that; based on gauging stations location and L-moment, the regional homogeneity test was conducted and the study area was regionalized in to three homogeneous regions as region -1, region-2 and region3. The most suitable flood frequency distributions which were found for the study area were General Extreme Value, General Pareto and Lognormal 3p to region -1, region-2 and region-3 respectively. These flood frequency distributions were selected by using Kolmogorov Smirnov, Anderson-Darling and Chi-Squared goodness-of-tests with easy fit software and linear moment ratio diagram.

Additional study made by Tefera (2015) on Awash river from Logiya to Dubti for flood mitigation alternatives for selected reach using Gumbel, Log-pearson type 3, Log-normal and Normal frequency distribution to forecast the flood event and the best fit model is selected based on the relative magnitude of the statistical test results with lowest RMSE, lowest RRMSE, lowest MAE or highest CC value. The statistical values indicate Log -Pearson III was the best fit to estimate the flood peak flow design for the selected River reach.

2.11. Evaluation of flow duration curve

It is a graph of river discharge plotted against exceedance frequency and is normally derived from the complete time series of recorded river flows. It is simple to construct and used in different water resources application over the entire range of river flows. The construction is based on the ranking data (normally daily discharge) and calculating the frequency of exceedance for each value. It effectively recorders the observed hydrograph from the one ordered by time to one ordered by magnitude. The percentage of time that any particular discharge is exceeded can be estimated from the plot (Kumar and Schei, 2009).

The flow-duration curve is a cumulative frequency curve that shows the percent of time specified discharges were equaled or exceeded during a given period. It combines in one curve the flow characteristics of a stream throughout the range of discharge, without regard to the sequence of occurrence. If the period upon which the curve is based represents the long-term flow of a stream, the curve may be used to predict the distribution of future flows for hydropower, water-supply, and pollution studies (Hall, 2009).

To prepare a flow-duration curve, the daily, weekly, or monthly flows during a given period are arranged according to magnitude, and the percent of time during which the flow equaled or exceeded the specified values is computed. The curve, drawn to average the plotted points of specified discharges versus the percent of time during which they were equaled or exceeded, thus represents an average for the period considered rather than the distribution of flow within a single year (Rotilio et al., 2017).

If the available head and efficiency of the power plant are known, the flow duration curve have seen that may be converted in to power duration curve (i.e. ɣQH). The power which is available for 95 % to 97 % of the time on the reservoir regulated schemes is usually considered to be the primary or firm power and the area of power duration curve under the minimum amount of flow a valuable for 95% or 97% of the time thus gives the total amount of the primary power. It is not necessarily produced continuously (Macavoy, 2012). If the

bondage and inter connection facilities are available the plant may be operated on the peak load only. The secondary or surplus power is all the available power in excess of the primary power and is given by the area under the power duration curve between the firm power line and the total installed capacity of power plant (Kumar and Schei, 2009).

2.12. Multi Criteria Decision Analysis

Multi-criteria decision analysis (MCDA) is a group of techniques for structuring and evaluation decision alternatives based on multiple attributes and objectives which is an approach having capability to integrate numerous notion of decision problems.

Selection of best alternative is complex problem since it is affected by many factors like geographical, environmental and human factors. In order to prioritize suitable alternatives, an analysis performed for selection of the best suitability one. To facilitate a favorable condition for local decision makers to make a reasonable decision as to which alternative should be given the top priority for project implementation, ranking of available alternative is essential (Mbaka and Mwaniki, 2016).

Various methods have been developed in the last three decades which use pairwise comparisons of the alternatives and criteria for solving multi-criteria decision making. Among multi-criteria decision making methods analytic hierarchy process (AHP) and Technique for Order of Preference by Similarity to Ideal Solution (TOPSIS) discussed as follows.

2.12.1. Technique for Order of Preference by Similarity to Ideal Solution

TOPSIS (Technique for Order of Preference by Similarity to Ideal Solution) is one of the multi criteria decision-making methods introduced by Hwang and Yoon. The principle used TOPSIS is the chosen alternative must have the closest distance from the ideal solution and furthest from the ideal solution from a geometric point of view using the Euclidean distance to determine the relative proximity of an alternative with the optimal solution. The positive ideal solution (A +) is defined as the sum of all the best attainable values for each attribute, while the ideal solution (A-) consists of all the worst values achieved for each attribute (Afhsari et al., 2010).

2.12.2. The Analytic Hierarchy Process

The Analytic Hierarchy Process (AHP), introduced by Thomas Saaty (1980), is an effective tool for dealing with complex decision making, and may aid the decision maker to set

priorities and make the best decision. By reducing complex decisions to a series of pairwise comparisons, and then synthesizing the results, the AHP helps to capture both subjective and objective aspects of a decision. In addition, the AHP incorporates a useful technique for checking the consistency of the decision maker's evaluations, thus reducing the bias in the decision making process.

2.12.2.1. Application of standardized criteria

In decision making, utilizing quantitative and qualitative data, the criteria scores need to be standardized (Carver, 2005). Variables are considered benefit criteria if the more desirable values are the higher values, conversely, most criteria are variables in which the more desirables values are the lower values (Jimoh & Yisa, 2010). The linear scale transformation methods convert the raw data into standardized criterion scores. A number of linear scale transformations exist for application of the maximum score and the score range procedures. The application of standardize is used to maximize or minimize the criteria score in decision making process from multiple alternatives (Reichl and Hack, 2017).

2.12.2.2. Criteria weighting methods

There are four different techniques for assigning weights, which are ranking, rating, pair wise comparison and trade-off. Ranking (arranging in rank order), is the simplest of the four methods to use, however it is limited in that the results can only be viewed as approximation of the true weights. The rating method in which weights are estimated based on a predetermined scale is also a relatively simple method and is sometimes criticized for its lack of theoretical foundations. The pair wise comparison method and trade-off analysis methods offer much more precision in terms of calculating weights with having underlying theoretical bases. However, research has shown that the pair wise comparison technique is simpler to use and just as effective analysis (Hudson et al. 2016).

3. MATERIAL AND METHODS

3.1. Description of the study area

Awash River basin is one of the major twelve basins in Ethiopia. The basin has a total catchment area of 117,600km2. Awash River basin is divided into three parts; upper awash from Koka reservoir to the beginning of the awash river, middle awash, from Koka reservoir to Kesem dam and lower awash downstream of Kesem dam based on climatological, physical, socioeconomic, agricultural, and water resources characteristics (Edossa et al., 2010). The study area including upstream of Koka reservoir watershed cover an area of 14,479 km^2. According to Edossa (2010) study the specific study area lies in the middle part of the basin and covers around 50km downstream of Koka Reservoir with an area of 2,872km^2. The geographical location of specific study area lies between latitude of 8°25‟06” N to 8°28‟12” N and longitude of 39°09‟35” E to 39°31‟48” `E and elevation ranges from 1274-1573 m.a.s.l.

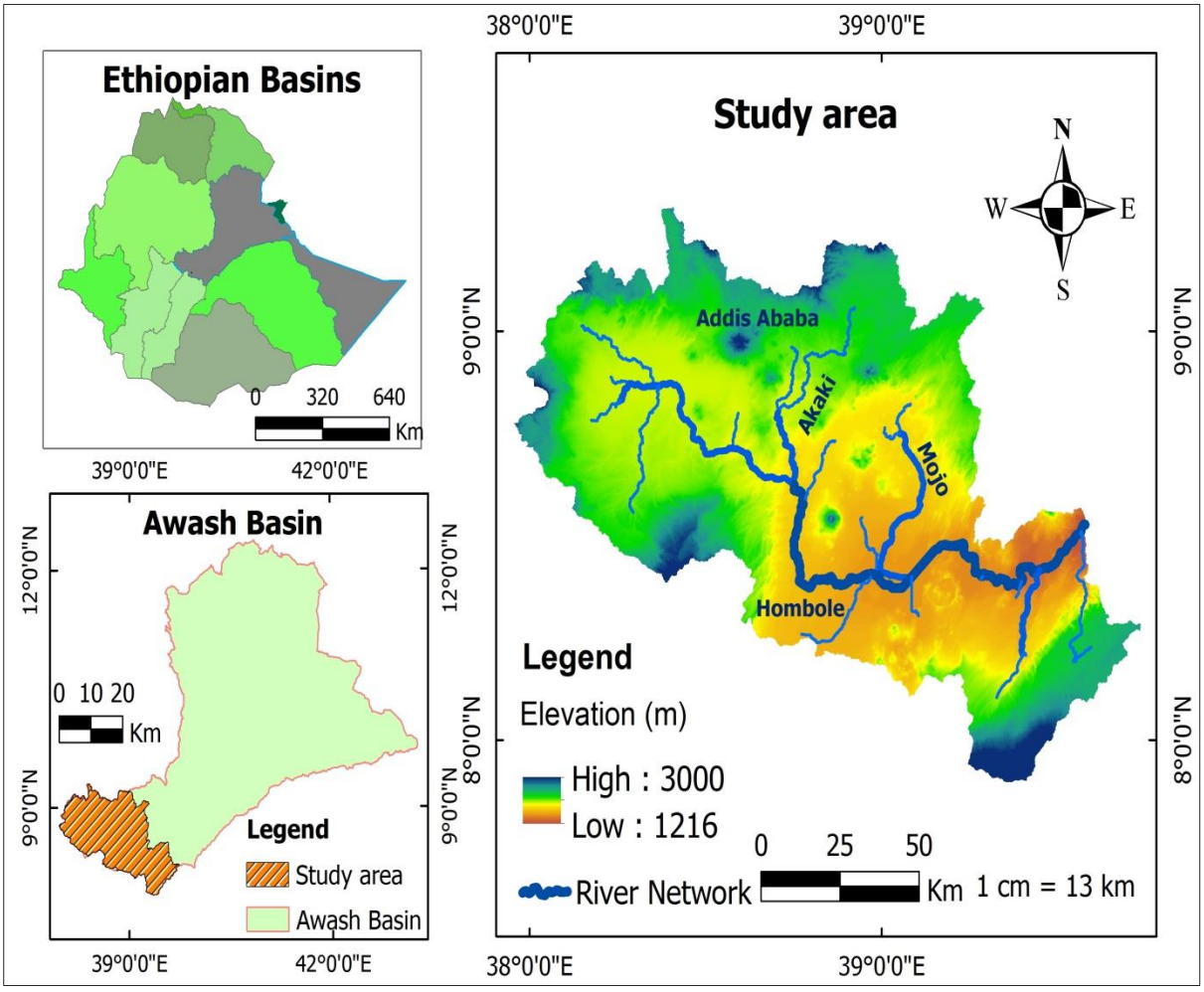

Figure 2: Location map of study area

3.1.1. Climate

The climate of Awash Basin varies according to the wide ranging altitudinal variation. It is broadly characterized by two main climatic zones – arid to semi-arid in the lowland areas and a zone of tropical humid to dry sub-humid along the highlands. The cycle of precipitation in the basin are results of the year round migration of the Inter-Tropical Convergence Zone (ITCZ), a zone of low pressure characterized by the convergence of dry tropical easterlies and moist equatorial westerly's. The main climatic seasons are recognized to be having heaviest summer rains in June and July, receding through August to September as a transition to a dry season from October to February, and a spring of relatively shorter rainy season from March to May. Near the origin of the Awash River on the highlands to the west of Addis Ababa, the rainfall distribution signifies a continuous rise from the spring rains all through the summer peak rainfall. Rainfall pattern over the highland varies in correspondence with the wide ranging altitudinal variation giving rise to a highly variable monthly and annual rainfall distribution. Annual rainfall ranges from about 1600 mm in the highlands near the origin of the river to 160 mm close to the northern limit of the basin with the mean of 850 mm (Kerim et al., 2016; Adey et al., 2016; Mulugeta et al., 2019).

3.1.2. Topography of study area

The landscape of the basin comprises highland, escarpment and rift. The terrain in the study area generally ranges from 1273 meters to 1572 m.a.s.l. Awash river, which is the longest river in the area, it crosses the study area from west of Addis Ababa to southeast and its tributaries crosses highland, escarpment and valleys. The flood prone area located at the lowest the part of the area, it occupies the major portion Metahara to Afar triangle. On the other hand, the highland regions are located around Addis Ababa, which is the capital city of Ethiopia. The slope of the specific study area at the downstream of Koka Reservoir is predominantly small about 0.0044. At the sides of the watershed (i.e. eastern and western part of the study area) comprises highland with escarpments area and gorges along the river.

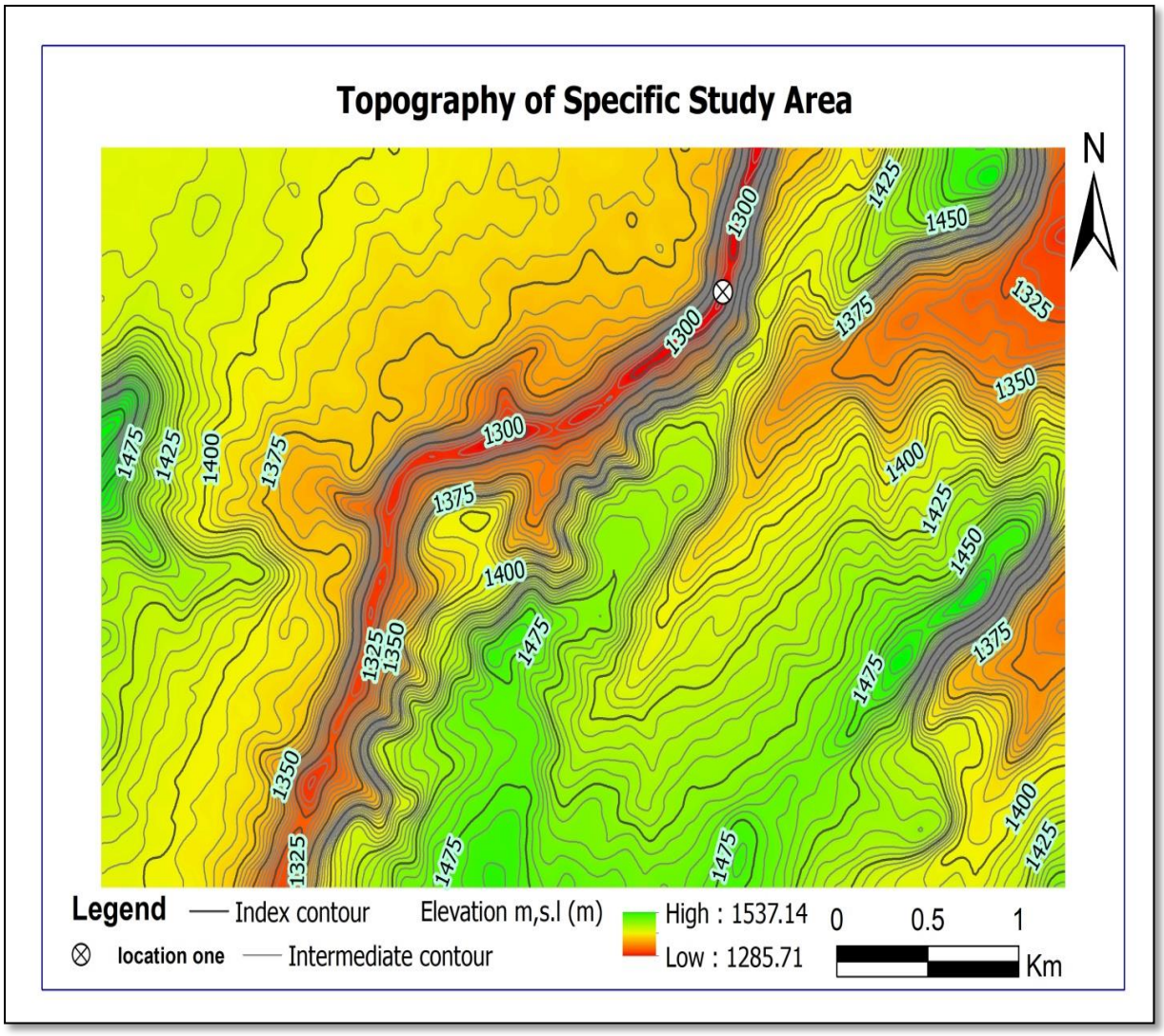

Figure 3: Topography of study area

3.1.3. Land use and Land cover of study area

According to land use land cover classification the study area generally comprised Settlement area, barren land (Exposed rock), vegetation, agricultural land, and forest and water bodies. The settlement areas combined with barren land cover the largest part of study area.

Table 1: Area and percent of area covered of LULC of study area

Land cover	Area(Square kilometers)	Percent of area covered (%)
Settlement area	924.77	32.2
Barren Land	920	32
Forest	533.38	18.57
Agricultural Land	332	11.56
Water Bodies	91	3.16
Vegetation	70.43	2.45
Total	2871.58	100

The Land Use Land Cover (LULC) of study area depicts that settlement area combined with barren land cover an aggregated area of 1,844.77km^2, or approximately 64.24% of the watershed. The other land area covered by forest, agricultural land, water bodies and vegetation comprises 1,026.81 km^2, or approximately 35.76%.

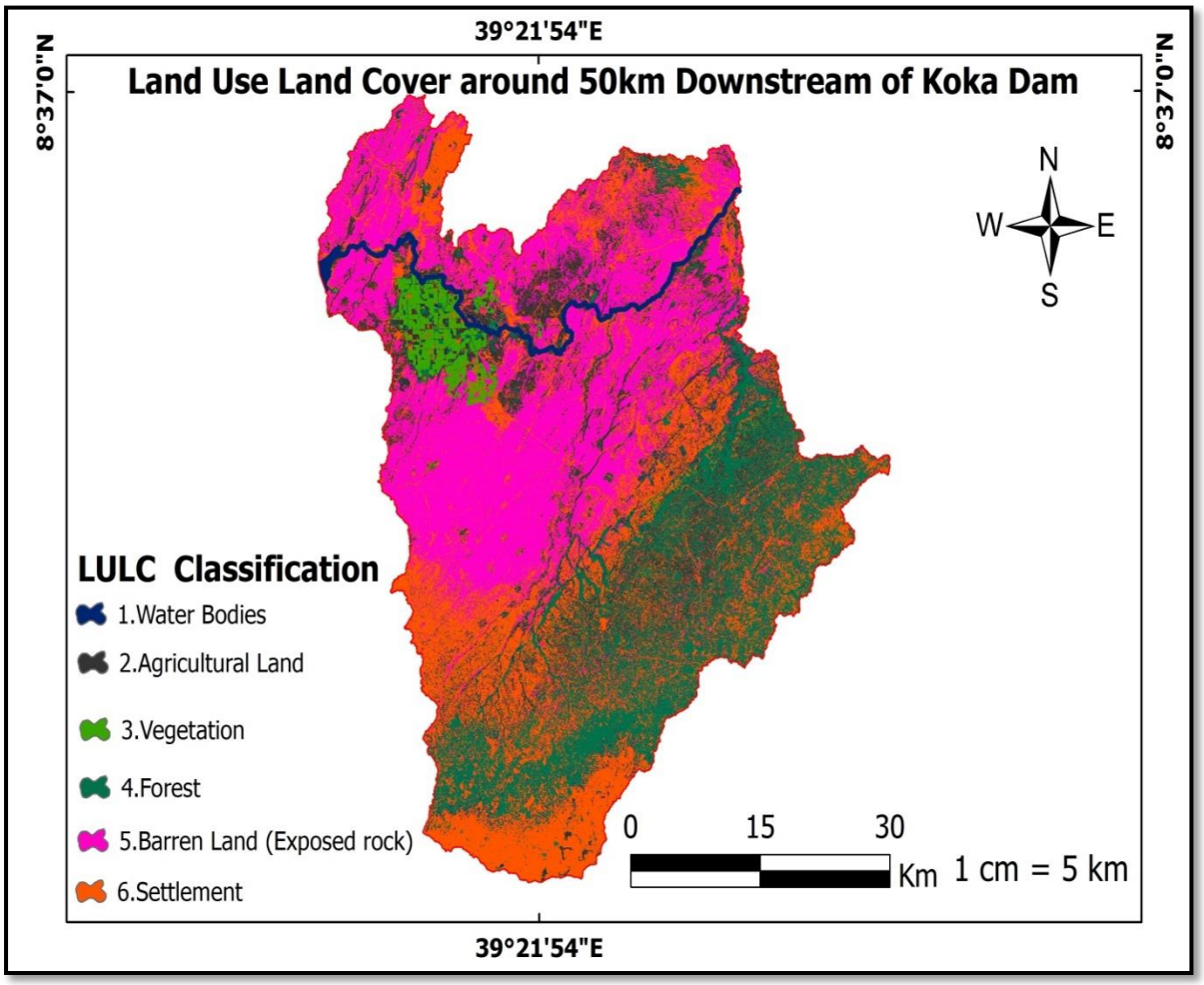

Figure 4: LULC of study area

3.1.4. Soil Classification of study area

According to Upper Awash Sub Basin Integrated Land Use Planning Study (OWWDSE, 2014) the most common soil types in the basin are Clay, Clay-Loam, Loam, Sandy-Clay-Loam and Silt-Loam. To know spatial distribution soil in specific study area, the study made soil map using FAO soil from the page FAO/UNESCO Soil Map of the world in ESRI shape file format and for further analysis SWAT2012 user soil downloaded and according to the number in SEQN soil textural classification shown in table 2 and soil map shown in figure 5 as follows.

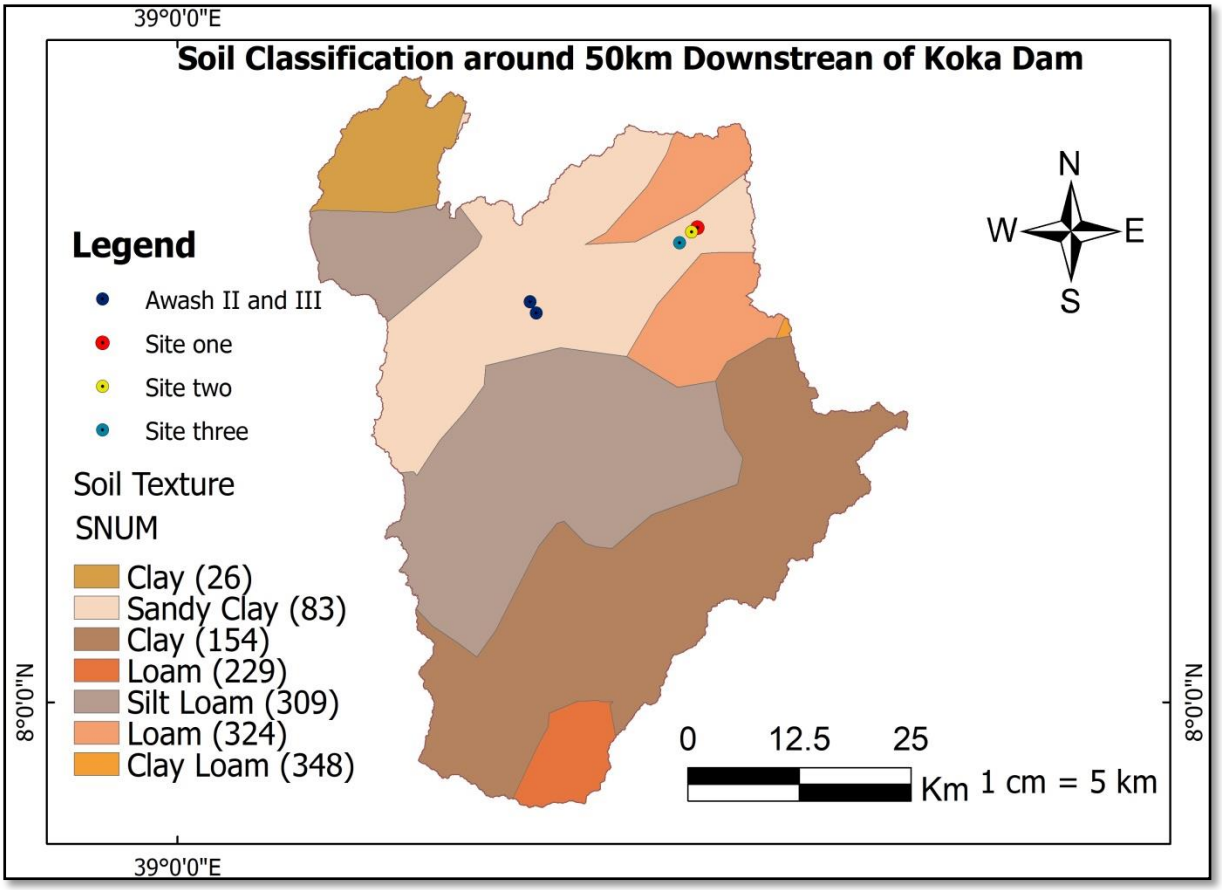

Figure 5: Spatial distribution of soils in the study area

According to FAO soil the study area generally comprises clay, sandy-clay, loam, silt-loam and clay-loamy. Soil type at selected specific site dominated by sandy-clay (83) and loamy (229) soil at the left and right side.

Table 2: Percent of each soil content in soil texture

SEQN	Soil texture	Clay (%)	Silt (%)	Sand (%)
26	Clay	43	28	29
83	Sandy clay	26	22	52
154	Clay	32	31	37
229	Loam	26	44	30
309	Silt loam	20	53	27
324	Loam	43	28	29
348	Clay loam	20	41	39

3.1.5. Geology of study area

The geology around 26.97km from specific study area to the upstream, which is at Awash II and Awash III dam site is basalt layer of volcanic ash and tuff in between (Awash II) and liparitic rock more than 30m thick with a layer of impermeable clay beneath at Awash III (EELPA, 1964). To know the geology of specific study area this research used world geologic maps of USGS pages to download geology of the study area. And using GLG codes from attribute table of geology map and searching for rock type from the legend of ArcGIS RESET Endpoint Directory quaternary undivided (Q), quaternary extrusive and intrusive rocks (Qv), and tertiary extrusive and intrusive rocks (Ti) were observed. As shown in the figure 6; the geology in the specific selected site is tertiary extrusive and intrusive rocks, and is igneous type rock.

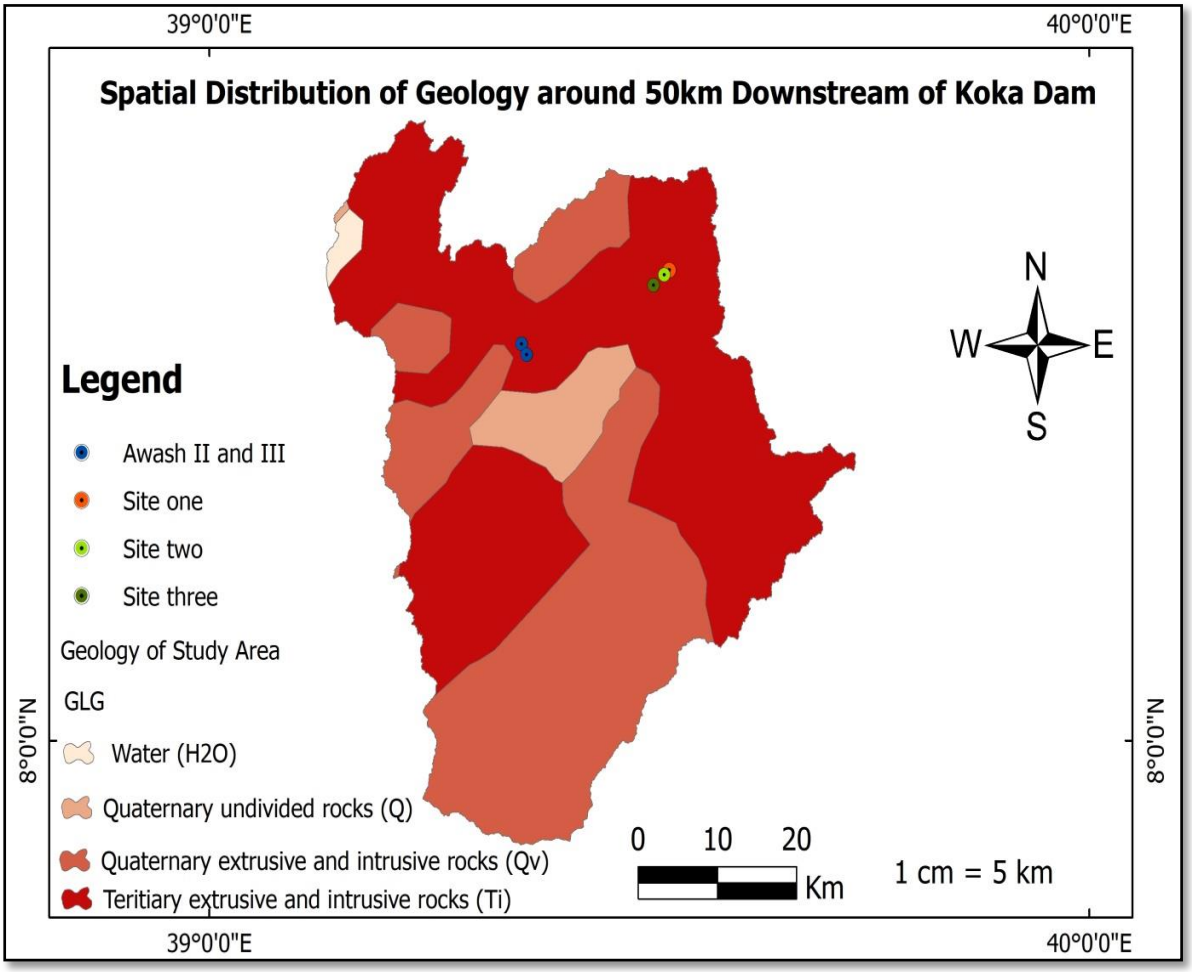

Figure 6: Spatial distribution of geology in the study area

3.2. Data Sources and Methods of Collection

3.2.1. Hydrological data

Daily stream flow of five stations (i.e. Metahara, Wonji, Awash below koka dam, Awash 7kilo and Awash melka seddi) from 1991-2016 were taken from Ministry of Water Resources and Energy (MWRE). Among the five stations, Wonji station is the nearest upstream station to the specific target site. So, it was used as the inflow flow data to rout the outflow at the downstream for specific targeted sites. The other four stations used to fill the missing stream flows of Wonji station. Stream flow is the most dominating input data for assessment of run of the river hydropower scheme.

3.2.2. DEM (Digital Elevation Model)

Digital elevation model is the representation of the topography. The study used ALOS PALSAR DEM (Digital Elevation Model). It was downloaded from Alaska satellite facility (htts://users.earthdata.nasa.gov/users/new).

3.2.3. Others important data

There are different parameters that directly or indirectly affect the final findings of the study. Among the other, Landsat image (Landsat8) one of important parameter, it has been downloaded from earth explorer USGS of the time range 5/25/2020 to 5/1/2023 at 1:11AM. Landsat is the critical parameter to know LULC of the study area. In addition Geologic data is the other influencing parameter to characterize the geology of the study area. It is downloaded from world geologic maps of USGS pages. Soils also other important construction material and it was downloaded from FAO/UNESCO Soil Map of the world. Finally one of indirectly influencing tool was online Google earth pro. It is used for visualizing the real study area to correlate with Landsat image for LULC accuracy assessment and to validate the spatial information of Digital Elevation Model (DEM) and to download specific study area high resolution images. To summarize essential data and modeling software were tabulated in table 3 and 4 as follows.

Table 3: Source, description and purpose of the data used in the study

No	Types of data	Source	Description	Purpose
1	DEM	Alasca.S.F	Cell size (12.5,12.5)	To analyze the spatial information
2	Landsat image	USGS	Number of bands: 7 Cell size (x,y): 30,30	LULC classification
3	Digital soil map	FAO/UNESCO	Soil map digitized at scale 1:5000	To know spatial distribution of soil of the study area
4	Geology map	USGS	World Geology map	To know the geology of study area
5	Stream flow	MWRE	1991-2016	To develop FDC
6	Water depth	MWRE	2012-2021	For accuracy assessment
7	Google earth pro	Online source	Earth data	For accuracy assessment
8	High resolution image	Google earth pro	Cellsize(x,y):0.079 number of band:3	For further detail analysis of spatial information at home

Additional supporting information was obtained from online journals, conference proceedings, thesis, government policy documents, Published books as well as project reports.

Table 4: Modeling Software

No	Modeling Software	Purpose
1	ArcGIS:10.41	To analyze spatial information of study area
2	HEC-GeoRAS:10.41	H Pre-processing of geometric data
3	HEC-RAS 6.3	Hydraulic Modeling(i.e. flood level forecasting)
4	HEC-HMS 4.10	To rout stream flow(Muskingum method)
5	Rainbow software	To test homogeneity test of stream flow
6	Easy fit software	To check fitness of frequency distribution
7	Microsoft excel	Statistical computation of all required data

3.3. Flow Data processing

Before beginning any flow data analysis and discussion, it is important to make sure that the data are consistence, homogeneous, sufficient, complete and statically logical with no missing. Lack of appropriate data processing leads to unreliability and finally bias in the final result. This session aimed to make ready and significant the flow data for further analysis and discussion.

3.3.1. Rough Screening of flow Data

The basic procedure begins with an initial, rough screening of the data. It is visual detection of whether the observations have been consistently or accidentally credited to the wrong day, whether they show gross errors (e.g. from weekly readings instead of daily ones), or whether they contain misplaced decimal points (Stol, 1965).

3.3.2. Filling stream flow

Flow data determine the potential site for run of the river hydropower plant. There are different imputation methods for the missing stream values, from these infilling methods the study discusses about the following

3.3.2.1. Normal ratio method

Normal ratio (NR) method is weighted based on the ratio mean of the available data between the target station and the i^{th} neighboring station. This method is used if any neighboring stations have the normal annual rainfall and stream flow data which exceeded more than 10% of the considered station (Silva et al, 2007; Cited by Ismail and Ibrahim, 2017). The estimated missing value is given by

$$V_o = \frac{1}{n} \sum_{i=1}^{n} \frac{N_t}{N_i} X_i \quad \text{.....3.1}$$

Where, Nt is the annual rainfall and stream flow amount at the target station and Ni is the annual rainfall and stream flow amount at the i^{th} nearby station.

3.3.2.2. Inverse distance method

Inverse distance (ID) method is the most commonly used for estimation of missing rainfall, stream flow, flood depth. In this method, it is based on the distance between target station and

nearby station. The closer stations are better correlated with the target station compared to further stations (Ismail and Ibrahim, 2017). The estimated missing value is given by

$$V_o = \frac{\sum_{i=1}^{n} V_i/d_i}{\sum_{i=1}^{n}(1/d_i)} \quad \text{.....3.2}$$

Where, Vo is the estimate obtained for missing stream value, Vi is the observed stream value at the i^{th} station, di is the i^{th} surrounding station distance, and n is the number of stations used. The distance between the target station and the surrounding stations is calculated using the Pythagoras formula

$$d_i = \sqrt{(X_a - X_i)^2 + (Y_a - Y_i)^2} \quad \text{.....3.3}$$

Where, di is the distance between the target station and the surrounding i^{th} station, X_a and X_i are the longitudes, and Y_a and Y_i are the latitudes of the target and the i^{th} surrounding stations, respectively. The study was inverse distance weighting methods due to it gives more weight to nearest surrounding station. The nearer the station, the common climate they share.

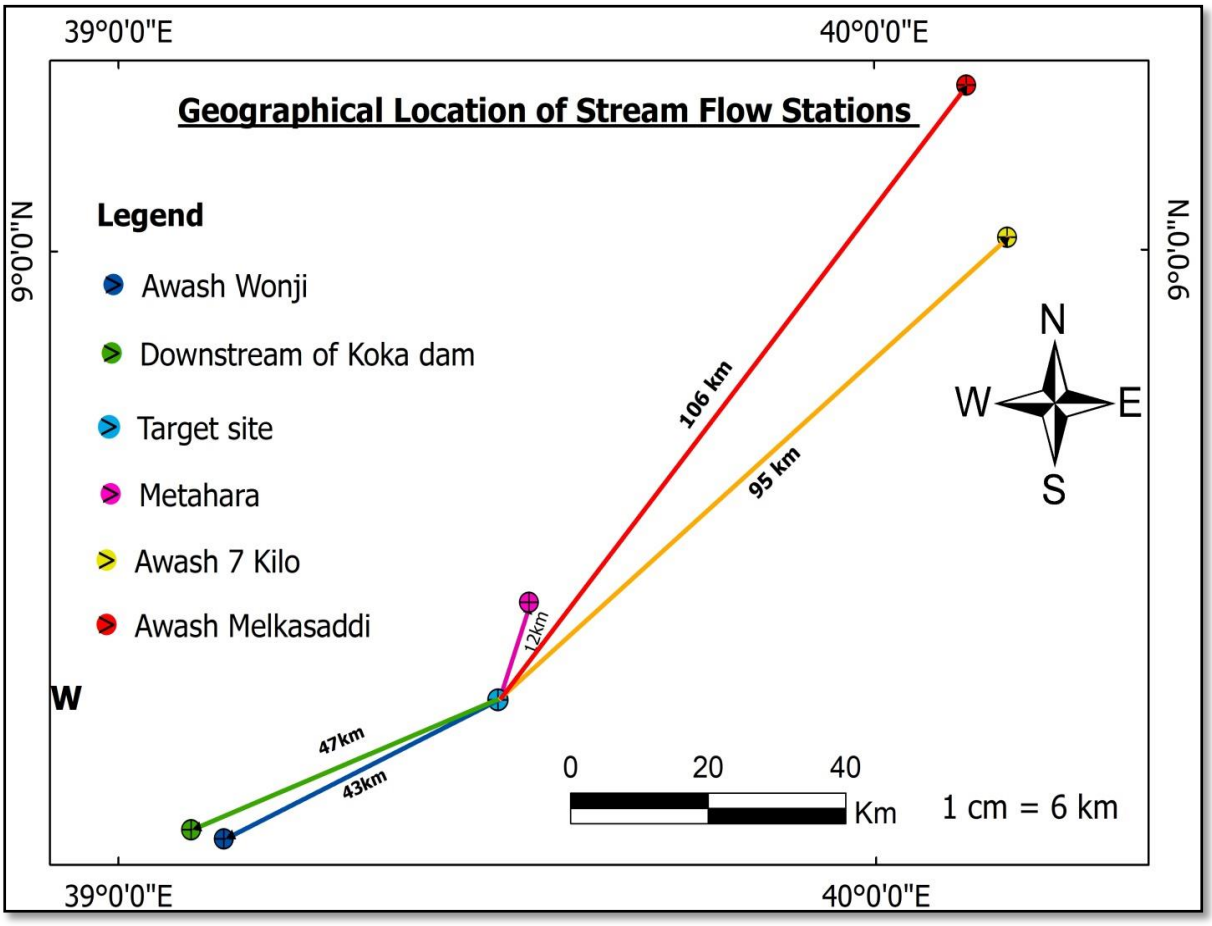

Figure 7: Location of surrounding station with respect to target site

Table 5: Location of target and surrounding stream flow stations

River Station	Longitude	Latitude	X	Y
Downstream of Koka	39.10	8.28	510683	916073
Awash Wonji	39.14	8.27	515419	914800
Metahara	39.51	8.51	556066	940864
Awash 7 Kilo	40.17	9.01	629229	996722
Awash Melka saddi	40.12	9.20	623302	1017451

3.4. Transporting stream flow data from gauged to un gauged location

The linear Muskingum Equation comprises continuity equation and a relationship a connecting inflow, outflow, and storage for the solution of the routing problem (Sajikumar et al., 2015; Khaeruddin et al., 2020).

$$\frac{d_s}{d_t} = I(t) - O(t) \quad \text{.....3.4}$$

Where;- S: is the absolute channel storage at time t and I is the rate of inflow at time t somewhere the upstream and O is the rate of outflow at time t somewhere the downstream and the total storage in a channel is represented by a so-called Muskingum equation (Chow et al., 1988) given by

$$S = K[XI + (1 - X)Q] \quad \text{.....3.5}$$

Where K: the storage time constant for the river reach, which has a value reasonably close to the flow travel time within the river reach; and X: a weighting factor is varying between 0 to 0.5. This value is specific for every channel/river.

Through writing the form of finite difference of equations 3.4 and 3.5, and their combination and finally simplification, the following equation is obtained based on which routing can be performed.

$$Q_{t+\Delta t} = C_o I_{t+\Delta t} + C_1 I_t + C_2 Q_t \quad \text{.....3.6}$$

Where I is inflow at t somewhere upstream and Q is outflow at t somewhere downstream (i.e. stream flow at ungauged site), Δt is time interval and for this study; it is 24hr and Co, C1 and C2 are coefficients the sum is 1.

$$\mathbf{C_o} = \frac{\Delta t - 2KX}{2K(1-X)+\Delta t} \quad \text{.....3.7}$$

$$\mathbf{C_1} = \frac{\Delta t + 2KX}{2K(1-X)+\Delta t} \quad \text{.....3.8}$$

$$\mathbf{C_2} = \frac{2K(1-X)-\Delta t}{2K(1-X)+\Delta t} \quad \text{.....3.9}$$

The Muskingum parameters K and X are estimated for the ungauged sites at the downstream using Wonji stream flow station as inflow data, which is located immediate upstream of the target sites along the same stream line. Muskingum parameters K and X are estimated for the ungauged basin using an inflow hydrograph of the current year, flow characteristics, and dimension of the channel (Biswadeep and Utpal, 2022). The parameter K and X can be estimated in equation 4 and 4.1 as follows; (Chow, 1959; Fread, 1993; Tewolde, 2005).

$$\mathbf{K} = \frac{\Delta L}{V_w} \quad \text{.....4}$$

$$\boldsymbol{X} = \frac{1}{2} - \frac{Q_o}{2SPV_w\Delta L} \quad \text{.....4.1}$$

Where, Qo: reference discharge (m^3/s), S: dimensionless channel bottom slope (m/m), Vw: kinematics wave celerity (m/s), ΔL: routing reach length (m), P: wetted perimeter (m), K: the storage time constant for the river reach (s), which has a value close to the wave travel time within the river reach, and X: a weighting factor varying between 0.0 and 0.5 (dimensionless).

The wetted perimeter can be estimated by the Lacey equation for stable river channels (Kong and Wang 2008; Xiao et al., 2011):

$$P = C\sqrt{Q_O} \quad \text{.....4.2}$$

Where C is a coefficient whose value is between 4.71 and 4.78 (**take: 4.75**). The reference discharge was defined by (Wilson and Ruffini, 1988; Xiao et al., 2011) as follows:

$$Q_o = Q_b + 0.5(Q_p - Q_b) \quad \text{.....4.3}$$

Where Q_b and Q_p are minimum discharge and peak discharge, respectively. The maximum and minimum discharge was determined from 1991-2016 inflow (i.e. Wonji station) stream flow data (i.e. **353m^3/s** and **3.97m^3/s**). The maximum and minimum discharge could be seen from Wonji river station daily time series stream flow (1991-2016) in the figure follow as;-

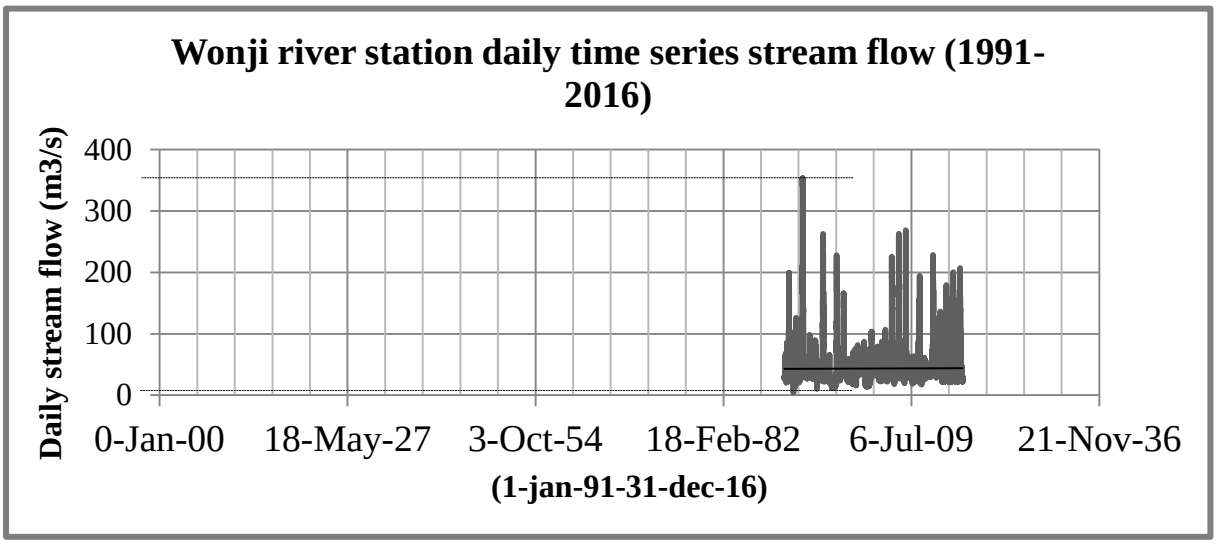

Figure 8: Wonji station daily time series stream flow

The relationship between flood wave celerity and velocity can be obtained from the following formula (Todini 2007):

$$V_m = \lambda V_{av} \quad \text{.....4.4}$$

Where $\boldsymbol{\lambda}$ is the wave celerity coefficient or shape coefficient of the channel cross section (dimensionless), V_m is flood wave celerity (m/s) and V_{av} is average velocity (m/s); average velocity (V_{av}) can be calculated from manning's formulas in equation 4.5 as follows:

$$V_{av} = \frac{Q_o}{A} = \frac{1}{n} R^{2/3} S^{1/2} \quad \text{.....4.5}$$

Where Vav, R, Qo, S and n, are average velocity, hydraulic radius, reference discharge, slope and manning's roughness coefficient, respectively. The roughness coefficient may be estimated using the method outlined by Cowan (1956) considering the most important factor that affects the selection of channel roughness coefficient. (i.e. the average of LOB, Channel and ROB, roughness coefficient 0.046, 0.0443 and 0.055 which is equal to **0.0484**). In addition, R is computed from the flow area and wetted perimeter P as follows:

$$R = \frac{A}{P} \quad \text{.....4.6}$$

Using equations 4.5 and 4.6 we can drive the following equation for hydraulic radius (R);

$$R = \left(\frac{nQ_O}{P\sqrt{S}}\right)^{3/5} \quad \text{.....4.7}$$

Using equations 4, 4.2, 4.4, 4.5, 4.6 and 4.7 we can estimate Muskingum parameter K as follows;

$$K = \frac{n^{0.6}LC^{0.4}}{\lambda Q_O^{0.2}S^{0.3}} \quad \text{.....4.8}$$

K value in equation 4 is in second; but Muskingum K value in HEC-HMS hydrologic modeling software of basin model in a given reach is in hour (hr). So to change the K value in equation 4.8 to hr multiply by 1/3600. Take λ =1.5 for natural channel from table 6.

Finally to estimate another Muskingum parameter X we can use equations 4.1, 4.2, 4.4, 4.5 and 4.6 as follows;

$$X = \frac{1}{2} - 0.5\frac{Q_o^{0.3}n^{0.6}}{C^{0.6}s^{1.3}\lambda L} \quad \text{.....4.9}$$

Wave celerity (wave speed) $\boldsymbol{\lambda}$ can be determined from average velocity as follows;

Table 6: Factors for computing wave speed from average velocity (US Army Corps of Engineers, 2008; Safa, 2012)

Channel shape	Factor ($\boldsymbol{\lambda}$) =$\mathbf{V_m/V_{av}}$
Wide rectangular	1.67
Wide parabolic	1.44
Triangular	1.33
Natural channel	1.5

The study determined reach length and slope from spatial analysis of study area topography using Digital Elevation Model in ArcGIS. This is done by digitizing from Wonji station to site one as follows;

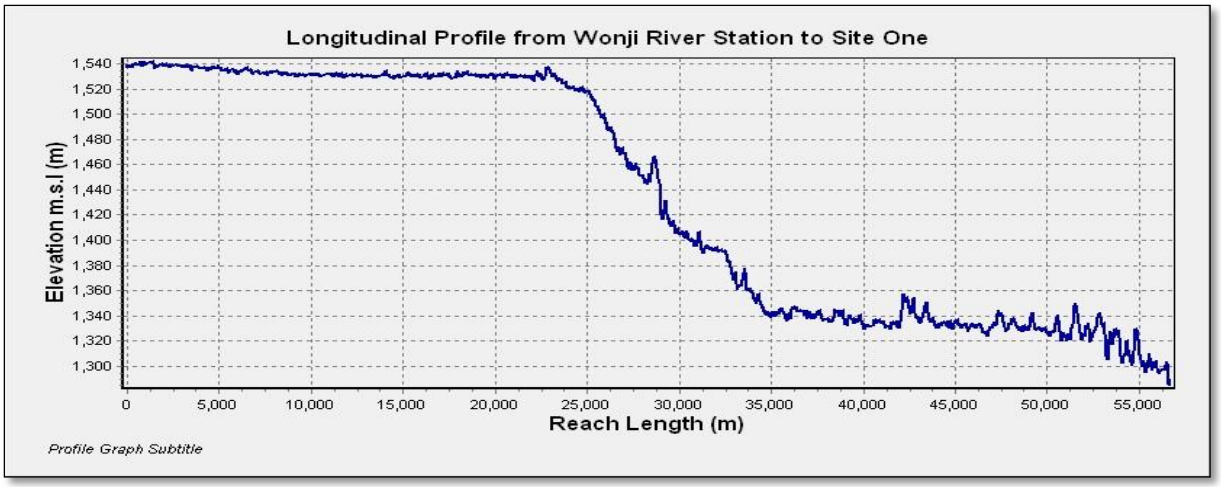

Figure 3: Topography of Longitudinal profile for site one

From the above longitudinal profile data of terrain data of study area in Arc-GIS;- the following parameter were computed as; reach length, elevation and slope can be estimated as; Reach length (m) = **56.663km**, elevation (m) = 1539-1289.6 = **249.3m** and slope (%) = elevation/reach length =249.3/56663 = **0.0044.**

Longitudinal profile for site two and site three can be available at annex 1 and 2. And reach length, slope and Muskingum parameter K and X estimated using equation 4.8 and 4.9 for site one, site two and site three tabulated as follows;

Table 7: Muskingum parameter of selected site

Sites	Reach length (m)	Slope (%)	Roughness (n)	K(hr)	X(dimensionless)
Site one	56663	0.0044	0.0484	**2.22**	**0.40**
Site two	55975	0.00445	0.0484	**2.18**	**0.38**
Site three	53982	0.0046	0.0484	**2.08**	**0.36**

The study used the above Muskingum parameters (K and X) and inflow data of Wonji Station as an input data to determine the flow data at the target sites in HEC-HMS 4.10. The Muskingum parameter X when calculated using equation 4.9 is around 0.49 for all sites. But with value the warning note from HEC-HMS software showed that the routing is unstable. Therefore, the study calibrated parameter X to stable Muskingum routing and found the above allowable tabulated weighting factors values.

To transfer inflow data from upstream (i.e. gauged site) to downstream (i.e. ungauged site) using HEC-HMS 4.10 modeling software can be shown in flow chart below as;-

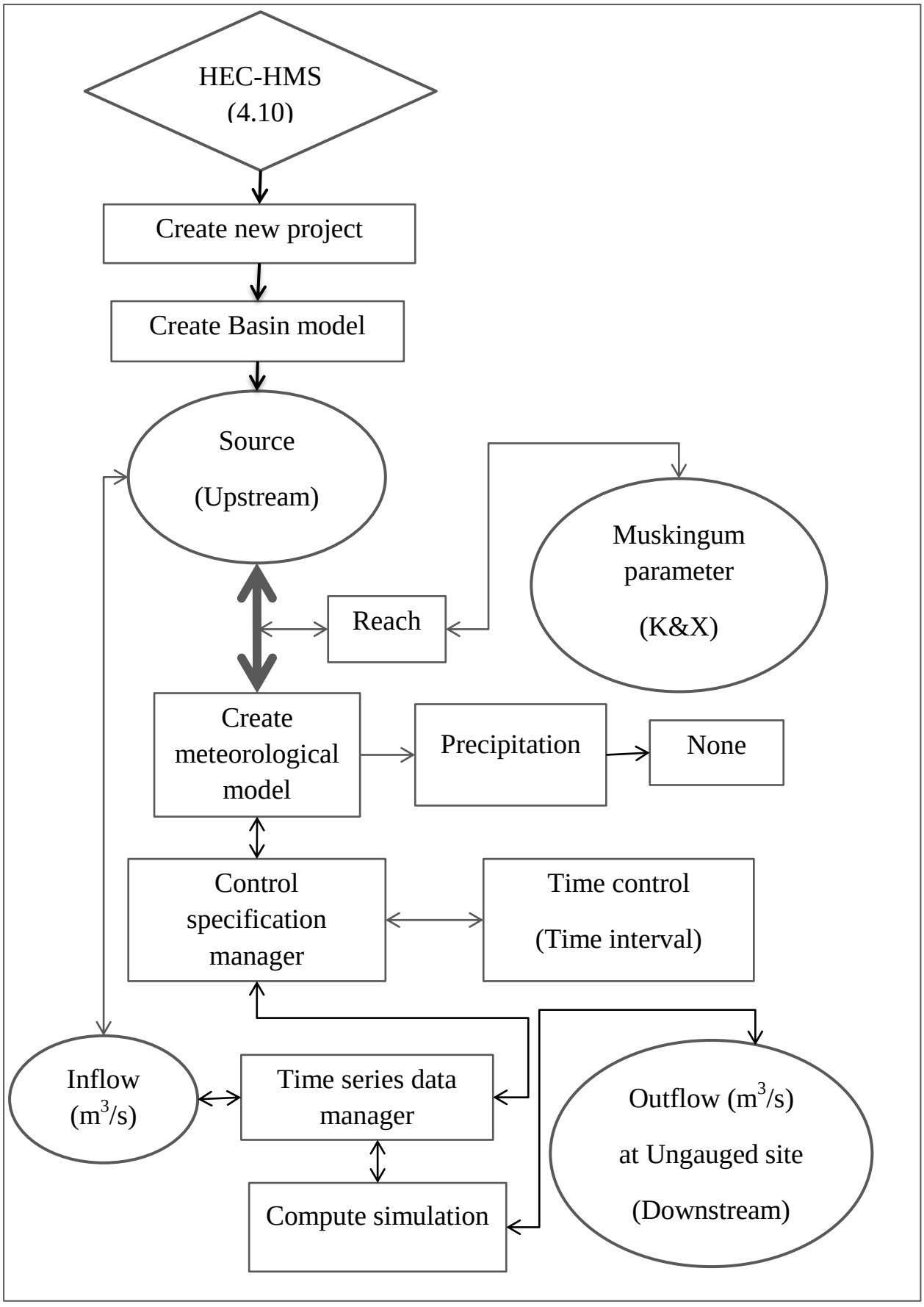

Figure 10: Schematic representation channel routing in HEC-HMS 4.10

3.5. Checking Consistency

A time series of hydrological data may exhibit jumps and trends called inconsistency and non-homogeneity (Yevjevich & Jeng, 1969; Cited by Aliyu, 2018). Inconsistency is a change in the amount of systematic error associated with the recording of data. The study were used a double mass curve technique to test the consistency of stream flow records of three selected site. It is used to check the consistency of many kinds of hydrologic data by comparing data for a single station with that of a pattern composed of the data from several other stations in the area (Mehari, 2017). The Double Mass Curve drawn cumulative annual flows of site one, site two and site three in y-axis and cumulative group stations (Metahata, Wonji, below koka dam, Awash melkasedi and Awash 7kilo) for each selected site drawn in x-axis as follows; annual flow data of selected site and surrounding station available at annex 12&13.

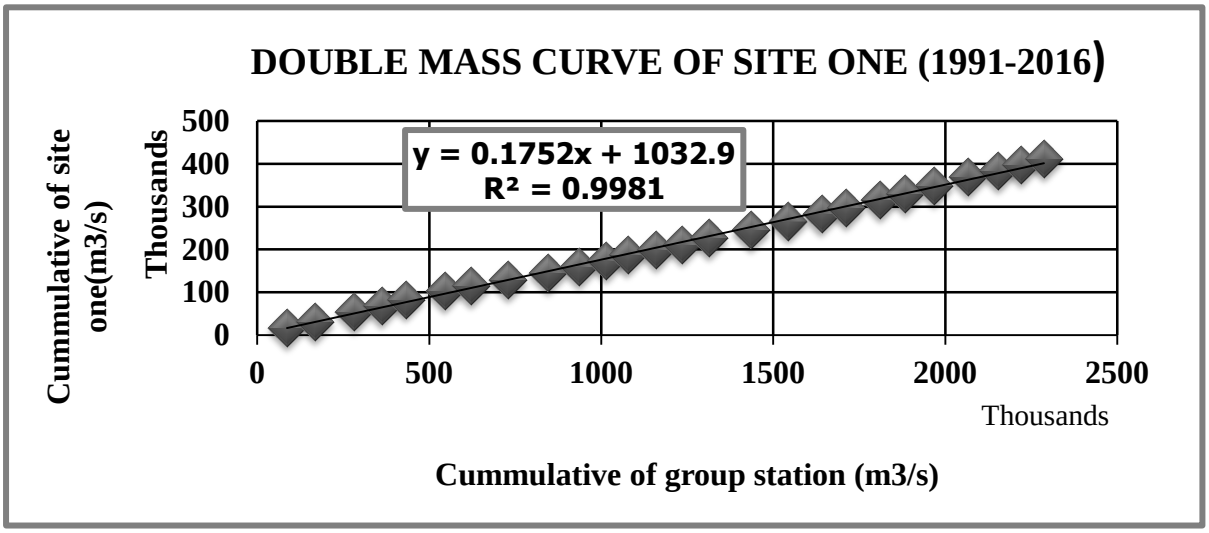

Figure 4: Double mass curve of site one

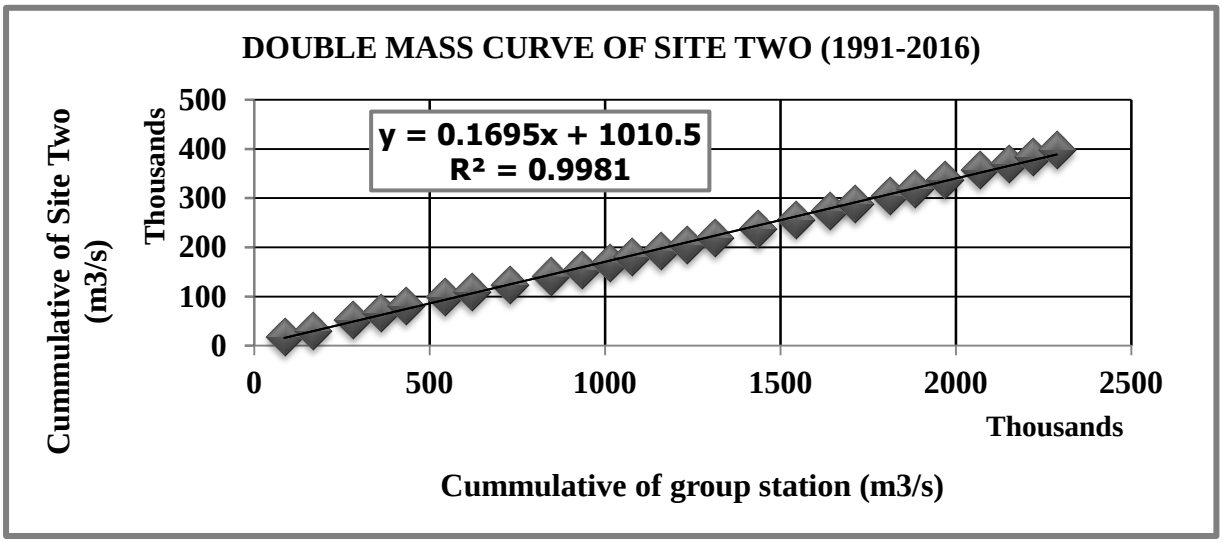

Figure 5: Double mass curve of site two

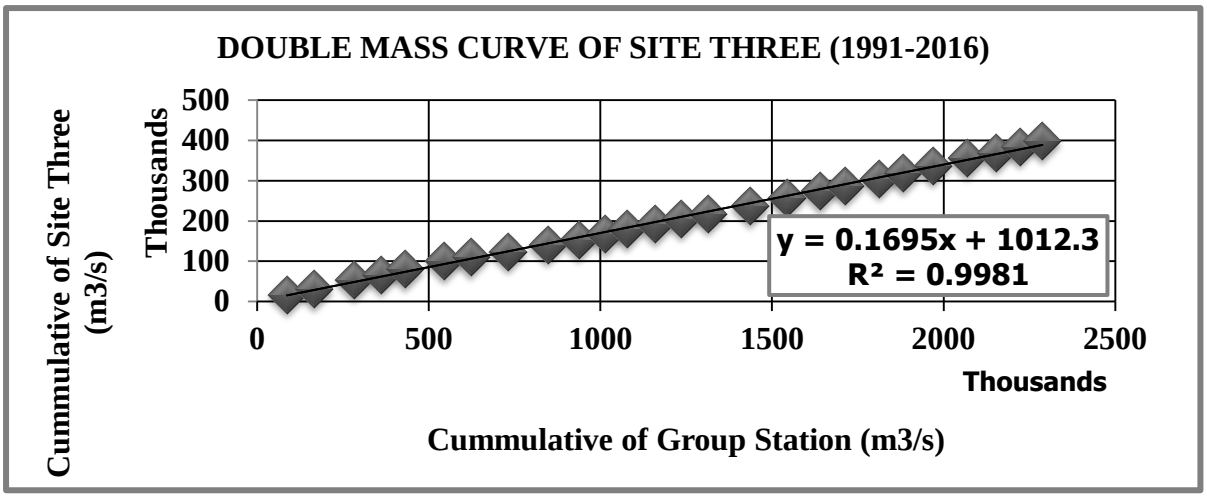

Figure 6: Double mass curve of site three

3.5.1. Homogeneity test

Homogeneity is an important issue to detect the variability of the data. In general, when the data is homogeneous, it means that the measurements of the data are taken at a time with the same instruments and environments (David, 1998). The study used one of popularly known Rainbow software. Rainbow is a software package for hydro meteorological frequency analysis and testing the homogeneity of historical data sets. It was used for checking the homogeneity of rainfall and flow data. RAINBOW homogeneity test is based on the cumulative deviations from the mean (Aliyu, 2018). The homogeneity of the data of a time series is tested by evaluating the maximum and the range of the cumulative deviations from the mean. In this study the stream flow of selected sites were homogeneous at 90%, 95% and 99% probability as shown in figures (14, 15 and16); annual flow data available at annex 13.

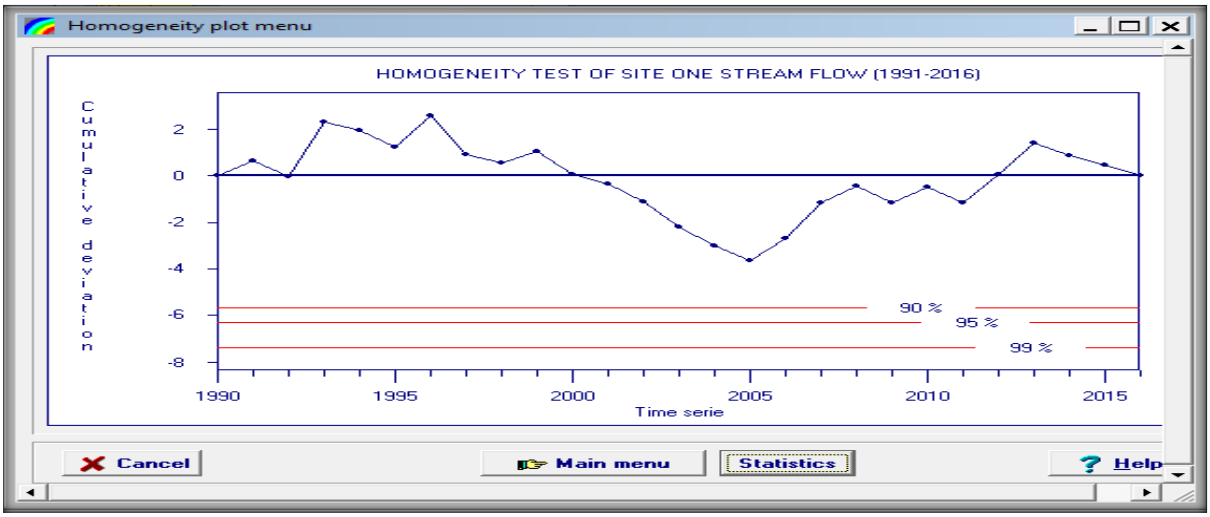

Figure 7: Site one stream flow homogeneity test

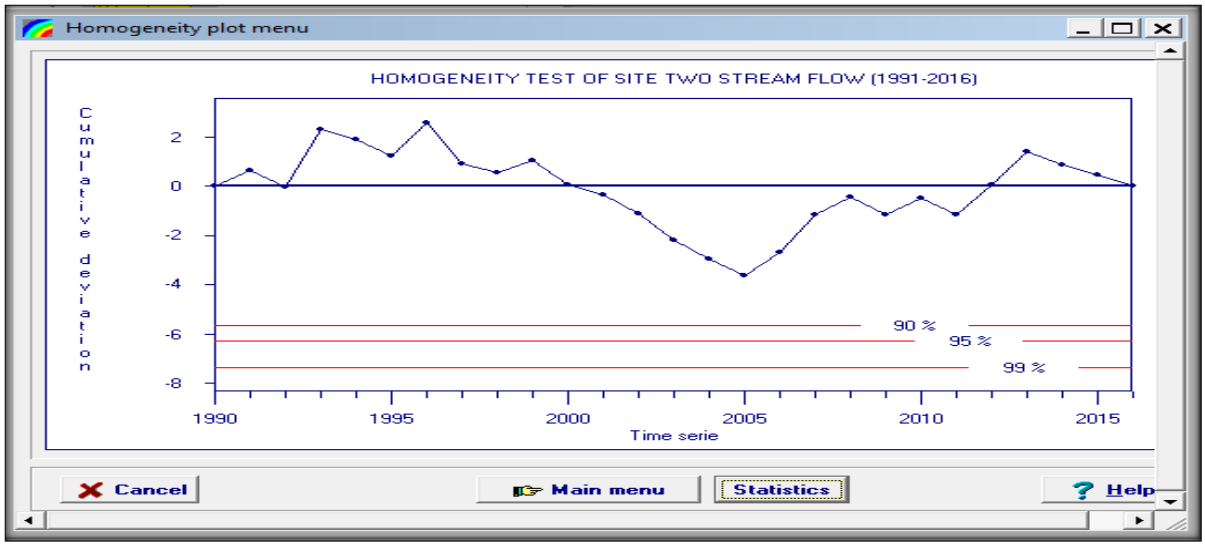

Figure 8: Site two stream flow homogeneity test

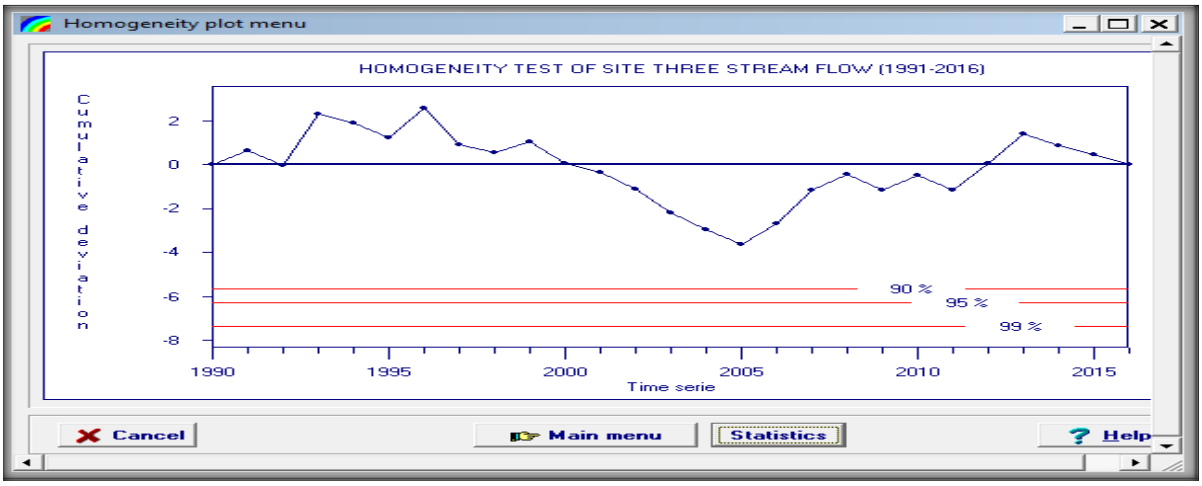

Figure 9: Site three stream flow homogeneity test

3.6. Graphical representation of the average yearly flow data

Trend of time series analysis is widely used to forecast logistics, production or other business process. Usually you want to understand if there is a trend or seasonality in the time series. This could support forecasting and planning. However, there are different approaches to understanding trend (Getnet, 2019). While trend often refers to historical changes of data and to verify the trend of the time series of yearly flow data plotted as shown below.

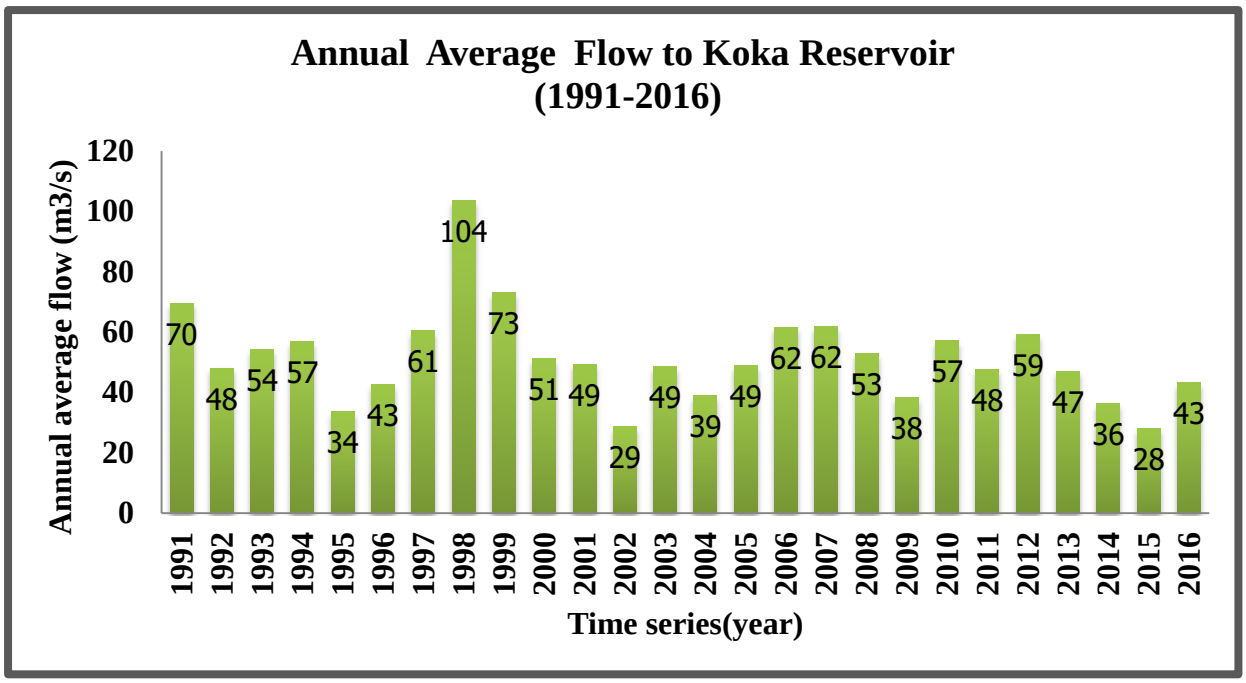

Figure 10: Annual average flow distribution to Koka reservoir

The flow data to Koka reservoir estimated by adding (1991-2016) year flow of Mojo river station and the routed Hombole river station (i.e. routing of hombole river station were done using the same procedure as selected sites routed in sub title 3.4). The annual average flow pattern at immediate downstream of Koka reservoir can be shown in figure as follows;

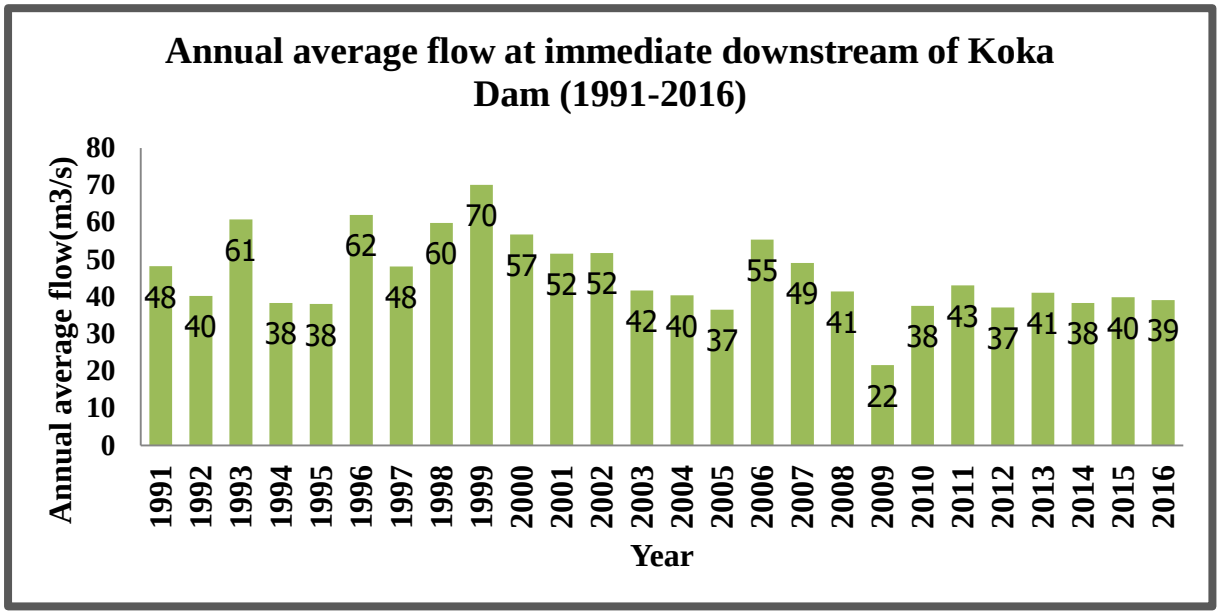

Figure 11: Annual average flow distribution at the downstream of Koka Dam

Wonji river station located near to downstream of Koka dam station (about 5km distance) and as shown in the figure they have more or less similar flow distribution. Wonji river station is the only station located upstream of selected sites.

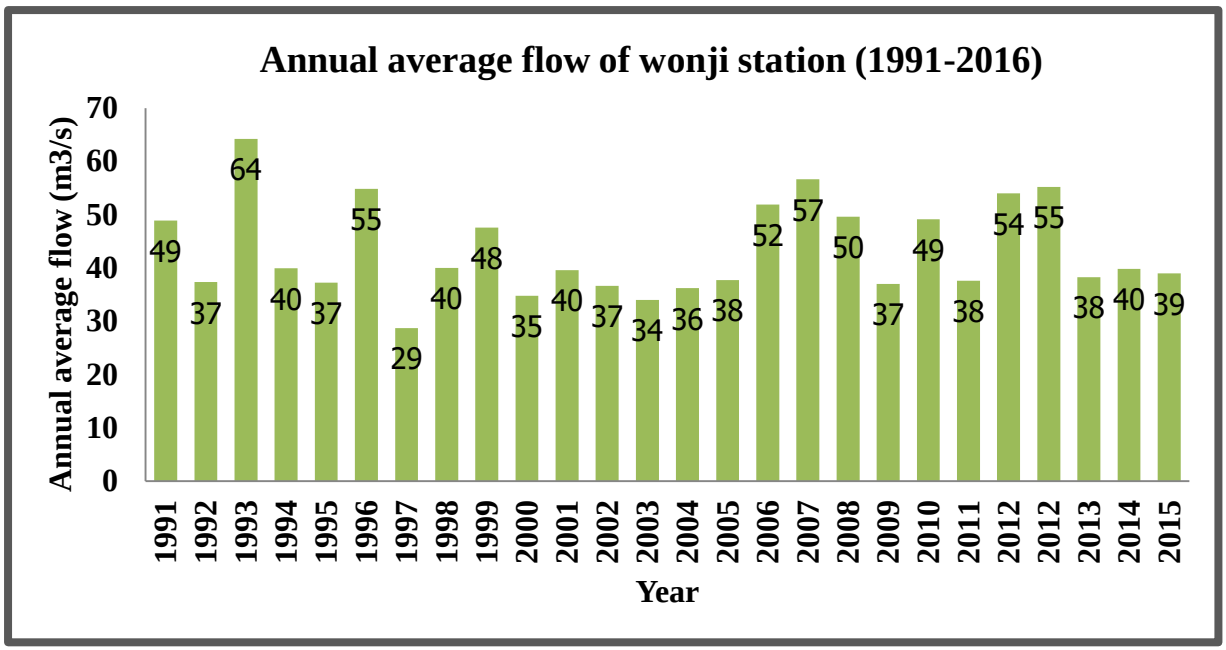

Figure 12: Wonji Station yearly flow distribution

The variation of stream flow to Koka reservoir, downstream of koka dam, Wonji river station, selected sites, Awash 7killo and flow to Awash melka saddi can be seen in the figure below.

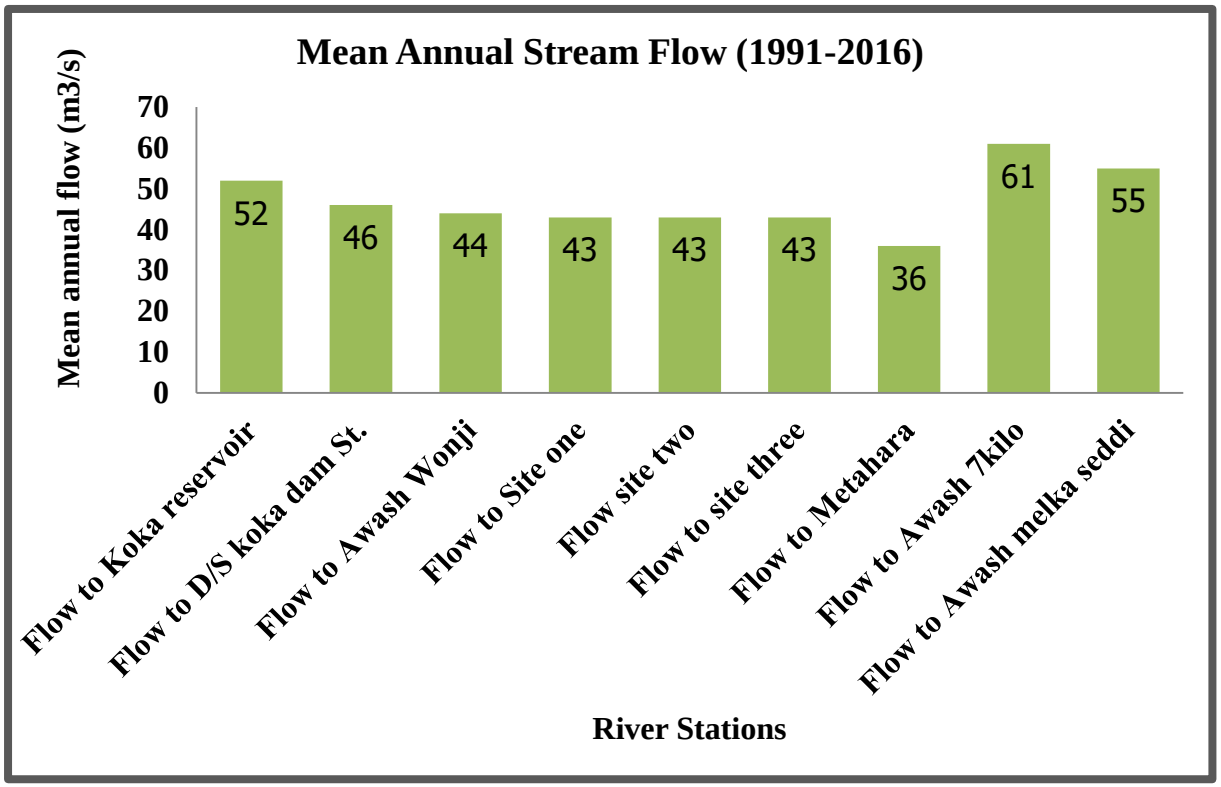

Figure 20: Mean annual stream flow of selected sites and surrounding river stations

3.7. Developing Flow duration curve

After making the flow data statistically significant and ready for further analysis, one of stream flow behavior indicators, which is flow duration curve for each target location were done using the following method. The basic time unit used in preparing a flow duration curve greatly affects its appearance. When mean daily discharges are used, a steep curve is obtained as the flow duration curve. When the mean flow over a long period is used mean monthly flow, the resulting curve will be flatter due to averaging of short term peaks with intervening smaller flows during a month. FDC is a curve with probability of exceedance (%) on the x - axis and the flow rate (m3/s) on the y - axis, which provides information on the probability of a specific flow being equalled or exceeded (Copestake and Young, 2002; Tallaksen and Van Lanen, 2004). The steps to draw flow duration curve from available to monthly average discharge data are listed below (Getenet, 2019)

Step 1: Transfer or input the mean monthly flow measurement data in to excel

Step 2: Compute the total number of months in the period of record

Step 3: Sort flow data according to magnitude and assign ranks. Highlight all of the data and select the sort command to rank data by flow from largest to smallest. Create a new column and assign each discharge value. Use the excel auto-fill feature to generate a list of rank numbers down to the last discharge row.

Step 4: Compute exceeded probability (p) for flow in each line of data by using the formula provided below. Apply the formula to all flows and calculate all the exceeded probabilities by copying the formula down the column to the last ranked discharge row and the percentage probability of any flow magnitude Q being equaled or exceeded is given as:

$$P = \frac{100m}{n+1} \quad \ldots\ldots 5.0$$

Where, P: Probability that a given flow will be equaled or exceeded (% of time), m: Ranked position on the listing (dimensionless) n: number of events for period of record (dimension less). The mean monthly flow of routing river station (i.e. Wonji river station used as inflow value for Muskingum routing in HEC-HMS 4.10) to get flow values of selected sites. Flow data is available at (Annex: 3, 4, 5 and 6).

3.8. Head Measurement

The head is the difference between the head of the full supply level and the head of tail water level. The head at which the waterfall was measured by total station tracking the coordinate's value from the selected site for the upstream side and downstream of the site. The minimum distance between two consecutive sites should not be less than 500 m. This will ensure that there is sufficient gap between the tailrace of one site and the diversion arrangement of the next, so that the river ecosystem will have sufficient opportunity to rejuvenate. This will also ensure that the tailrace of the upstream site is not influenced by the reservoir/pondage of the downstream site and the maximum distance of river considered to find the head should not be more than 3000 m (Kusre et al. 2010). The gross head is determined by surveying or using GIS equipment with respective spatial data.

3.9. Developing Theoretical power

Concisely and within hydrological context, it involves the determination of the technologically feasible limits of the gross hydropower potential of the studied river. By definition, gross hydro potential is the theoretical optimum limits of hydroelectricity production of any river which represents the potential that possible feasible fall and flow within the river constitutes. Conceptually gross hydropower potential is proportional to the product of gross head and discharge which can determined a useful way of treating time variability of water discharge in the existed small-scale hydropower generation. It is a curve which is connected by arranging the monthly power value in descending order and follow the same procedure in case of flow duration curves (Getnet, 2019; Mehari, 2017).

Theoretical power is the power that is available at a given location without considering any losses. It is as a function of available water flow in cubic meter per second (m^3/s) and the vertical head in meters (m) and unit weight of water (Singh, 2009).

$$P = Q * H * 9.81(Kw) \quad \text{.....5.1}$$

Where, P: Power at the generator terminal, in kilowatts (kW), H: The gross head from the pipe line intake to the tail water in meter (m) Q : Flow in pipe line, in cubic meters per second (m^3/s) 9.81 is a constant and is the product of the density of water and the acceleration due to gravity (g).

Depending on the available head and water flow, different turbine configurations may be used to achieve maximum generation. Pelton, turgo and crossflow are impulse turbines best

suited for high and medium available head. For medium and low available head reaction turbines such as Francis, propeller and Kalpan are most appropriate (Okot, 2013; Cobb & Sharp, 2013).

3.10. Developing Technical power potential

Due to physical and technical reasons hydropower plants can not able to fully use theoretical power potential and technical potential of hydropower describes the energy capacity that is actually usable when technical, infrastructural and other consideration. In this study the technical hydropower potential is calculated for each selected site by estimating total system efficiency losses considering each specific loss at each site (Rajput, 2008). Technical power is the power that is actually usable power and is consider physical and technical issues that lower the gross theoretical power of the given plant. It includes conveyance and overall efficiency of generator and turbine efficiency. For small scale hydro power plant overall efficiency is between 75-80% (Getnet, 2019; Mehari, 2017). This study took (77.5%) average values for overall efficiency. Therefore, power output is obtained after all losses are considered.

P_{out} = power input ×overall efficiency……5.2

P_{out} = 0.775×power input……5.3

3.11. Developing Annual energy

The pattern of annual energy demand of a country can be seen from the energy curve. The annual energy mostly used for planning, allocation the resource and to know the demands of the total population. The energy demands of the study area developed by multiplying technically available power with the number of hours per year (Getnet, 2019).

$$\text{Annual energy (E)} = \text{technical power} * 8760\text{hr} \quad \text{……5.4}$$

The annual energy curve developed using the same procedure as flow duration and power curve developed, but the only thing is multiplying technical power with total hours in a year (i.e. 1year = 365*24hr is equals 8760hr).

3.12. Prediction of Dependable and plant capacity

The only problem often counter in hydropower development has been how to determine the potential capacity of the proposed site because the hydropower potential is limited by the

intermittent nature of river flows, which have high water discharge during rainy and low discharge in dry season. Therefore, the study of maximum flow is very important from the point of design or installed capacity; the average flow is important for the consideration of energy output and minimum flow is required to predict dependable capacity. The selection of design flow depends on the available flow of the site, for run of river projects; design flow is usually the flow is about 30% (Q_{30}) of the time (Getenet, 2019).

The minimum flows are required to predict dependable or firm plant capacity. For computation of water availability, long time series river flow data should be collected. The firm flow of rivers is specified from flow duration curve usually selected by users between 90 % and 100% (Adedoken, 2013).

A hydropower station generates firm power for consumer needs with a firm power for consumer needs with a firm flow that guarantee a consumer a highly dependable electric energy supply at the very driest season of the year. Accordingly, the dependability of flow for an isolated hydropower station is must be greater than 90%. However, the installed capacity of a hydropower station is always greater than the firm power to utilized seasonal hydro energy when the additional flow is coming during rainy reason to meet maximum power generation (Getenet , 2019). The study accepted the design flow at 30% (Q_{30}) and firm flow of the river at 95% (Q_{95}). This flows used to determine the installed capacity of the plant and the flow at driest period of the year.

$$P_{ins}=7.603\times Q_{30}\times H\ (kW) \quad \ldots\ldots 5.5$$

$$P_{dep} = 7.603\times Q_{95}\times H\ (kW) \quad \ldots\ldots 5.6$$

Where, 7.603 is overall efficiency multiplied by acceleration due to gravity, Q_{30}, Q_{95} are design flow and firm flow, Pins and Pdep are installed and dependable power.

3.13. Selecting Suitable Site Using Analytic Hierarchy Process (AHP)

The analytic hierarchy process is a mathematical device in multi-criteria decision making which designing the decision factors in a hierarchic problem structure (Saaty, 1990). The main target of the AHP is to decide and help decision makers in making resolutions for the complex problems by structuring the criterion hierarchy of Multi-criteria decision making. AHP main strength is its ability to structure a problem and then relate both tangible/intangible

factors in a common framework. In the pairwise comparison AHP method, criteria and alternatives are presented in pairs of one or more referees (e.g. experts or decision makers), (Rajnish and Jayant, 2014). Application of AHP to decision making involves four steps (Kshitij et al., 2015):-

1) Structuring of the decision problem into a hierarchical model.
2) Making pair-wise comparisons of criteria and obtaining the matrix.
3) Making pair-wise comparison for alternatives and obtaining matrix.
4) Aggregation of all priorities.

The analytic hierarchy process (AHP) needs criteria or decision problem as the first input criteria for further analysis. This research has selected eight Criterions that determine the selection of suitable and cost effective site. Based on experience and knowledge on the area of study to get suitable hydropower site; the study used the following demanding criteria. These selected criteria sorted based on their relative importance and suitability for hydropower development;-

Power: power is the final output of a given RoR hydropower scheme. It the combination all factor that affect the output result. The flow to rotate the turbine, the head to create the potential, the structure to facilitate, good management and other influencing criteria determine the final output. Mean annual power of each hydropower site was considered as the first weighted comparison criterion to evaluate feasible hydropower sites.

Discharge: discharge is one of the most important criteria that determine the selection of potential hydropower site. The study selected discharge as the second influencing parameter that determines the existence of the plant. ROR hydropower generates electric power as and when water is available in the river.

Head: if we have discharge, we need head to create potential difference to do the work in producing the electric power. Therefore, head was taken as one of high weighted comparison criterion parameters to evaluate the suitability of the RoR hydropower sites.

Road Accessibility: the accessibility of the road determines the cost of the plant and time of implementing the scheme. If the site is good in terms of discharge and head and not accessible, it needs an investment to construct the road and it consume its own time to construct the road. But in our case the sites are accessible on foot as well as at any transport.

Geology: the geology of the site determines the stability of the project, the cost of the project as well as generally determines the life of the project. According to world geologic map and study conducted by EELPA (1964) the geology of the study area comprises quaternary undivided (Q), quaternary extrusive and intrusive rocks (Qv), and tertiary extrusive and intrusive rocks (Ti). The specific location of the study area is rich in tertiary extrusive and intrusive rocks, which are igneous intrusive and extrusive rocks and known by its soundness for foundation.

Soil: soil is one of the construction material, it influence the cost the project as well as the stability of the project. According to FAO soil map and study effected by Upper Awash Sub Basin Integrated Land Use Planning Study (OWWDSE, 2014) the study area comprises clay, sandy clay, loam, silt loam and clay loamy.

Gorge: Narrow gorge more preferable than wide gorge for construction of structure on it. Narrow gorge directs the flow to the targeted location. The spatial analysis of the study area terrain at selected site indicates that the topography was endowed by gorges and valley shape.

Distance from nearby town: Long distance consumes more time to transport construction materials and also require long power transmission line to supply electric energy for residential, industries and different institution. So, the farthest site consumes more budgets. The distance between towns and the selected hydropower sites in this study were measured using real site KML shape file (i.e. using Google earth) and ArcGIS 10.41 tool and the length of distance from end users to the feasible site was considered as one of prioritization factor to select the best suitable site.

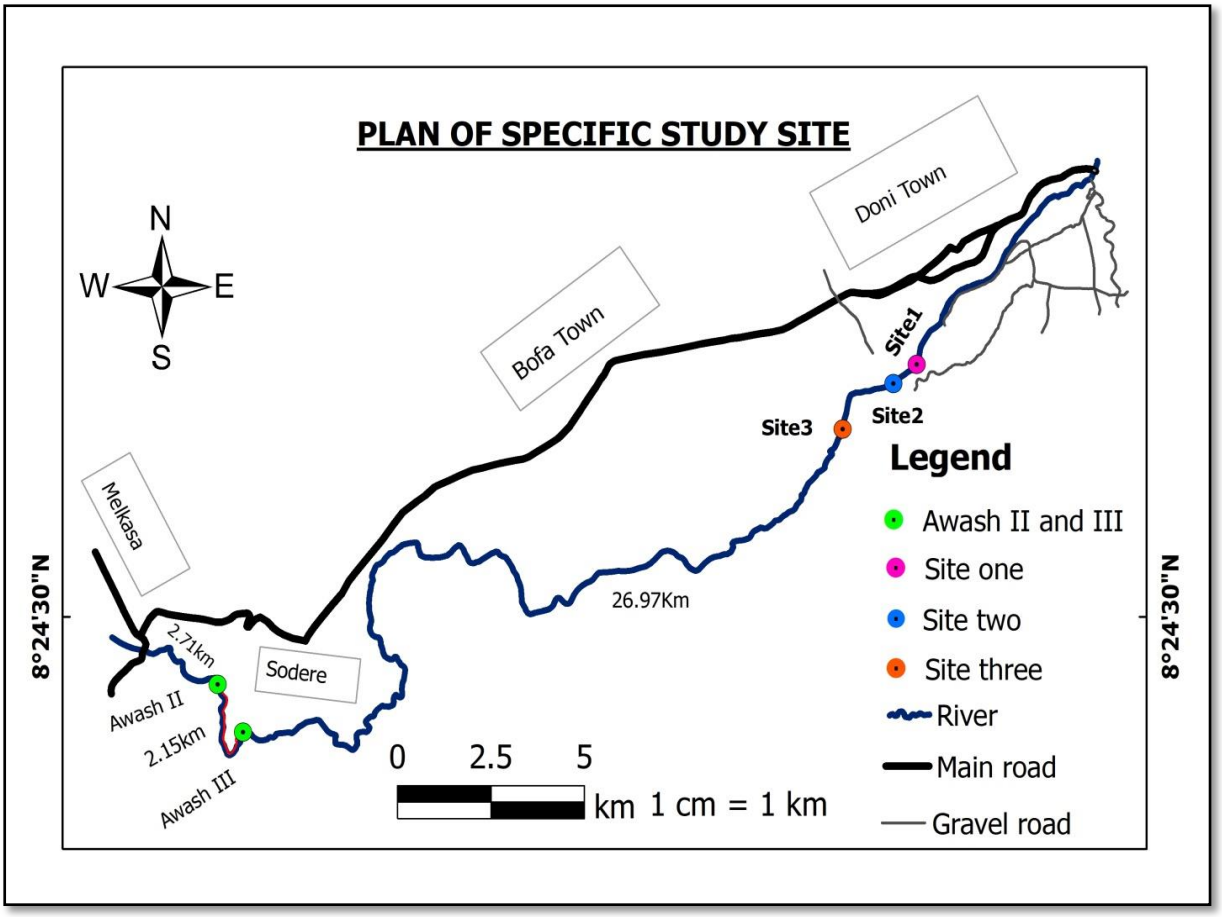

Figure 21: Plan of specific study sites

To give the order of best operating site from all selected hydropower sites in the study area; the requirement of suitability estimated based on the judgments given numerical values for each selected site. The main reason of selecting appropriate site for hydropower plant development and ranking these sites according to comparison criteria is to facilitate a way of favorable condition for determining the best hydropower site. The selected site has to be economically feasible for future project implementation. The ranking procedure in the study considers eight main criteria that directly affect the hydropower potential site selection and safety issue. These selected criteria sorted based on their influence to the suitability of hydropower plant implementation in proposed site.

3.13.1. Criteria of weighting

For this analysis, factors selected to evaluate the hydropower sites, are standardized using the pair wise comparison method. In the process, each factor is rated for its importance relative to every other factor using a 9 point reciprocal. This leads to generate n×n matrix of rating where n the number of factors being considered.

Table 8: pairwise comparison scale for AHP preference (Saaty and Windi, 1980; Saaty, 2008)

Rank of importance	Definition	Explanation
1	Equal importance	Two activities contribute equally to the objective
3	Weak importance of one over another	Experience and judgment slightly favor one Activity over another
5	Essential or strong importance	Experience and judgment strongly favor one activity over another
7	Demonstrated importance	An activity is strongly favored and its Dominance demonstrated in practice
9	Absolute importance	the evidence favoring one activity over another is of the highest possible order Of affirmation
2,4,6,8	Intermediate values between the two adjacent judgments	When compromise is needed

3.13.2. Pair-wise comparisons

Pair wise comparison of alternative and criteria can be seen from the following diagram to decide the judgment value for making upper and lower triangular matrix.

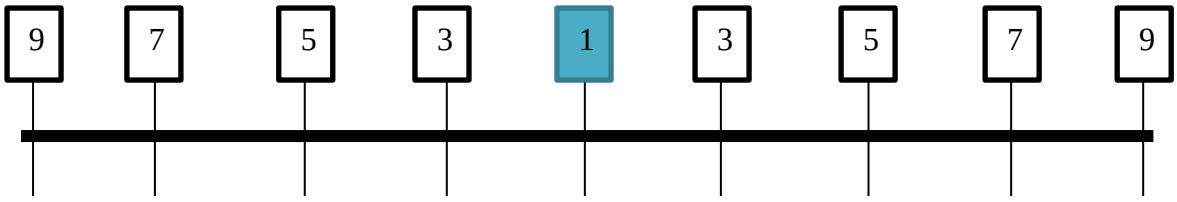

Figure 13: Intense of relative importance between two alternatives and criterion

The diagonal elements of the matrix are always 1 and we only need to fill up the upper triangular matrix. To fill up the upper triangular matrix the following rules could be used:

A. If the judgment value is on the left side of 1, we put the actual judgment value.
B. If the judgment value is on the right side of 1, we put the reciprocal value.

Pairwise comparison is comparing each criterion in pair. To check whether one criterion slightly, strongly, very strongly and extremely important over another or either criterion equally important AHP is used the standard scale number (i.e. 1 to 9). By comparing each criterion in pair we can make a comparison matrix as follows (Saaty, 1980).

3.14. Consistency analysis in Analytic Hierarchy Process (AHP)

Impeccable consistency rarely occurs in practice. In the AHP the pairwise comparisons in a judgment matrix are considered to be adequately consistent if the corresponding consistency ratio (CR) is less than 10% (Saaty, 1980). If the Consistency Ratio is greater than 10%, we need to revise the subjective judgment. To check consistency of judgment first we need to find consistency index as:

$$\text{Consistency index(CI)} = \frac{\lambda_{max} - n}{n-1} \quad \ldots\ldots\ldots\ldots\ldots\ldots\ldots\ldots\ldots\ldots\ldots\ldots\ldots\ldots\ldots\ldots 5.7$$

Where, λmax is the largest principal eigenvalue of a positive reciprocal pairwise comparison matrix of size n, where n is number of criteria, which is 8. λmax = (sum of elements in priority vector)*(sum of each criteria values)

Priority vector $\mathbf{(W_{ij})} = \frac{\sum_{i=1}^{n} X_{ij}}{n}$ **,** where, $\sum_{i=1}^{n} X_{ij}$ is normalized matrix column sum and n is number of criteria.

Normalized matrix $\mathbf{(X_{ij})} = \frac{C_{ij}}{\sum_{i=1}^{n} C_{ij}}$ **,** where, C_{ij} is criteria values in pairwise comparison matrix and $\sum_{i=1}^{n} C_{ij}$ is column sum of pairwise comparison matrix.

Generally, AHP hierarchy method follows the following representative flow chart to select the best suitable site. The figure 23 depicts that the study used 8 criteria based on their influence to determine feasible scheme for the run of the river hydropower. To choose the best site; each criterion made pairwise comparison to know their relative weight to select from alternatives. Then after, using the weight each criterion and qualitative and quantitative value of each site; the pairwise comparison made between each alternatives to get the most suitable site.

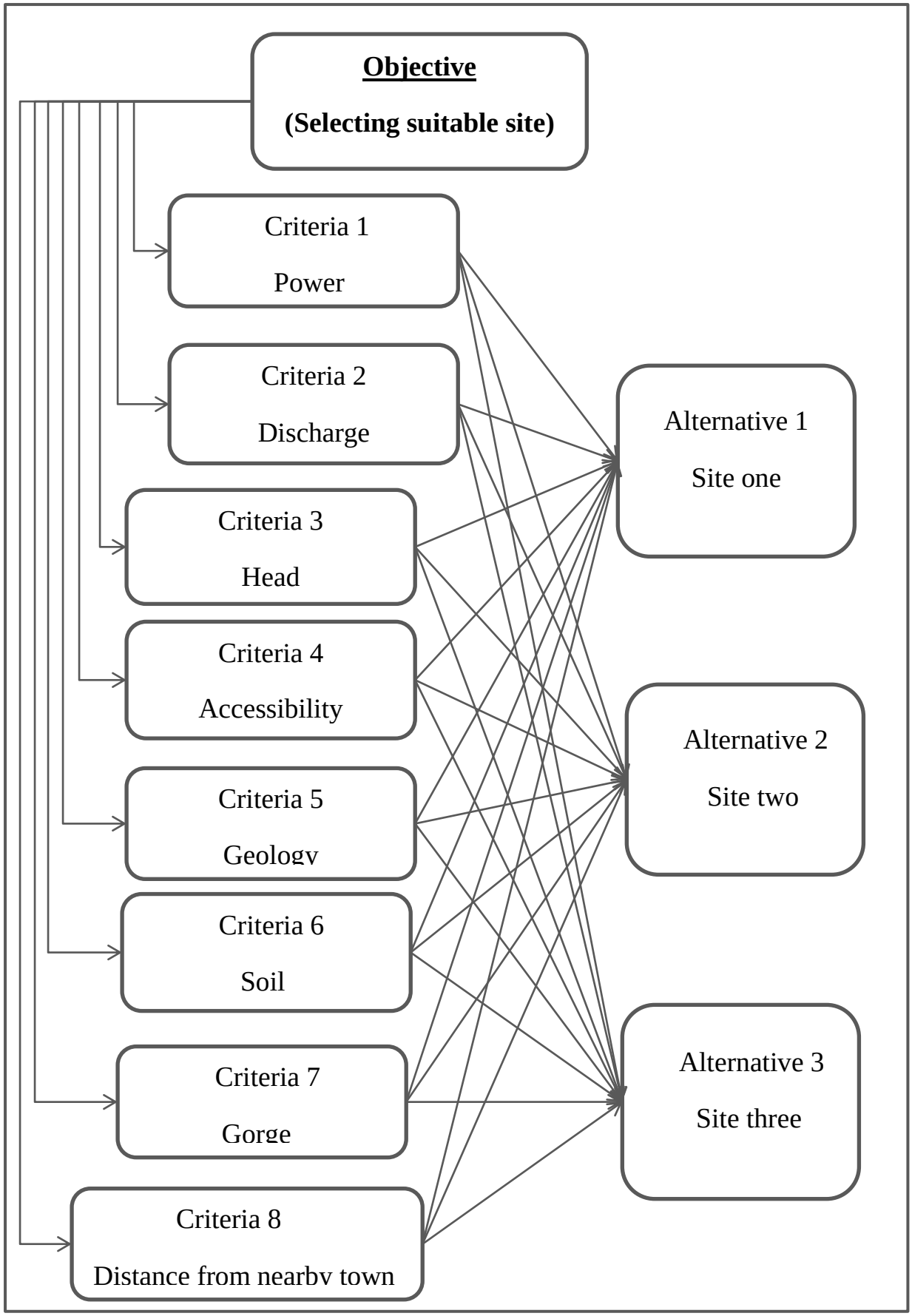

Figure 23: Typical AHP hierarchy

3.15. Selection of frequency distribution

The choice of distribution is influenced by many factors, such as methods of discrimination between distributions, methods of estimation parameters, the availability of data, etc. Generally, there is no general global agreement as to a preferable technique of model choice and no single one distribution accepted universally (Yaynshet, 2020). For example, Log Pearson type II distribution was recommended by U.S. Water Resource council (1967) for USA, General Extreme Value (GEV) distribution was recommended by the Natural Environmental Research council. (NERC, 1975) for U.K. and Ireland, Pearson type III was selected by the institute of Engineers in Australia etc. In general the chosen distribution should be widely accepted, simple and convenient to apply, consistent, flexible or robust (low sensibility to outliers), theoretically well based (established) and documented in the Guide (WMO) or elsewhere (Cunnane, 1989).

Based on their popularity, acceptance by statistical test and suitability for different region of the world; the study used Gumbel and log-pearson type three distribution. The best suitable distributions selected using easy fit software and importance of the project. Finally the selected distribution dedicated to forecast the flood event of specific study area.

3.15.1. Log -Pearson Type III distribution

Log pearson type III distribution is suitable for both the annual non extreme series and the extreme flood frequency analysis. The recommended technique for fitting a log Pearson Type III distribution to observe the annual peaks is to compute the base 10 logarithms of stream flow and water depth at selected probability, P, by the following equation (Phien and Ajirajah, 1984)

$$\log X_T = \overline{X} + K * S \quad \text{.....5.7}$$

$$X_T = \text{antilog}(\log X_T) \quad \text{.....5.8}$$

Where, X_T= stream flow and water depth for selected return period, $\overline{X}$ = mean logarithm, $\sum_{i=1}^{n} \frac{\log X_i}{n}$, and n is number of sample, Xi is stream flow and water depth to be forecasted

S= standard deviation of the logarithm, $\sqrt{\sum_{i=1}^{n}\left(\frac{\log Xi-\log \bar{X}}{n-1}\right)^2}$, K = a factor that is a function of the skew coefficient (G) and desired recurrence interval or selected probability (annex 7). G = skew coefficient of logarithm, $\frac{n\sum_{i=1}^{n}(\log Xi-\log \overline{Xi})^3}{(n-1)(n-2)S^3}$

3.15.2. Gumbel distribution

It is one of the most widely used probability function for extreme values in hydrologic and meteorological studies for prediction of flood peak, maximum water depth, maximum rainfalls, maximum wind speed, etc (Mayank, 2020).

The following steps are necessary to apply the Gumbel Method:

$X_T = \overline{X} + K_T * S$……5.9

Where, X_T = design food for certain return period ($\frac{m^3}{s}$), $\overline{X}$ = the mean stream flows ($\frac{m^3}{s}$), S= standard deviation of stream flow ($\frac{m^3}{s}$) and K_T = the frequency factor for a return period

$K_T = \frac{Y_T - Y_n}{S_n}$……5.8

Where,Yn = reduced mean, it is a function of sample size n only, S_n = reduced standard deviation Which, is also a function of sample size only and Value of Yn and S_n as a function of sample size can be available at (annex 8&9) and YT is reduced variate given by: $Y_T = -\ln(-\ln\left(1-\frac{1}{T}\right))$. Annual maximum flow data of selected sites are available at annex.13.

3.16. Fitness of Distribution

Easy Fit software is a data analyzer and simulation software which allows to fit probabilistic distributions to given data samples, simulate them, choose the best fitting probability distribution and implement the results of analysis to take better decisions (Pakgohar, 2014). To validate the specified probability distribution function the software is uses several methods. Among the methods this study discussed about the following:-

3.16.1. Kolmogorov–Smirnov (K–S)

Kolmogorov-Smirnov (K-S) test measures the greatest discrepancy between the observed and hypothesized distribution. The process can be summarized as follows (Melo et al., 2009; Wang, Wang, 2010). The test statistic (D) is:

D=max|F_O (X)-F_e (x)|……6.1

Where, Fo(x) is the observed cumulative relative frequency and Fe(x) is the expected cumulative relative frequency.

3.16.2. Anderson–Darling (A–D)

Anderson-Darling test compares the fit of an observed cumulative distribution function to an expected cumulative distribution function. The A-D test is preferred, because it is a modification of the Kolmogorov-Smirnov (K-S) test and is the most powerful test available at present (Millington et al., 2011).

$$A^2 = \sum_{i=1}^{n}\left[(2i-1)\ln Fx(xi) + \ln\frac{[1-Fx(X_{n+1-i})]}{n}\right] n \ldots\ldots\ldots\ldots\ldots\ldots\ldots\ldots 6.0$$

Where, FX(xi) is the cdf (cumulative distribution function) of the projected distribution at xi , for i = 1,2,…,n. The annual maximum stream flow and annual maximum water depth data essentially ordered in ascending order, as x1 < x2 < ... < xn. The study used Anderson-Darling method, since it is the modification of Kolmogorov-Smirnov test. The best fit distribution from the candidate selected by comparing p value with test statistic. Where, P_{value} indicate the probability of the Null hypothesis to be true.

Table 9: Anderson-Darling P values formula for a given test statistics from easy fit software and sample size (n)

Anderson-Darling statistics	Formula for P value Calculation
AD≥0.6	exp(1.2934-5.709(AD^*)*(0.0186(AD^*)^2)
0.34<AD^*<0.6	exp(0.9177-4.279(AD^*)-1.38(AD^*)^2)
0.2<AD^*<0.34	1-exp(-8.318+42.796(AD^*)-59.938(AD^*)^2)
AD^*≤0.2	1-exp(-13.436+101.14(AD^*)-223.73(AD^*)^2)

$AD^* = AD * \left(1 + \frac{0.75}{n} + \frac{2.25}{n^2}\right)$; AD = $\sum_{i=1}^{n}\left[(2i-1)\ln Fx(xi) + \ln\frac{[1-Fx(X_{n+1-i})]}{n}\right] n$

Where, AD is test statistics from easy fit software and n is number of sample which is 26.

3.17. Hydraulic modeling with HEC-RAS

There are two main ways for specifying the inputs to build a hydraulic model in HEC-RAS. One is to do a physical survey of the study site, and collect data manually regarding the river geometry and the other way is to use geospatial datasets like DEM and Landsat image to develop the geometric data in GIS. This research were used the second choice due to shortage of cost, time and required materials. The main input parameters for hydraulic modeling in Hec-RAS;-

1) River geometric data
2) Flow data and
3) Boundary conditions

Steps in creating a hydraulic model with HEC-RAS are as follows:- starting a new project, entering geometric data, entering flow data and boundary conditions, editing geometric, flow data and performing the hydraulic calculations, and finally viewing the required result.

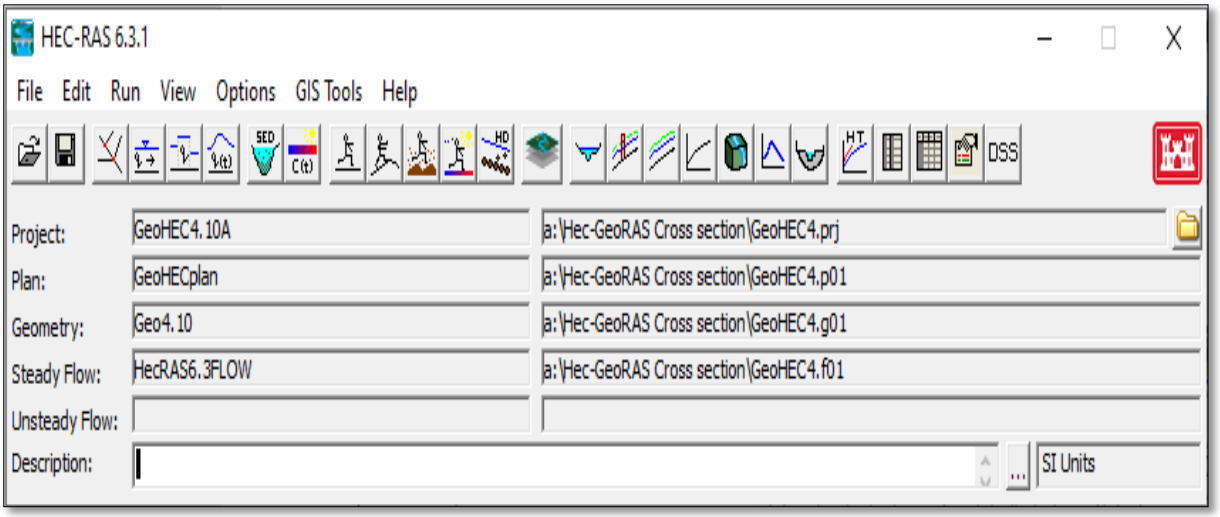

Figure 14: Saved project, plan, geometry, and flow data of the study

3.17.1. Cross section data

The first components to analyze hydraulic modeling is geometric data, to analyze stream flow, Hec-RAS represents a stream channel and flood plain as series of cross section along the channel. The study had used Digital Elevation Model (DEM) by converting into TIN (Triangulated Irregular Network) for spatial analysis of river geometry. Hec-GeoRAS is one of the intermediate models between ArcGIS and Hec-RAS for pre-processing of cross section data by assigning elevation data to shape files created in ArcGIS. To create cross section data in Hec-GeRAS the following steps has to be followed;-

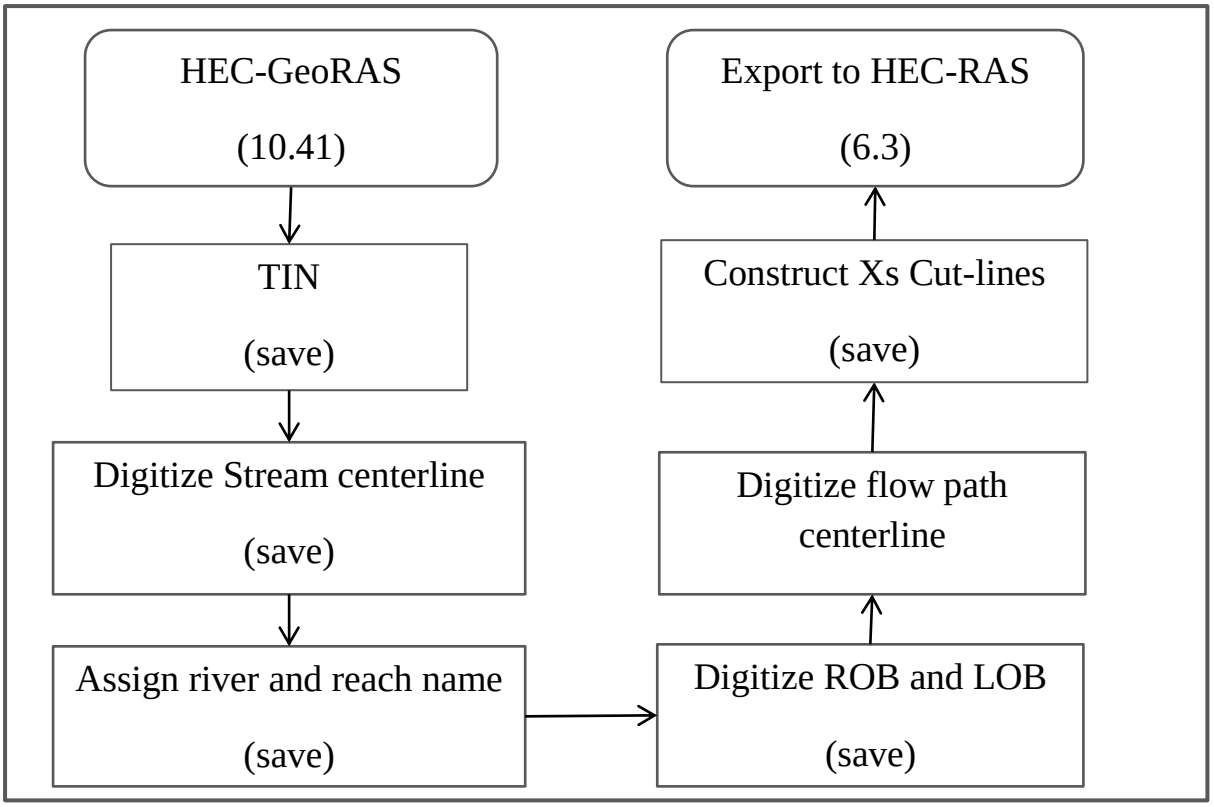

Figure 15: Schematic representation of cross section data preparation in Hec-GeoRAS

To prepare the cross section data the study took 150m for total width of the river by assuming that no flow of forecasted profile overflow from this boundary and 50m for cross section interval. To analyze the flood plain digitization of river station (RS) starts at 3.55km upstream of selected site and 26km downstream of Awash III. The selected site endowed with gorges and valley topography along the river.

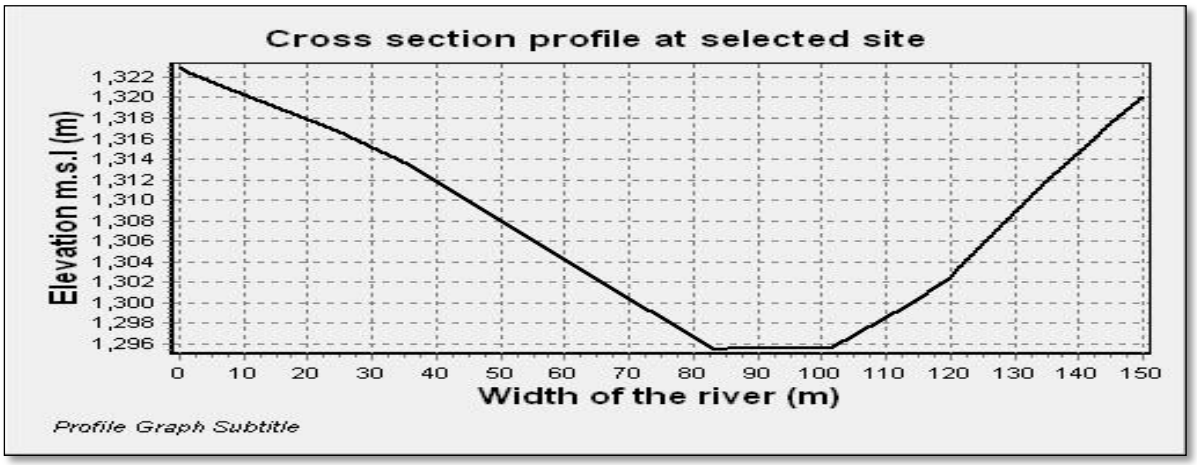

Figure 16: Cross section at site one

50m interval successive cross sections along 4.65km reach length (upstream to downstream) shown in the figure below:

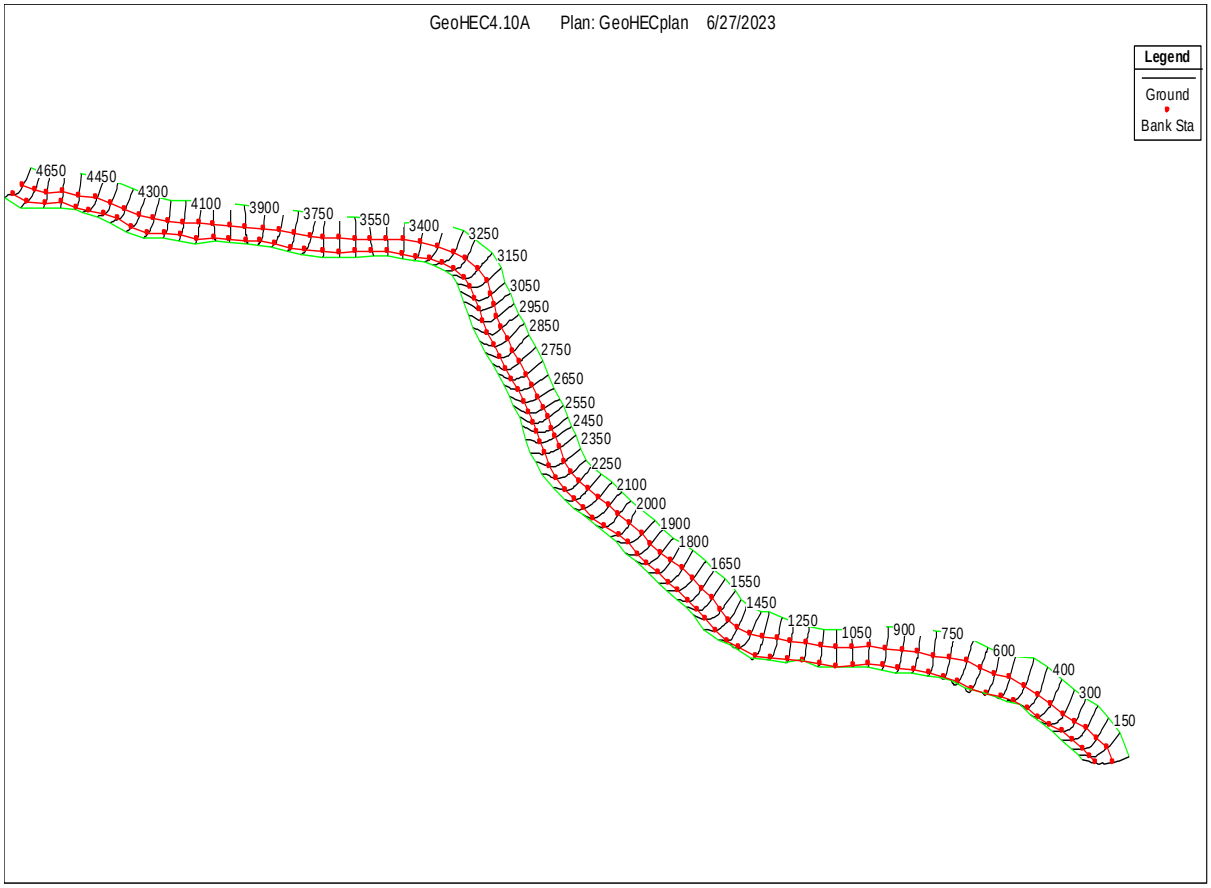

Figure 17: Perspective view of successive cross sections

3.17.2. Flow Data and Boundary Conditions

Boundary conditions were important inputs in hydraulic model for establish a starting water surface elevation and are required to establish a water surface elevation at the ends of all river reach. Then HEC-RAS can begin to perform hydraulic calculation. The study was used normal depth as a boundary condition due to available flow data and simplicity. Normal depth requires the energy slope or when this is not available the slope of the channel bottom. The slope of the channel bottom was obtained from terrain data (DEM) of the study area. Discharge information was other boundary condition that required at each cross section in order to compute the water surface profile. Flow data forecasting made using one of the best frequency distribution methods are Log-pearson type III or Gumbel-distribution for 2, 5, 10, 25, 50, 100 and 200year profile and are entered from upstream to downstream for all reaches.

3.17.3. Manning's coefficient (n)

The study considers different roughness coefficient values for channel, left bank and right bank and used cowan (1956) important factors that affect the best channel roughness values. To choose Cowan roughness value the study used GE high resolution image and LULC of

study area as bench mark and according to United State Geological Survey Water Supply (George et al., 1989) paper the following roughness value selected for LOB, channel and ROB, respectively as shown in table 10. The study assume the base roughness coefficient (nb) rock cut roughness values and add all the adjustment n values on it to be more reliable and smoothly approach to the real n values. The base of values of manning's n and adjustment values are based on the US Geological survey guide to select manning's coefficients for natural and flood plain which is available at (Annex, 10 and 11).

Table 10: Different roughness values for different land cover of study area

Items	Description	LOB		Channel		ROB	
		min	max	min	max	min	max
nb	Base value	0.025	0.025	0.025	0.025	0.025	0.025
n1	Degree of irregularity	0.0065	0.008	0.0055	0.0068	0.0075	0.01
n2	Variation of channel XS	0	0	0	0	0	0
n3	Effect of obstruction	0.0045	0.007	0.0048	0.0075	0.008	0.01
n4	Amount of vegetation	0.003	0.006	0.002	0.005	0.0085	0.01
m	Degree of meandering	1	1	1	1	1	1
n= (nb+n1+n2+n3+n4)m		0.039	**0.046**	0.0373	**0.0443**	0.049	**0.055**

The following Google earth image is used to select appropriate manning's roughness values;-

Figure 18: Different land cover of left and right bank of study area (Source: Google earth image, imagery date at 12/25/2023)

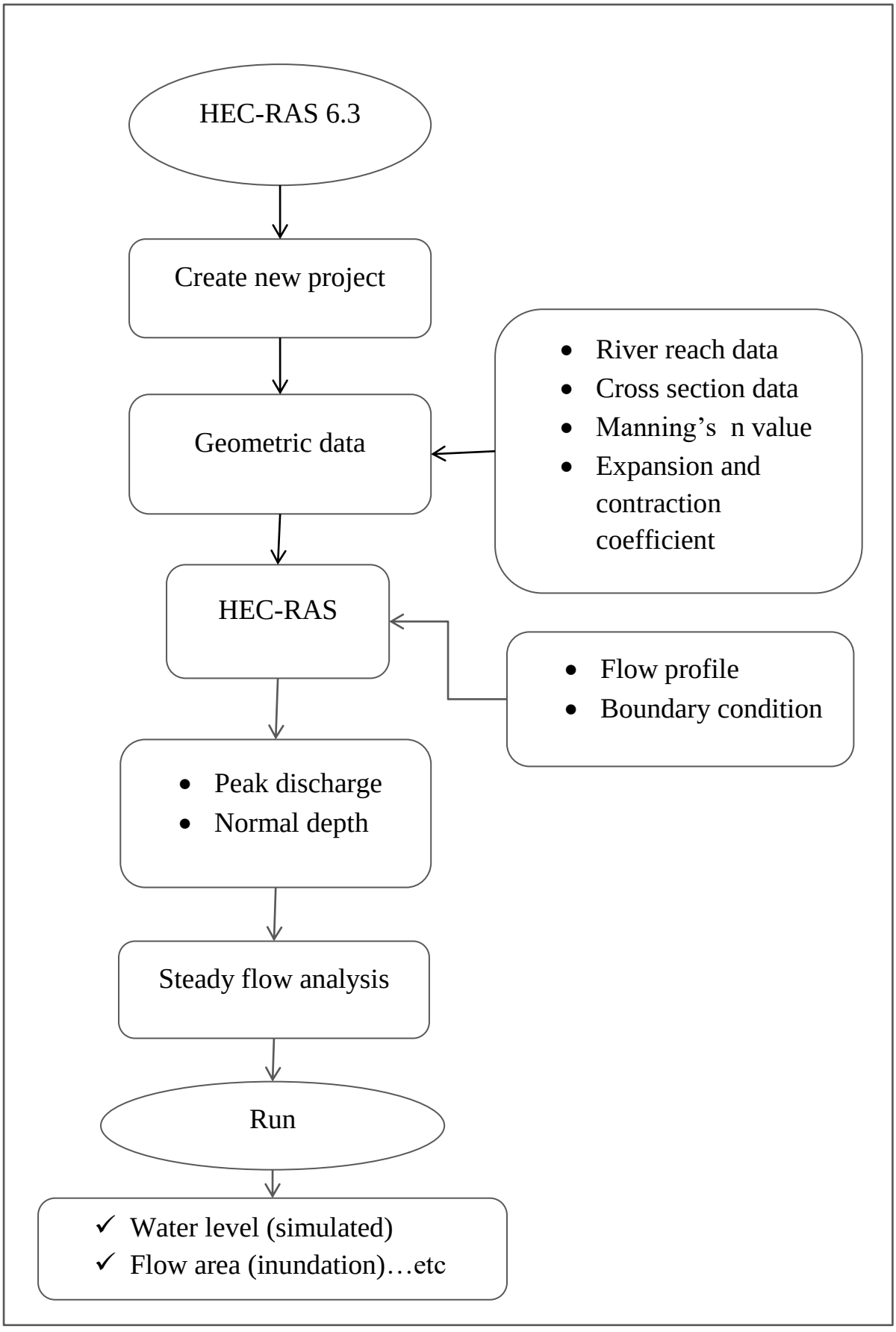

Figure 29: Schematic representation of 1D steady flow simulation in HEC-RAS

3.18. Calibration and Validation of the models

To check the applicative performance of the model the study was used ENS, RMSE, PBIAS and R model efficiency criteria. To evaluate the efficiency of the spatial data in ArcGIS 10.4 using terrain data in estimating elevation information of study area, the study compared DEM spatial information with Google earth (GPS) elevation data and geographical location. In addition simulated water level in Hec-RAS 6.3 compared with observed water level using Moriasi (2007) statistical test. The study made validation of flow depth for 25, 50, 100 and 200year flow profile. The choice of selected profile is to indicate that the proposed scheme can be designed and planned by considering the consequence the high flood event occur at minimum 25 year and maximum 200 year. Moreover, to get the best parameter for model reliability; the calibration made for manning's roughness value in HEC-RAS as shown in flow chart of figure 30 below.

$$RMSE = \sqrt{\frac{\sum_{i=1}^{n}(X_{ob}-X_s)^2}{n}} \quad \text{.....6.2}$$

$$ENS = 1 - \frac{\sum_{i=1}^{n}(X_{ob}-X_S)^2}{\sum_{i=1}^{n}(X_{ob}-mX_{ob})^2} \quad \text{.....6.3}$$

$$PBIAS = 1 - \frac{\sum_{i=1}^{n}(X_{ob}-X_s)}{\sum_{i=1}^{n}X_{ob}} * 100 \quad \text{.....6.4}$$

$$R = \frac{\sum_{i=1}^{n}(X_{ob}-mX_{ob})(X_s-mX_s)}{\sqrt{\sum_{i=1}^{n}(X_s-mX_s)^2}\sqrt{\sum_{i=1}^{n}(X_{ob-mX_o})^2}} \quad \text{.....6.4}$$

Where, Xob, Xs, mXob and mXs are observed, simulated, mean of observed and mean of simulated values. Ideal condition when **RMSE** = 0

Table 11: Summary of performance evaluation criteria for recommended statistical performance measures for watershed models (Moriasi et al., 2007)

Rate of performance	Evaluation Criterion		
	NSE	PBIAS	R
Un satisfactory	< 0.5	>25	< 0.5
Acceptable	0.5<NSE <0.65	10 to 25	0.5 < R^2 < 0.6
Good	0.65<NSE <0.75	10-15	0.6 < R^2 < 0.7
Very good	>0.75	< 10	>0.7

To validate hydraulic simulation the study follows the following flow chart (HEC-RAS 6.3);-

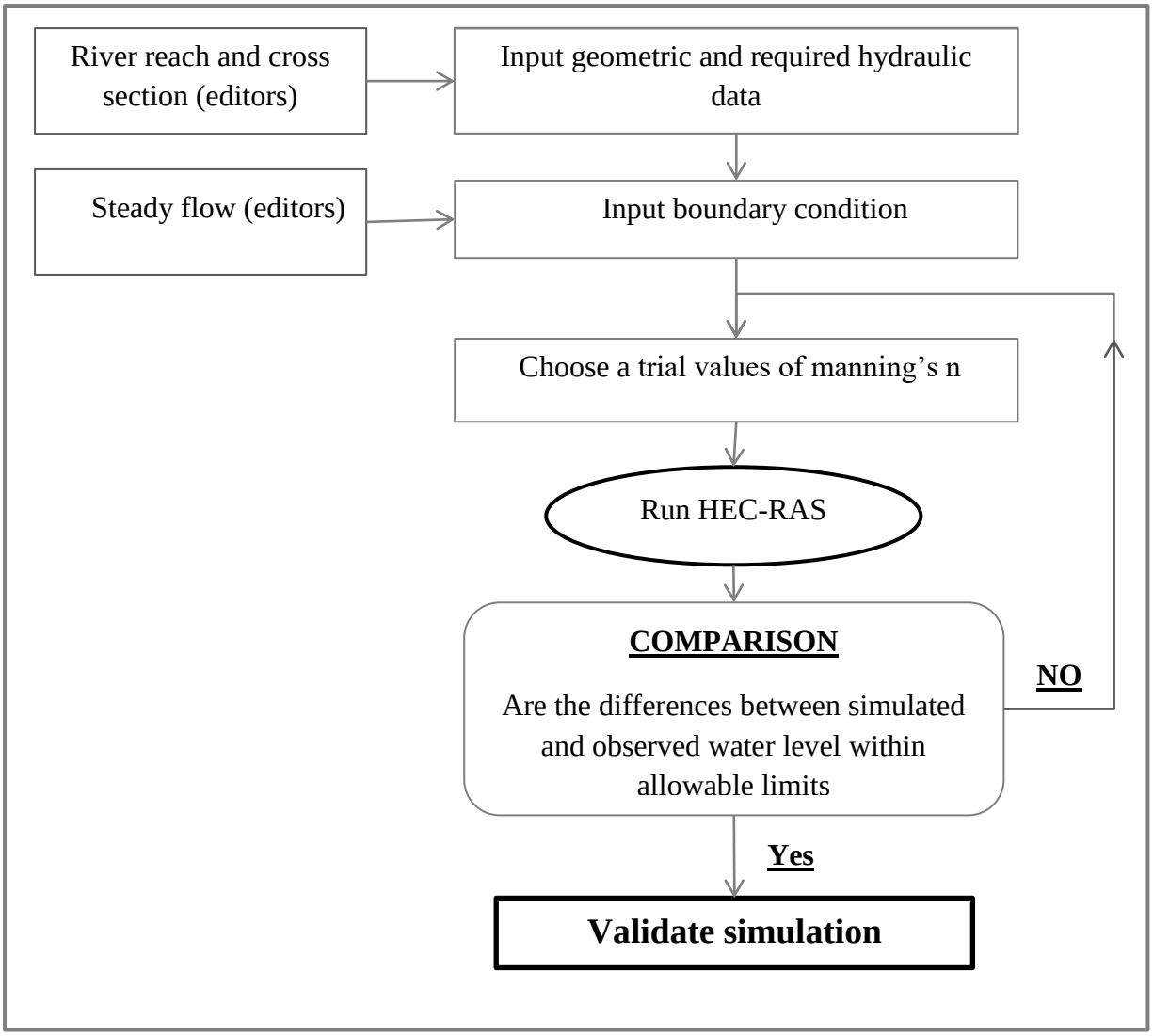

Figure 30: Schematic representation of calibration in HEC-RAS

3.19. Land use accuracy assessment

The final step of land use land cover classification is accuracy assessment. It is known that accurately classified land use directly or indirectly affect the final result of the study in underestimating or overestimating the roughness value as well the applicative performance of hydraulic analysis and incorrectly represent the study area land cover.

To do the accuracy assessment the study were taken 50 sample points for water bodies, agricultural land, vegetation and settlement, individually. And 30 sample points for forest and barren land (Exposed rock) respectively. Totally 260 sample points was taken from unclassified image and by converting sample points to kml format to see it where is it lays in truth Google earth image before selecting training areas. The error matrix resulted from classifying test pixels used to determine user accuracy, overall accuracy and kappa coefficient in the following equations.

$$\text{User accuracy} = \frac{\text{Number of correctly classified pixel in each category}}{\text{total number of classified pixels in that category(row total)}} * 100 \ldots\ldots\ldots\ldots\ldots 6.7$$

$$\text{over all accuracy} = \frac{\text{total number of correctly classified pixel (diagonal)}}{\text{total number of reference pixels}} * 100 \ldots\ldots\ldots\ldots\ldots\ldots 6.8$$

$$\text{Kappa coefficient(k)} = \frac{N\left(\sum_{i=1}^{r} X_{ii}\right) - \left(\sum_{i=1}^{r} (X_{i+} * X_{+i})\right)}{N^2 - \sum_{i=1}^{r} (X_{i+} * X_{+i})} \ldots\ldots\ldots\ldots\ldots\ldots\ldots\ldots\ldots\ldots\ldots\ldots 6.9$$

Where, r is the number of rows in the error matrix, X_{ii} : is the sum of diagonal matrix or is the number of observations in row I and column I (on the major diagonal), X_{i+} : is the sum of row or is the total number of observation in row I (shown as the marginal total to the right of the matrix), X_{+i} : is the total number observations in column I (shown as the marginal total at the bottom of matrix) and N: total number of observations included in matrix. According to (Anderson, 1976) the minimum accuracy value for reliable land cover classification is 85%.

4. RESULT AND DISCUSSION

4.1. Land Use Classification Accuracy Assessment

To know how well the land cover correctly classified the study used user accuracy, overall accuracy and kappa coefficient land cover accuracy assessment tool in table 12 below.

Table 12: Error matrix of LULC

Description	Water bodies	Agricultural land	Vegetation	Forest	Barren land (Exposed rock)	Settlement	user
Water bodies	**46**	3	0	1	0	0	**50**
Agricultural land	0	**46**	4	0	0	0	**50**
Vegetation	0	5	**45**	0	0	0	**50**
Forest	0	0	0	**30**	0	0	**30**
Barren land (Exposed rock)	0	0	0	0	**30**	0	**30**
Settlement	0	0	0	0	0	**50**	**50**
Producer (total)	**46**	**54**	**49**	**31**	**30**	**50**	

Table 13: User accuracy of land cover

User accuracy	Water bodies	92%
	Agricultural land	92%
	Vegetation	90%
	Forest	100%
	Barren land (exposed rock)	100%
	Settlement	100%

The user accuracy tells us how often the class on the map will actually be present on the ground. And Overall accuracy is equal to 95% to imply that from 100% of classification the perfect classification where 95% of reference site were classified correctly. The Kappa coefficient (94%) shows the agreement between the classified image and ground truth (i.e. ideal value is 100%; to show a complete agreement). Based on this point the assessment of LULC accuracy shows almost perfect agreement between the classified image and ground truth.

4.2. Head determination

4.2.1. Site one head determination

The gross head one of influencing parameter that determines the potential assessment of the study area. The elevation difference using 3D analyst tool of Arc-Map from terrain data (DEM) of study area estimated in figure 31 below as:

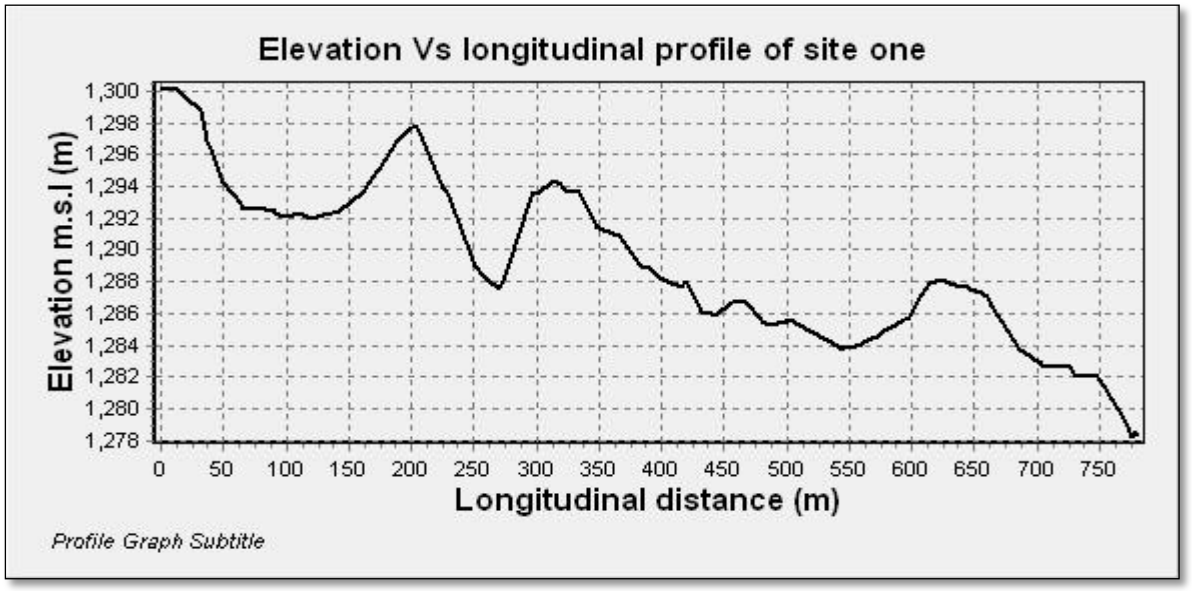

Figure 31: Elevation versus longitudinal profile of site one

The elevation value and longitudinal distance from the profile data of the above figure 31 is the difference between 1300.083m-1278.3706m and 780.57m-0m equaled **21.7124m** and **780.57m** were obtained (the exact values is taken from profile data of terrain information in ArcGIS). The terrain of site one can be represented by contour map with contour interval 5m and intermediate contour 25m. For detail information about the topography of site one, the study used contour map to show what it looks the specific longitudinal profile and the surrounding topography. As it is known about the contour map and shown in figure 32 the steeper the terrain the smaller the distance between the contour line and the flatter the terrain the larger the gap between the contour line. So as it can be seen in figure 32 the terrain endowed relatively with narrow gorge, valley shape along the river, and relatively gentle slope at the left side as compared to the right side of the river and escarpment land area at right side of the river.

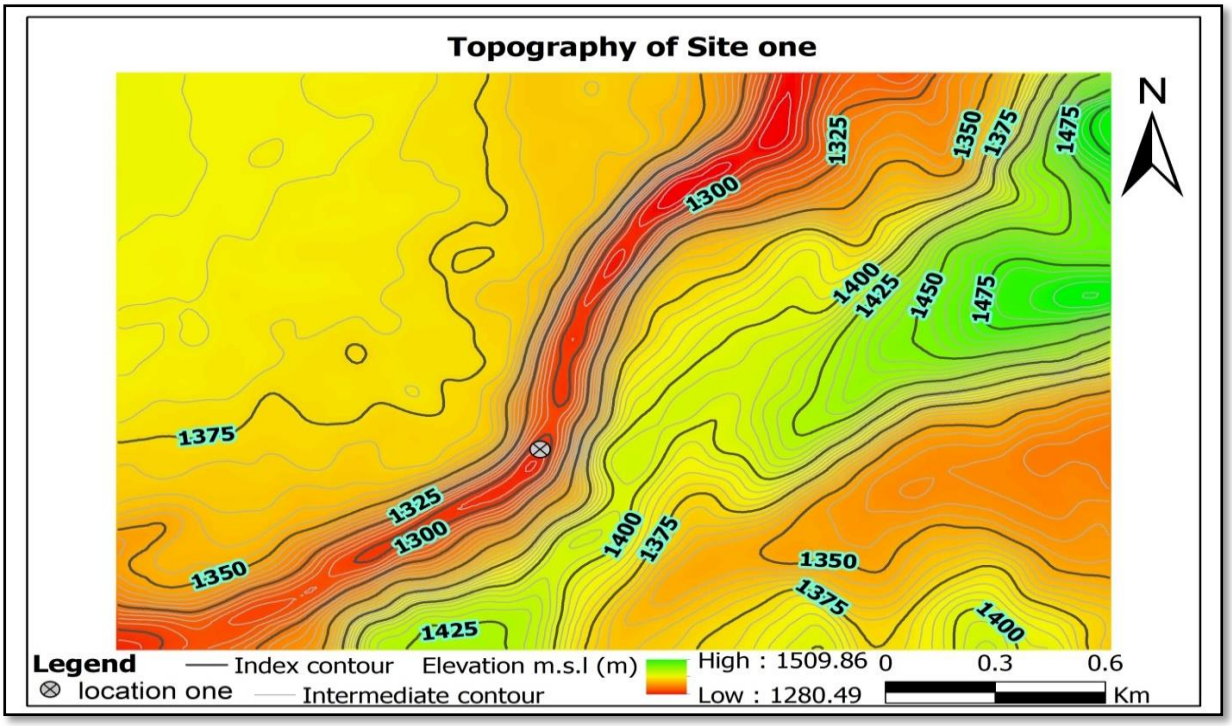

Figure 32: Topography of site one

4.2.2. Site two head determination

Site two located around 600m upstream of site one. The same procedure followed as site one above to determine the head difference of site two.

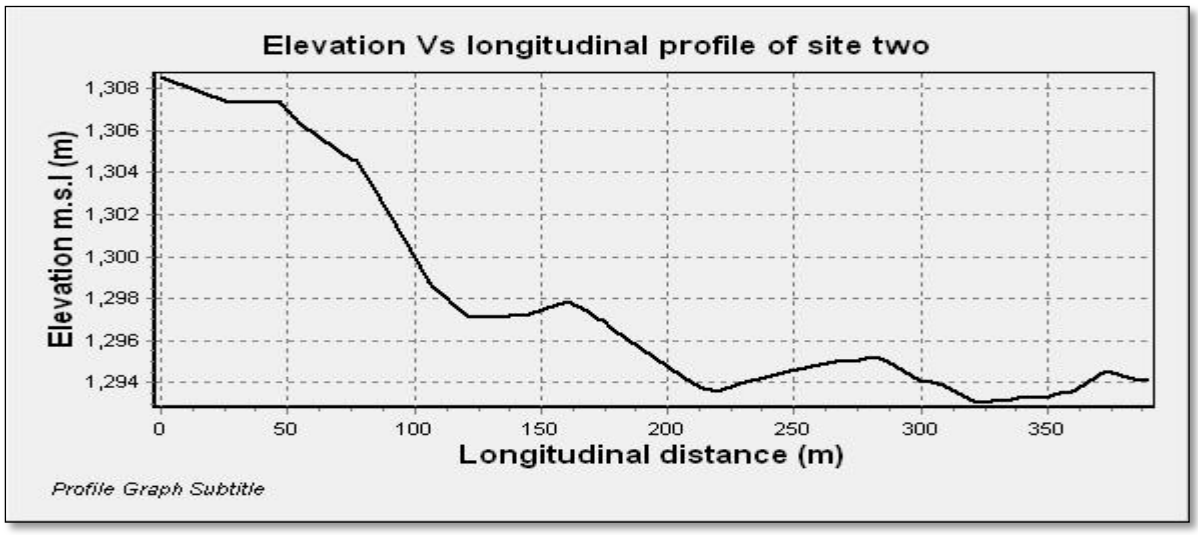

Figure 33: Elevation versus longitudinal profile of site two

The elevation difference between the highest point and the lowest point and the longitudinal distance is 1308.55m-1293.044m and 321.44m-0m equaled **15.5m** and **321.44m** were estimated. Topography of site two can be shown in contour map in the figure 34 as follows:

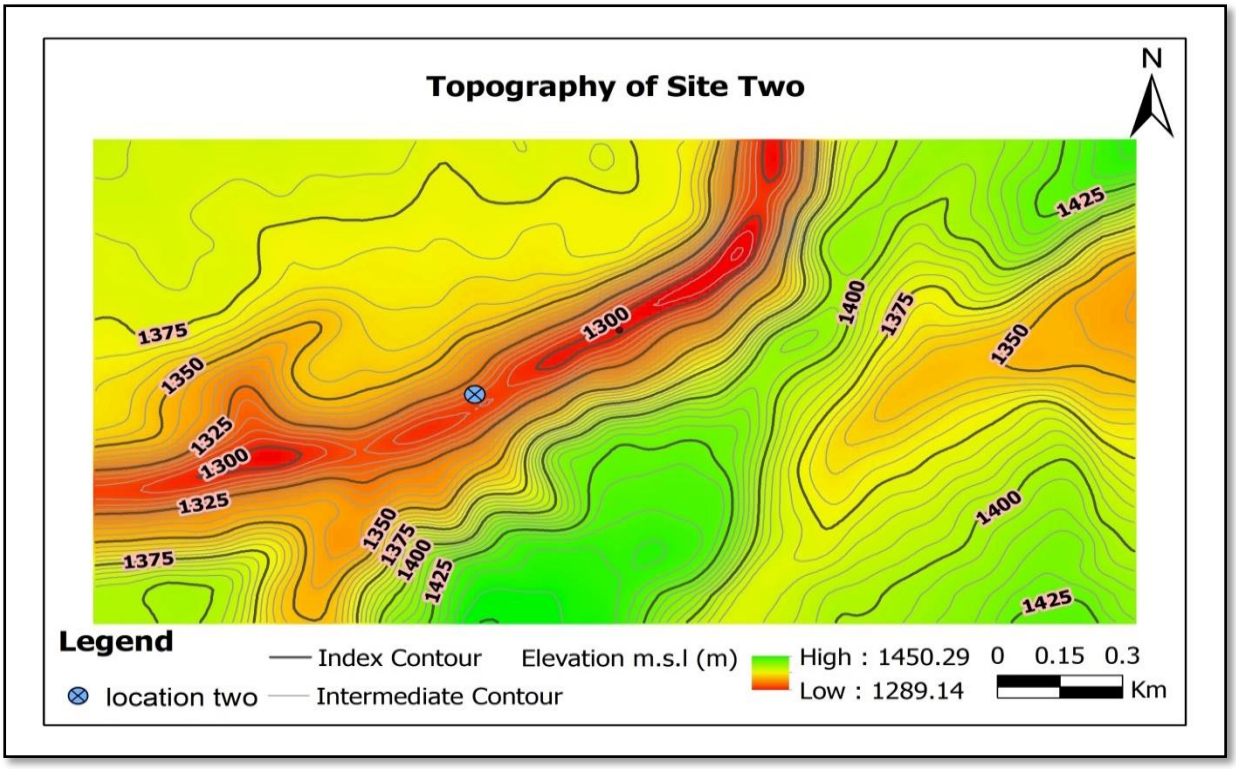

Figure 34: Topography of site two

4.2.3. Site three head determination

Site three located around 2km upstream of site two. The variation of distance between each sites depend on searching for suitable topography and elevation.

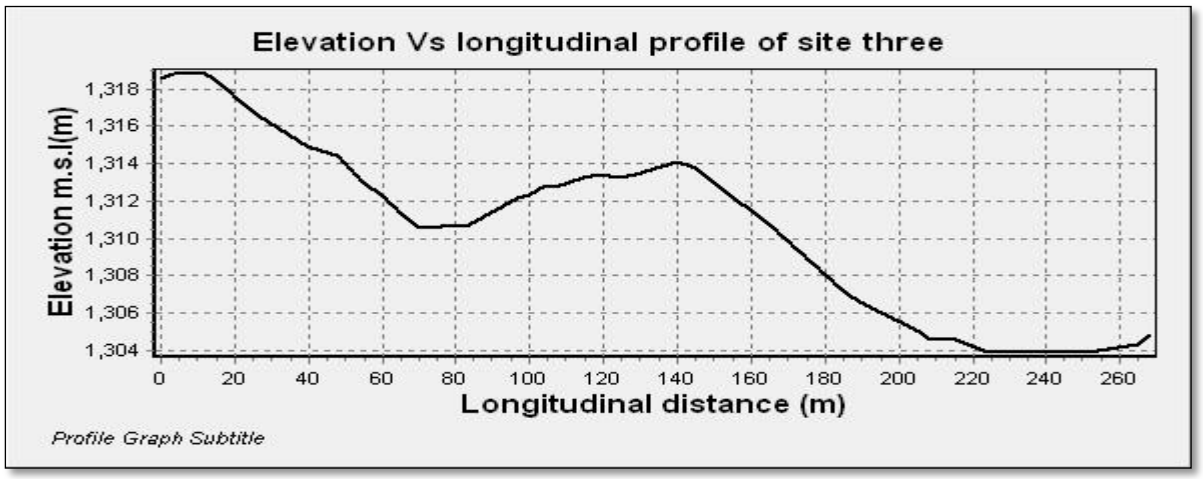

Figure 35: Elevation versus longitudinal profile of site three

The above figure indicates the relation between elevation and longitudinal distance and estimated **14.63m** and **224m**. To elaborate the topography of site three can be shown in the figure below.

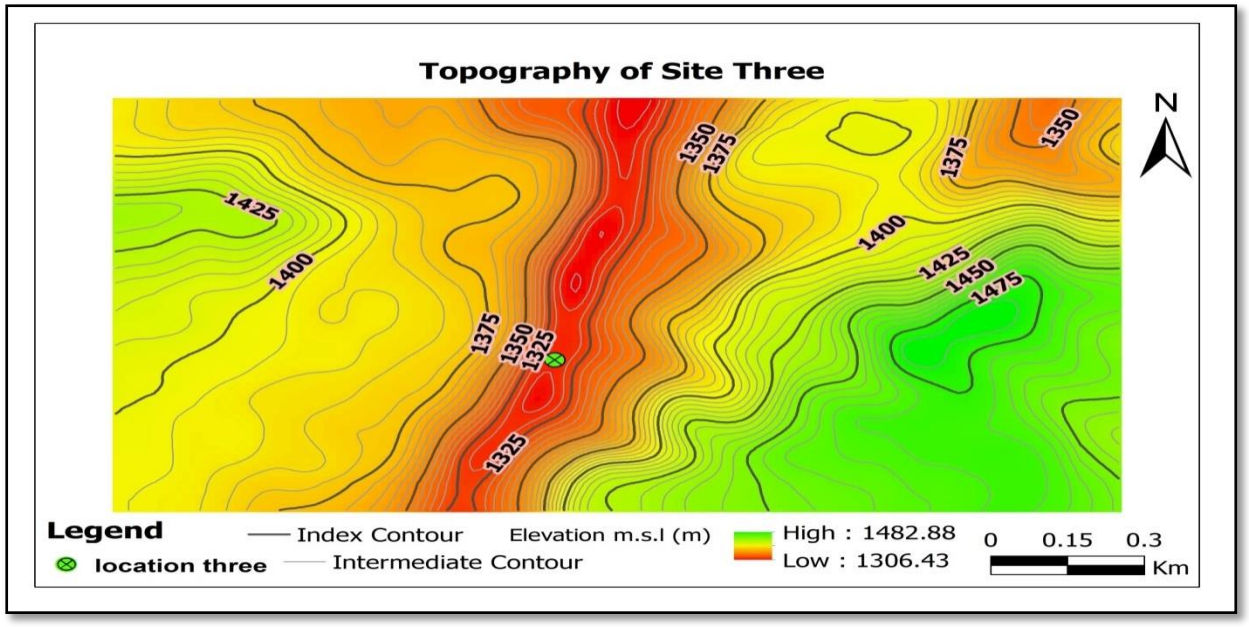

Figure 19: Topography of site three

4.2.4. Accuracy assessment of elevation

The applicative capacity of spatial analysis in ArcGIS was checked with the real geographical information of the study area using Google earth. Since we are checking the performance of elevation information to predict the reality, the accuracy of geographical location and elevation has to be considered.

Table 14: Geographical location from DEM and GE of study area

Sites	DEM				GE		
	Points	Latitude	Longitude	Elevation (m)	Latitude	Longitude	Elevation (m)
one	Point1 Point2	8.4654 8.4706	39.5228 39.5245	21.71	8.4667 8.4732	39.5233 39.5261	21
two	Point1 Point2	8.4617 8.4633	39.5169 39.5200	15.5	8.4614 8.4641	39.5173 39.5211	14
three	Point1 Point2	8.4508 8.4540	39.5051 39.5059	14.6	8.4508 8.4536	39.5053 39.5055	11

Using the above geographical data from DEM and GE the RMSE values computed in table 15 as follows:-

Table 15: The RMSE values for geographical location of selected site

Selected site	RMSE		
	Latitude	Longitude	Elevation
Site one	0.0020554	0.001185	0.71
Site two	0.0006041	0.0008200	1.5
Site three	0.0002828	0.0003162	3.6

The RMSE for latitude and longitude almost ideal for all sites (i.e. is near to 0). The RMSE for elevation committed error accordingly (i.e. we had 0.7, 1.5, and 3.6 error for site one, site two, and site three). The error we got does not mean that the assessment with an error, but it indicate that there is some deviation from the reference value. So, if we know the reference value, we can identify the applicable value. Based this point site one had the lowest error value, which is **0.71**.

4.3. Result of Flow duration curve for location one

The final result of stream flow analysis concluded in this study by developing flow duration for each selected sites. Flow duration curve indicate the timely flow behavior of river for RoR hydropower assessment, the research used average monthly flows for three selected stations. The flow duration curve at each potential site reflects the percentage of time that stream flow is likely to equal or exceed a value of interest for generation of hydropower. The frequencies converted into percentages of the total number of 312 months and the analysis of flow FDC in hydropower potential sites were constructed using this mean monthly flow values. But here the study analyzed and discuss about site one taking as sample due to its highest flows and head over the other two sites. The other sites full average monthly stream flow data (1991-2016) and the flow duration curve could be available at annex 4, 5, 6, 16 and 17.

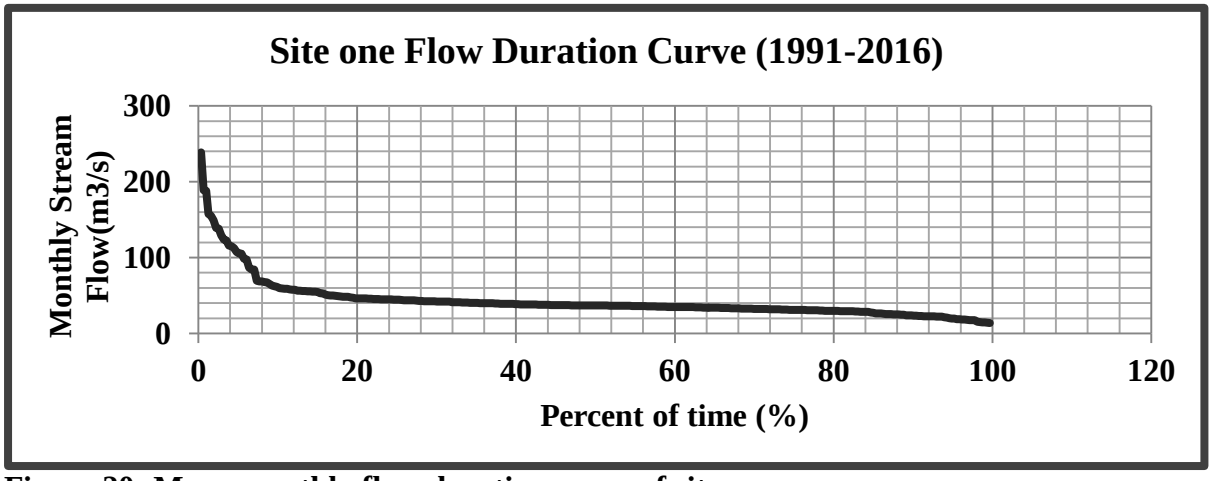

Figure 20: Mean monthly flow duration curve of site one

To elaborate the above flow duration curve from (1991-2016) of 312 months indicates that there is highest flow from 59.67 to 238.54 m^3/s with percent of time (10%-0%). The curve in this region relatively steep slope to depict that there is the flood event with high intense and short duration rain which occur 0% up to 10% of the year. The flow duration curve from percent of time (10%-20%) of the year have relatively moderate slope with flow of 46.32m^3/s to 59.67m^3/s. The shape of the curve from 20% to 85% of the year have almost flat slope to imply more of the 73 to 292 days of the year (i.e. 365 day of the year) got constant flows from (46.32m^3/s to 26.47m^3/s). And the flow ranges from 13.82m^3/s to 26.47m^3/s which occur with percent of time 85% to 100% available most of the year (292 to 365 days of the year).

In general, from the long term (1991-2016) monthly flow duration curve of site one the highest the flood event in a short time indicated by steep slope and the flattest the slope indicates the continuous flow for a most days of the year. To summarize the final result of flow duration curves of three selected site for the key exceedance percentages of Q_{30}, Q_{40}, Q_{50}, Q_{60}, Q_{70}, Q_{80}, Q_{90}, Q_{95}, Q_{97} and Q_{100} are considered to visualize the flow condition of each sites in table below.

Table 16: Mean monthly flow at key percent of time of selected sites

%(time)	site one	site two	site three
	flows (m^3/s)	flows (m^3/s)	flows (m^3/s)
Q_{30}	**42.17**	**42.17**	**42.17**
Q_{40}	38.74	38.74	38.73
Q_{50}	36.81	36.80	36.80
Q_{60}	34.82	34.82	34.82
Q_{70}	32.36	32.37	32.37
Q_{80}	29.58	29.58	29.59
Q_{90}	23.61	23.61	23.61
Q_{95}	**19.71**	**19.71**	**19.71**
Q_{97}	17.77	17.77	17.77
Q_{100}	13.82	13.82	13.82

As it can be seen easily the flow values from flow duration curve at key percent of time, each site have almost the same flow patterns due to they are located near each other. The distance between site one and site two is around 600m and site two and site three is about 1200m. In addition to distance gap they have almost the same climate pattern, land use, soil type, geology and allied in same stream line.

To summarize the design discharge (installed capacity) at Q_{30} is **42.17m^3/s** and the firm flow (dependable) flow at any time at Q_{95} is **19.71m^3/s**.

4.4. Result of Theoretical Power

It is the gross hydropower potential. It considers the gross head without considering any losses and the timely flow of the river. To represent the timely variation of hydropower potential of the each site, the study was developed average monthly power duration curve for site one, two and three. Full data to construct the curve and site two and site three power duration curves are available at annex 18&19.

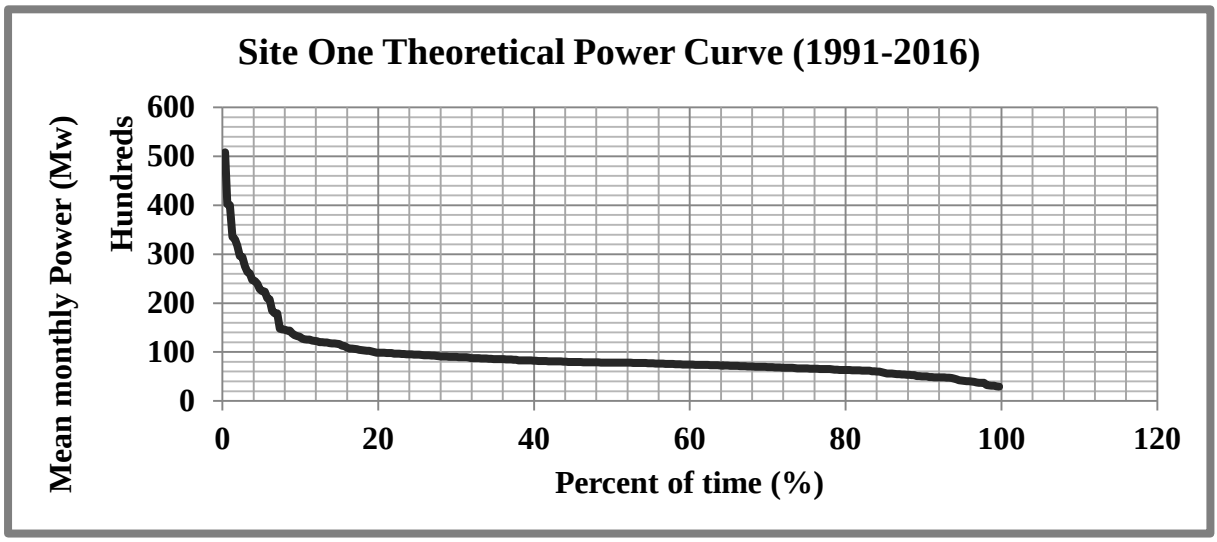

Figure 21: Mean monthly theoretical power duration curve of site one

The theoretical power from each power curves summarized in table 17 as follows.

Table 17: Mean monthly theoretical power at key percent of time of selected sites

%(time)	site one	site two	site three
	Theoretical Power: 9.81*H*Q (Kw)	Theoretical power: 9.81*H*Q(Kw)	Theoretical power: 9.81*H*Q (Kw)
P_{30}	**8980.68**	**6411.82**	**6040.44**
P_{40}	8250.38	5889.92	5547.47
P_{50}	7838.90	5596.13	5271.19
P_{60}	7415.79	5294.56	4987.13
P_{70}	6892.58	4922.02	4635.75
P_{80}	6300.51	4498.38	4238.53
P_{90}	5028.27	3590.46	3381.52
P_{95}	**4196.98**	**2997.45**	**2822.94**
P_{97}	3785.28	2702.02	2545.13
P_{100}	2943.87	2101.97	1979.27

Therefore, the maximum (installed) theoretical power (P_{30}) at Q_{30} are 8980.68kw, 6411.82kw and 6040.44kw and the minimum (dependable) theoretical power (P_{95}) at Q_{95} are 4196.98kw, 2997.45kw and 2822.94kw for each selected potential site.

4.5. Result of Technical power

From technical point of view, head losses in the water way (channel and penstock losses), efficiency losses in the hydraulic and electrical machines are considered as infeasible. Hence the technically usable hydro potential is substantially less than the theoretical value. Because the theoretical power is never developed as there is always some head loss associated within a hydroelectric plant known as transfer losses. These transfer losses are exists when we divert natural stream flow in to the canal/ channel using diversion weir and then in to the penstock conduit from the intake. These transfer losses are when we divert natural stream flow in to the canal/channel using diversion weir and then in to the penstock conduit from the intake. In addition to these transfer losses hydraulic machine losses (turbine and generator losses) and transformer losses are also necessary to determine the total system losses since the efficiency of the turbine, generator and transformer is never being 100%. Then after determining the total system losses, the net technical power potential calculated and the power curve developed using the equation of flow duration curve expression (equation 5.0 and 5.3); technical and energy curve site 1&2 available at annex 20&21.

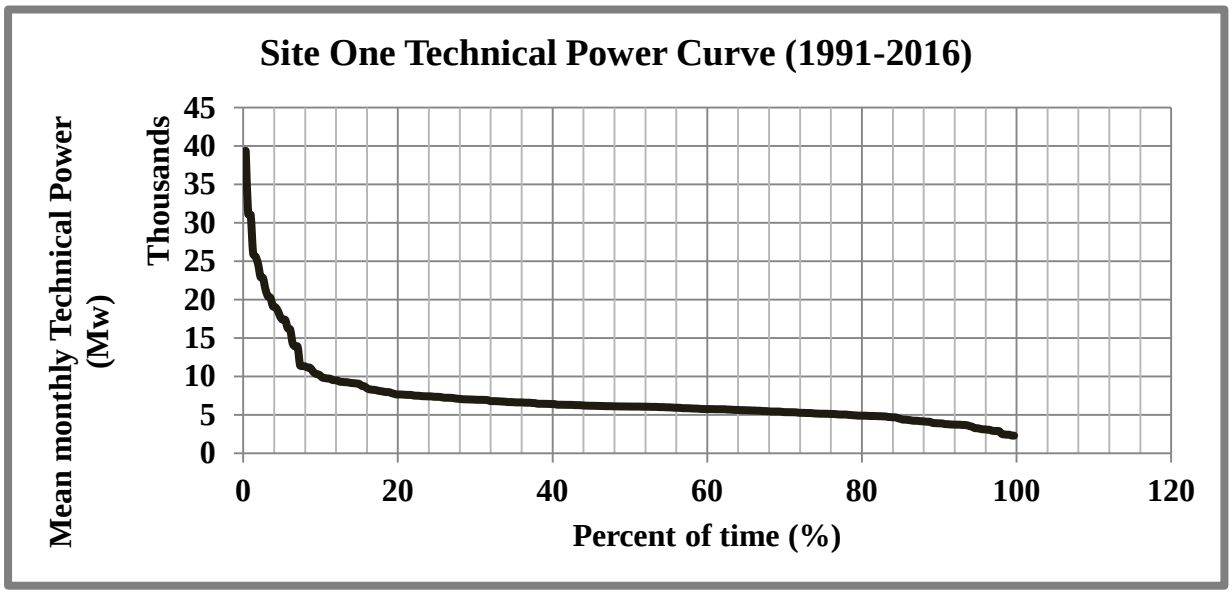

Figure 22: Mean monthly technical power curve of site one

The technical power from each power curves summarized in table 18 as follows.

Table 18: Mean monthly technical power at key percent of time of selected sites

%(time)	site one	site two	site three
	Technical Power : 0.775*9.81*H*Q(Kw)	Technical power : 0.775*9.81*H*Q(Kw)	Technical power: 0.775*9.81*H*Q(Kw)
TP_{30}	**6960.26**	**4969.32**	**4681.50**
TP_{40}	6394.26	4564.84	4299.43
TP_{50}	6075.35	4337.14	4085.31
TP_{60}	5747.43	4103.42	3865.15
TP_{70}	5341.93	3814.69	3592.82
TP_{80}	4883.06	3486.36	3284.97
TP_{90}	3897.04	2782.70	2620.76
TP_{95}	**3252.77**	**2323.10**	**2187.85**
TP_{97}	2933.69	2094.13	1972.54
TP_{100}	2281.57	1628.94	1534.00

Therefore, the maximum (installed) technical power (TP_{30}) at Q_{30} are 6960.26kw, 4969.32kw and 4681.50kw and the minimum (dependable) technical power (TP_{95}) at Q_{95} are 3252.77kw, 2323.10kw and 2187.85kw for each selected potential site.

The annual energy output describe the annual energy demand that can be exploited from study area can be indicated by energy curve as shown in the figure below; site two and site three annual energy curve available at annex 22&23.

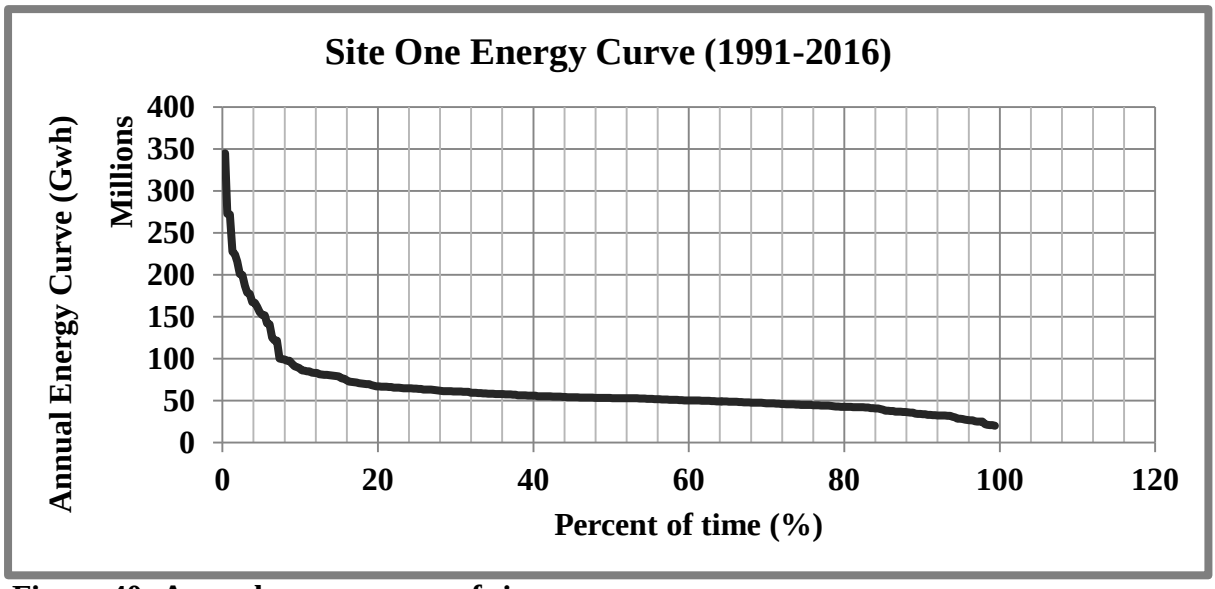

Figure 40: Annual energy curve of site one

The annual energy output from each power curves summarized in table 19 as follows.

Table 19: Annual energy output at key percent of time of selected sites

%(time)	site one	site two	site three
	Annual energy (kwh/yr): 0.775*9.81*H*Q*8760	Annual energy (kwh/yr): 0.775*9.81*H*Q*8760	Annual energy (kwh/yr): 0.775*9.81*H*Q*8760
E_{30}	**60971834.97**	**43531250.21**	**41009902.72**
E_{40}	56013675.50	39988008.91	37662987.77
E_{50}	53220065.93	37993381.63	35787314.31
E_{60}	50347474.07	35945916.54	33858734.29
E_{70}	46795292.53	33416694.96	31473129.42
E_{80}	42775591.84	30540475.49	28776358.70
E_{90}	34138070.70	24376434.48	22957891.85
E_{95}	**28494257.94**	**20350326.65**	**19165558.03**
E_{97}	25699093.60	18344598.99	17279428.73
E_{100}	19986560.04	14269538.49	13437847.89

Therefore, the maximum annual energy output (E_{30}) at Q_{30} are 60971834.97kwh/year, 43531250.21kwh/year and 41009902.72kwh/year and the minimum (dependable) annual energy output (E_{95}) at Q_{95} are 28494257.94kwh/year, 20350326.65kwh/year and 19165558.03kwh/year for each selected potential site.

Installed and firm capacity at Q_{30} and Q_{95}

The final result of the power assessment is to get the design capacity (installed power) that is to be harmed from the pant and the plant deserve at worst time of flow (dependable) are essential point that has to achieve from the research finding.

Table 20: Installed and firm capacity at Q30 and Q95

Sites	Q_{30} (m3/s)	Q_{95} (m3/s)	Head (m)	Firm capacity (P_{dep}) 0.775*9.81* Q_{95}*H (Kw)	Installed capacity (P_{ins}) 0.775*9.81* Q_{30}*H(Kw)
One	**42.17**	**19.71**	**21.71**	**3252.77**	**6960.26**
Two	**42.17**	**19.71**	**15.5**	**2323.10**	**4969.32**
Three	**42.17**	**19.71**	**14.6**	**2187.85**	**4681.50**

The final result power assessment depicts that, if we want to solve the diversified energy demand at 50km downstream of Koka Dam, specifically 31.83km below Awash Melkasa, we can get the sites that have the capacity to produce **6960.26kw**, **4969.32kw** and **4681.50kw** from three selected hydropower sites.

4.6. Result of Analytical Hierarchy Process (AHP)

4.6.1. Structuring of the decision problem into a hierarchical model

The first step in analytical hierarchy process is arranging criterion to select suitable hydropower site according to relative importance and influence on overall implementation the water resource project (i.e hydropower plant). A criterion's to select best hydropower sites arranged according to relative importance as follows:

1. Power, 2. Discharge, 3. Head, 4. Road accessibility 5. Geology, 6. Soil type 7. Gorge and 8. Distance from nearby town

4.6.2. Making pair-wise comparisons for each criterion and alternative sites and obtain the matrix

Table 21: Pairwise comparison matrix for criteria

	Pair wise comparison							
Criteria	Power	Discharge	Head	Accessibility	Geology	Soil	Gorge	Distance
Power	1	2	2	5	3	3	3	5
Discharge	1/2	1	3	5	3	3	3	5
Head	1/2	1/3	1	3	3	3	3	5
Accessibility	1/5	1/5	1/3	1	4	4	4	4
Geology	1/3	1/5	1/3	1/4	1	4	4	3
Soil	1/3	1/3	1/3	1/4	1/4	1	4	3
Gorge	1/3	1/3	1/3	1/4	1/4	1/4	1	4
Distance	1/5	1/5	1/5	1/4	1/3	1/3	1/4	1
Sum($\sum_{i=1}^{n} C_{ij}$)	3.4	4.6	7.53	15	14.83	18.58	22.25	30

The pair wise comparison matrix of criteria can be normalized by divided each column entry to the sum of column values: $\boldsymbol{X_{ij} = \frac{C_{ij}}{\sum_{i=1}^{n} C_{ij}}}$

Table 22: Normalization matrix for criteria (X_{ij})

	Normalization matrix							
Criteria	Power	Discharge	Head	Accessibility	Geology	Soil	Gorge	Distance
Power	0.29	0.43	0.27	0.33	0.20	0.16	0.13	0.17
Discharge	0.15	0.22	0.40	0.33	0.20	0.16	0.13	0.17
Head	0.15	0.07	0.13	0.20	0.20	0.16	0.13	0.17
Accessibility	0.06	0.04	0.04	0.07	0.27	0.22	0.18	0.13
Geology	0.10	0.04	0.04	0.02	0.07	0.22	0.18	0.1
Soil	0.10	0.07	0.04	0.02	0.02	0.05	0.18	0.1
Gorge	0.10	0.07	0.04	0.02	0.02	0.01	0.04	0.13
Distance	0.06	0.04	0.03	0.02	0.02	0.02	0.01	0.03
Sum($\sum_{i=1}^{n} X_{ij}$)	1	1	1	1	1	1	1	1

4.6.3. Evaluation of matrix consistency for criteria

In pairwise comparison sometimes inconsistency may be a rise due subjective judgment in evaluating criterion to make decision; to solve this problem matrix consistency is checked as follows: $\mathbf{(W_{ij})} = \frac{\sum_{i=1}^{n} \mathbf{X_{ij}}}{\mathbf{n}}$ (i.e. formula of priority vector or weight of each criteria)

$$1/8 \begin{vmatrix} 0.29 & +0.43 & +0.27 & +0.33 & +0.20 & +0.16 & +0.13 & +0.17 \\ 0.15 & +0.22 & +0.40 & +0.33 & +0.20 & +0.16 & +0.13 & +0.17 \\ 0.15 & +0.07 & +0.13 & +0.20 & +0.20 & +0.16 & +0.13 & +0.17 \\ 0.06 & +0.04 & +0.04 & +0.07 & +0.27 & +0.22 & +0.18 & +0.13 \\ 0.10 & +0.04 & +0.04 & +0.02 & +0.07 & +0.22 & +0.18 & +0.1 \\ 0.10 & +0.07 & +0.04 & +0.02 & +0.02 & +0.05 & +0.18 & +0.1 \\ 0.10 & +0.07 & +0.04 & +0.02 & +0.02 & +0.01 & +0.04 & +0.13 \\ 0.06 & +0.04 & +0.03 & +0.02 & +0.02 & +0.02 & +0.01 & +0.03 \end{vmatrix}$$

$$1/8 \begin{vmatrix} 1.99 \\ 1.76 \\ 1.22 \\ 1.01 \\ 0.76 \\ 0.58 \\ 0.44 \\ 0.23 \end{vmatrix} = \begin{vmatrix} 0.25 \\ 0.22 \\ 0.15 \\ 0.13 \\ 0.10 \\ 0.07 \\ 0.06 \\ 0.03 \end{vmatrix}$$

λmax=(0.25*3.4)+(0.22*4.6)+(0.15*7.5)+(0.13*15)+(0.1*14.8)+(0.07*18.58)+(0.06*22.25)+(0.03*3)=8.74

$$\textbf{Consistency index}(\mathbf{CI}) = \frac{\lambda_{max} - n}{n-1} = \frac{8.74-8}{7} = 0.105, \quad \textbf{Consistency Ratio } (\mathbf{CR}) = \frac{\mathbf{CI}}{\mathbf{RI}} \quad ,$$

Where, CI is consistency index and RI is Random consistency index for n=8, RI=1.41

Table 23: Random consistency index (RI), (Saaty, 1980)

n	1	2	3	4	5	6	7	**8**	9	10
RI	0	0	0.58	0.9	1.12	1.24	1.32	**1.41**	1.45	1.49

$\textbf{Consistency Ratio } (\mathbf{CR}) = \frac{\text{CI}}{\text{RI}}, \frac{0.105}{1.41} = 0.074 < 0.1$(The judgement is consistent)

The normalized principal Eigen vector is also called priority vector. Since it is normalized, the sum of all elements in priority vector is 1. The priority vector shows relative weights of each criterion and alternatives that we compare.

Table 24: The relative weight of each criterion

Criteria	Power	Discharge	Head	Accessibility	Geology	Soil type	Gorge	Distance nearby town
Priority vector	25%	22%	15%	13%	10%	7%	6%	3%

The final result of the normalized principal Eigen vector of priority vector encourages to summarized that from 100% cumulative importance of each criterion, power, discharge, head, accessibility, geology, soil type, gorge and the lowest distance from nearby town have relative weights 25%, 22%, 15%, 13%, 10%, 7%, 6% and 3%, respectively.

Likewise the above procedure of Criterion evaluation, best alternative selection from a given alternatives site of the pairwise comparison matrix, normalization matrix, evaluation of matrix consistency and the relative weight of each alternative were done for site one, site two and site three as shown in table 25, 26 and 27) ;-

Table 25: Pairwise comparison matrix for alternatives

Alternatives	Pairwise Comparison		
	Site one	Site two	Site three
Site one	1	3	5
Site two	0.333	1	3
Site three	0.2	0.333	1
Sum	1.533	4.333	9

The pair wise matrix of alternative can be normalized by divided each column entry to the sum of column values:

Table 26: Normalization matrix for alternatives

Alternatives	Normalization Matrix		
	Site one	Site two	Site three
Site one	0.65	0.69	0.56
Site two	0.22	0.23	0.33
Site three	0.13	0.08	0.11
Sum	1	1	1

4.6.4. Evaluation of Matrix Consistency for Alternatives

After a number of revision of the subjective judgment the consistency of the final decision were made as follows:-

λ= (0.63*1.533) + (0.26*4.333) + (0.11*9) = **3.08**, $\mathrm{CI} = \frac{\lambda - \mathrm{N}}{\mathrm{N}-1}$, N is the number of alternatives, which is 3, $\mathrm{CI} = \frac{\lambda - \mathrm{N}}{\mathrm{N}-1} = \frac{3.08-3}{3-1}$ = **0.04,** $\mathrm{CR} = \frac{\mathrm{CI}}{\mathrm{RI}}$, for RI(random consistency index for N= 3, from table 23 is **0.58.**, $\mathrm{CR} = \frac{\mathrm{CI}}{\mathrm{RI}} = \frac{0.04}{0.58}$ = **0.06<0.1** (the judgment is consistence).

Table 27: The relative weight of each Alternative

Alternatives	Site one	Site two	Site three
Priority vector	**63%**	**26%**	**11%**

The final result of Analytical Hierarchy Process (AHP) indicates that Site one had 63%, site two had 26% and site three had 11% weight (importance) to select the best site from each.

Table 28: Qualitative and quantitative values of each criterion

Criterion	Site one	Site two	Site three
Power (Installed capacity(kw)	6960.26	4969.32	4681.50
Discharge(m^3/s)	42.17	42.17	42.17
Head(m)	21.71	15.5	14.6
Accessibility	Very good	Good	Good
Geology	Good	Good	Good
Soil	Good	Good	Good
Gorge	Narrow	Slightly narrow	Slightly narrow
Distance from nearby town	Minimum	Minimum	Minimum

Based on relative weight of each alternative and qualitative and quantitative values of each criterion, site one is selected as the most suitable site for RoR hydropower scheme with installed capacity of **6960.26kw,** annual maximum energy capacity of **60.09GWh/year**, discharge of **42.17m^3/s** and head of **21.71m**. So, the study assessed the level of flooding for site one for further precaution in the following session.

4.7. Result of flood frequency analysis for site one

4.7.1. Result of Gumbel Distribution

Based on the procedure in method (page:54) to forecast the occurrence of flood at a given return period using Gumbel distribution for annual maximum flow of 26 year (1991-2016) flow data, which is available at annex.13 and using the flow data the following is computed: mean (Xmean): 158.8m^3/s, standard deviation (S): 83.3, reduced mean (Yn): 0.532, reduced standard deviation (Sn): 1.0961. Where, the value of Yn and Sn is available at (Annex-8 and 9) for a given sample size. For this study the sample size is 26.

Table 29: Forecasted floods for specified return period (Gumbel-distribution)

Return period	YT	K	XT (m3/s)
2	0.37	-0.15	**146.26**
5	1.5	0.88	**232.42**
10	2.25	1.57	**289.47**
25	3.20	2.43	**361.55**
50	3.90	3.07	**415.02**
100	4.60	3.71	**468.09**
200	5.3	4.35	**520.98**

4.7.2. Result of Log-pearson type III

Based on the procedure in method (page: 53) to forecast the flow magnitude at specified return period using log-pearson type III for 26 year (1991-2016) and using the annual maximum flow which is available at annex 13 the following is computed: logarithm of skew (G): -0.139, logarithm of mean: 2.14 and logarithm of standard deviation (s): 0.24. To get K factor for a given return period and logarithm of skew (G) interpolated using K values for log-pearson type III distribution at annex.7.

Table 30: Forecasted floods for specified return period (Log-pearson type III)

Return period	K factor	$\log X_T = \overline{X} + K * S$	$X_T = \text{antilog}(\log X_T), (m^3/s)$
2	0.02	2.14	**139.55**
5	0.85	2.34	**221.23**
10	1.27	2.44	**279.44**
25	1.7	2.55	**356.71**
50	1.98	2.61	**416.37**
100	2.22	2.67	**477.39**
200	2.45	2.73	**540.55**

Table 31: Summary of forecasted flow data for Gumbel and Log-pearson type III

Return period(yr)	Pro. Of Exceedence	Site one	
		Log-Pearson type III	Gumbel-Distribution
		$Q(m^3/s)$	$Q(m^3/s)$
2	0.5	**139.55**	**146.27**
5	0.2	**221.23**	**232.43**
10	0.1	**279.44**	**289.47**
25	0.04	**356.71**	**361.55**
50	0.02	**416.37**	**415.02**
100	0.01	**477.39**	**468.09**
200	0.005	**540.55**	**520.98**

4.7.3. Checking for goodness of fit test

Using the Anderson-Darling test the best fit distribution from candidate distribution obtained. The test statistic from easy fit software for 26 year (1991-2016) annual maximum stream shown in table 32. Based on Anderson-Darling formulas for Pvalue in table 9, $AD^* = AD^*(0.75/n+2.25/n^2)$ and AD is the test statistic from easy fit software for Log-pearson type III and Gumbel-Distribution are 0.7817 and 0.6037. For AD value and sample size (i.e n, 26) AD^* computed are 0.0194 and 0.0251. Finally, if $AD^* \leq 0.2$, then Pvalue = $(1-\exp(-13.436+101.14(AD^*)-223.73(AD^*)^2)$ formulas used and Pvalue computed in table 32 as follows;-

Table 32: Pvalues and test statistics of Anderson-Darling test

Distribution	Anderson-Darling (A-D)		P_{value} (%)
	Statistics	Rank	
Log-pearson type III	0.7817	2	100
Gumbel-Distribution	0.6037	1	99.9

The above table result of easy fit software for Anderson-Darling test showed that Gumbel-distribution ranked first and log-pearson type three second, but the Pvalue of both distributions have almost equal value. Since Pvalue indicates the probability of the Null hypothesis to be true and as mentioned in table 32 log-pearson type III and Gumbel-Distribution have 100% and 99.9% true to fit with a given flow data. Besides this point, as it

is shown in table 31 the result of forecasted flow magnitude of the two frequency distributions for specified return period, especially for higher profile in log-pearson type III gives slightly larger forecasts than Gumbel-Distribution. Consequently, the study consider the forecasts of log-pearson type three to be used as an input flow value in Hec-RAS for further flood level forecasting at required river stations. The choice of log-pearson type three is due to the purpose of the study is about assessment of suitable site for hydropower development and it needs thorough precaution in early planning and designing stage of the scheme to be protected from the consequence of high flood event.

4.8. Result of hydraulic modeling

Knowing the level of flood at specified place is important to give care and any care before implementation of construction (i.e. hydropower development) related directly with flowing water. In hydraulic analysis to discuss the final result, it is important to deal about each ways that directs our discussion to target point. Based on this reason the study followed the following points to deal step by step.

4.8.1. Cross section result

Standing from the cross section view of a given stream flow topography, we can decide our first judgments weather the proposed site is suitable for RoR hydropower development. The narrowness and the wideness of the cross section determine overall cost of the project and influence the stability of the structure constructed along the river. The narrow the cross section the suitable the site for hydraulic structure constructed along the river. The study made hydraulic analysis for 4.65km length of the river (i.e. 93 river stations with 50m interval) and channel width is 50m and total width of cross section including the left and right over bank is 150m. Since it is bulky and takes time to discuss about all river station the study choses river station 1100 and 2050 to deal about. The river station 1100 (RS.1100) is the location that study prioritize to be the best cross section because it is the starting location of the highest head from three selected site (i.e. site one), it has narrow cross section, highest velocity and it holds all forecasted flow safely within the total width of cross section. The river station 2050 (RS.2050) is the location around 1km upstream of river station 1100. It is chosen as a sample river station to know the flood event upstream of mostly prioritized site (site one). RS.1100 is the location where the study starts head measurement.

4.8.1.1.Result River Station 1100 (RS.1100)

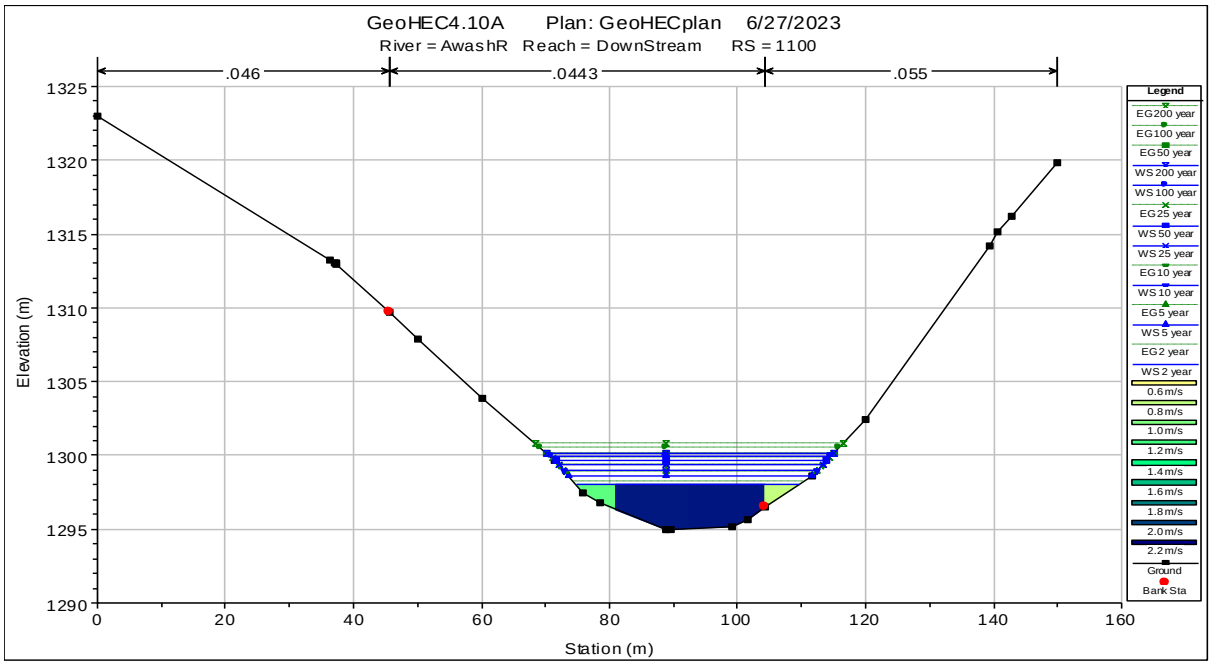

Figure 41: Cross section view of RS.1100 with different flow profile and velocity distribution

The cross sectional view RS 1100 shows Energy grade line profile (EG), the water surface label profile (WS) and velocity distribution for 2, 5, 10, 25, 50, 100 and 200 years flow condition. The cross section view shows the sufficiency to hold the forecasted flood for 2, 5, 10, 25, 50, 100 and 200 return period.

Table 33: Overall result of river station 1100 cross section from detail output table of the model

Description	2yr	5yr	10yr	25yr	50yr	100yr	200yr
Top width(m) LOB	0	0	0	0	0	0	0
Channel	29.57	30.73	31.42	32.22	32.78	33.46	34.17
ROB	5.28	7.32	8.10	8.97	9.58	10.16	10.72
Maximum depth(m)	3.06	3.65	4.00	4.41	4.69	4.96	5.22
Total velocity(m/s)	1.96	2.39	2.63	2.91	3.10	3.27	3.44
(Inundation area) (m^2)	71.02	92.48	105.05	122.50	134.26	145.79	157.30
Flow (m^3/s)	139.55	221.23	279.44	356.71	416.4	477.39	540.5

The detail output table result in table 33 of river station (RS.1100) indicates; at pre-determined return period of 2, 5, 10, 25, 50, 100 and 200 years flow, the flood depth are 3.06, 3.65, 4.00, 4.41, 4.69, 4.96 and 5.22 meters and inundation area: 71.02, 92.48, 105.05, 122.50, 134.26, 145.79 and 157.30m^2. From detail output table Water level-inundation area and water level-return period relationship can be depicted in the figure 42 and 43 for river station (RS.1100) shown as follows:-

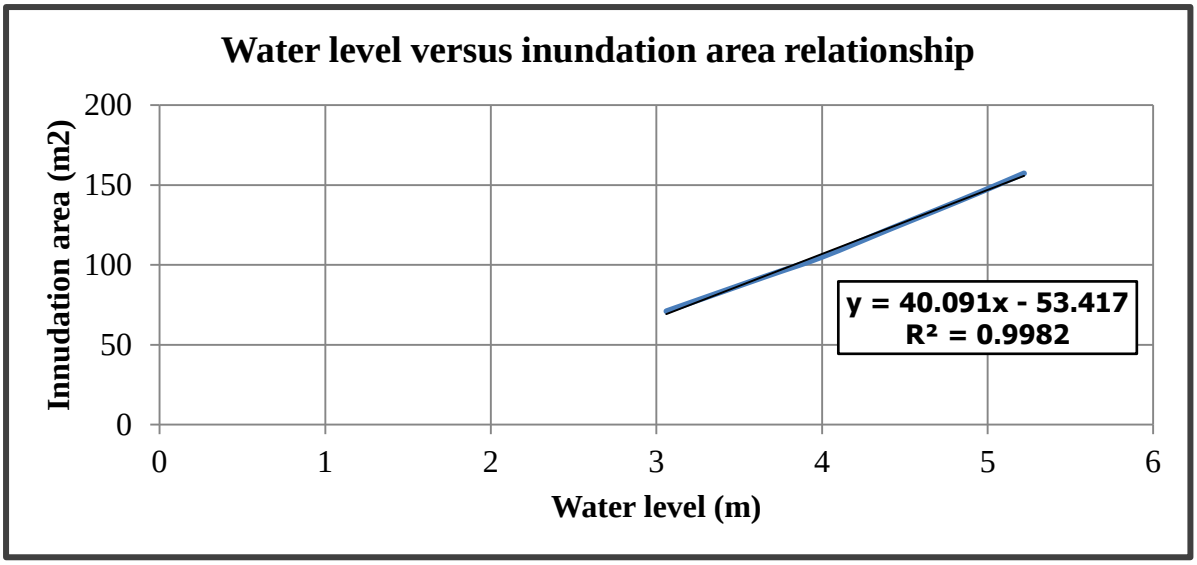

Figure 42: Water level-inundation area relationship of river station 1100

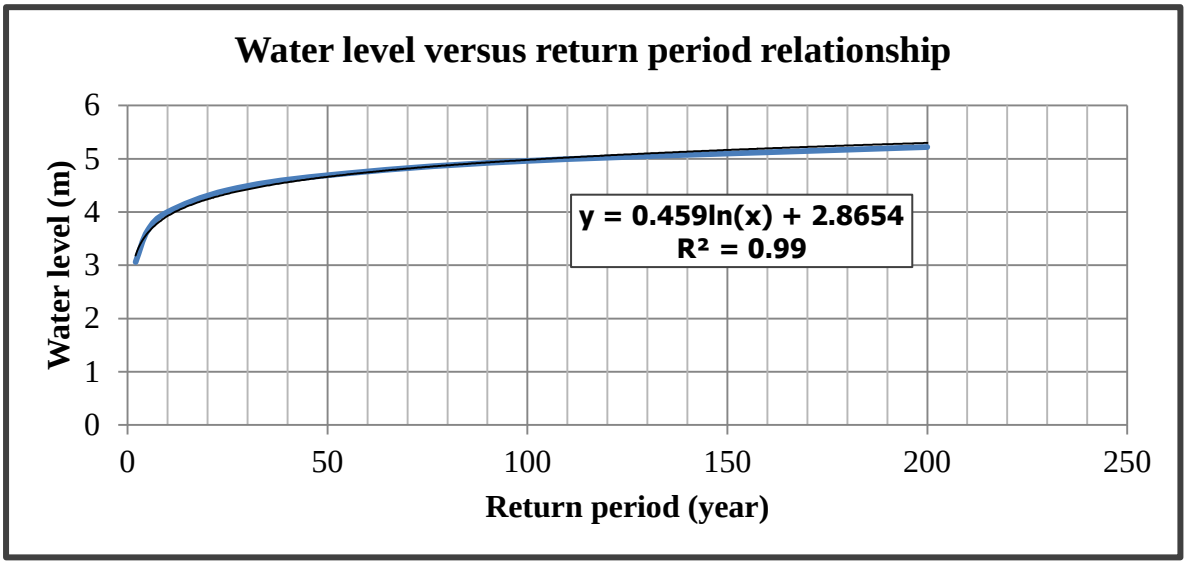

Figure 43: Water level-return period relationship for river station 1100

From the above figures we can determine water level at any required return period and at any water level we can estimate the inundation area. The inundation area indicates the extent of flooding area whether it needs early mitigation measure.

4.8.1.2.Result of River Station 2050 (RS. 2050)

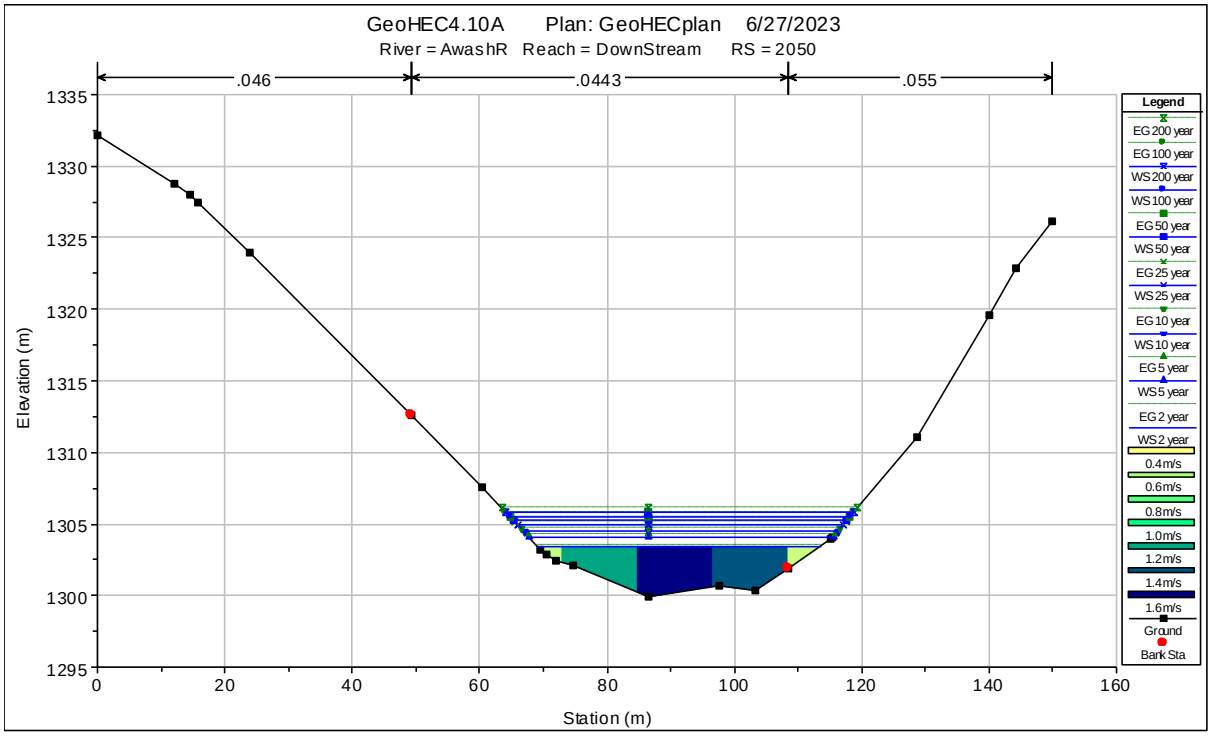

Figure 44: Cross section view of RS 2050 with different flow profile and velocity distribution

The total width of river station 2050 (RS.2050) is 150m and the lowest elevation at the bed of cross section is 1300 m.a.s.l and the highest bank level is between 1326.5 and 1334 m.a.s.l , the forecasted flood level at any profile not greater than 1310 m.a.s.l but the highest bank level is greater than 1326.5 m.a.s.l. This forces to conclude the cross section sufficiently holds all forecasted flood level.

Table 34: Overall result of river station 2050 cross section from detail output table of the model

Description	2yr	5yr	10yr	25yr	50yr	100yr	200yr
Top width(m) LOB	0	0	0	0	0	0	0
Channel	39.23	40.59	41.38	42.31	42.96	43.58	44.18
ROB	5.26	7.20	7.92	8.75	9.34	9.90	10.43
Maximum depth (m)	3.54	4.19	4.57	5.01	5.32	5.62	5.90

Total velocity (m/s)	1.37	1.68	1.86	2.07	2.21	2.34	2.46
Flow area (inundation), m^2	101.85	131.75	150.08	172.35	188.44	204.09	219.3
Flow (m3/s)	139.55	221.23	279.44	356.71	416.4	477.39	540.5

The detail output table result in table 34 of river station (RS.2050) depicts that at forecasted return period of 2, 5, 10, 25, 50, 100 and 200 years flow, the flood depth are 3.54, 4.19, 4.57, 5.01, 5.32, 5.62 and 5.90 meters and inundation area: 101.85, 131.75, 150.08, 172.35, 188.44, 204.09 and 219.37m^2.

The relationship between water level-inundation area and water level-return period can be developed in the figure 45 and 46 using the HecRAS model detail output table of river station (RS.2050) shown as follows:-

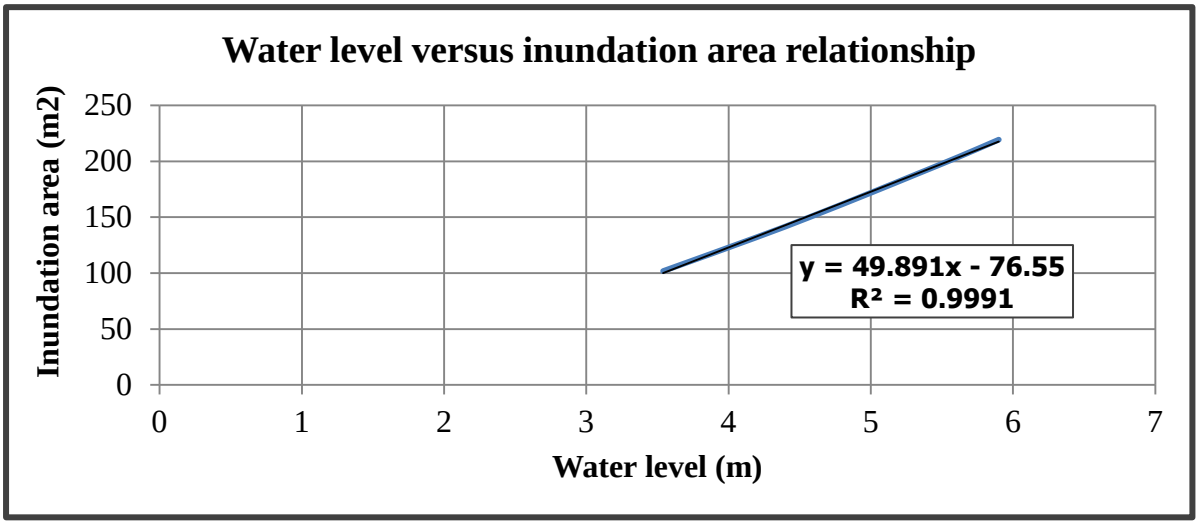

Figure 45: Water level-inundation area relationship of river station 2050

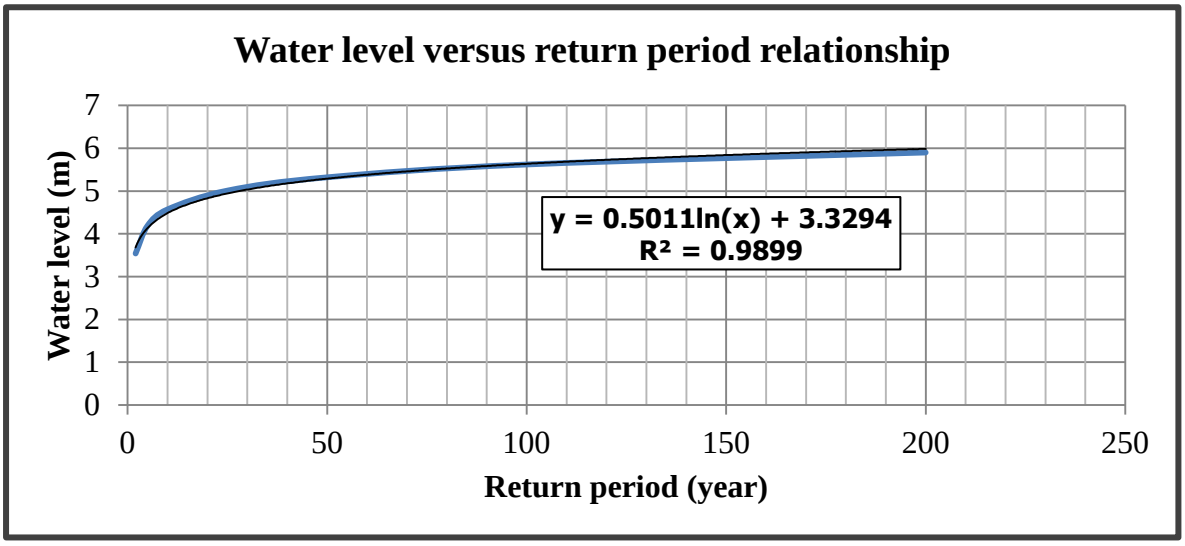

Figure 46: Water level-return period relationship for river station 2050

4.8.1.3. Result of X, Y, Z perspective view of series of the cross section

The areas susceptible to flood event can be recognized by analyzing x, y and z perspective view of series of river cross section. From the figure 47 the x, y and z perspective view of 17 successive river station with 50m interval (i.e. stands from river station 1100 to river station 300), it can be clearly see that the cross section end points extends to the right and left over bank (i.e.150m total width of cross section) to hold all profile simulated water. So, no flows over flood from each cross section. That means each cross section have the capacity to hold any of forecasted flood events sufficiently within the total width of cross section (150m). In addition, the settlement and the land in the vicinity of the cross sections are not venerable to inundation. The xyz perspective view can lead us to set our preliminary decision where is good location for the plant and encourages as to review our design and planning in terms of cost, stability, suitability and over all analysis of the hydropower development.

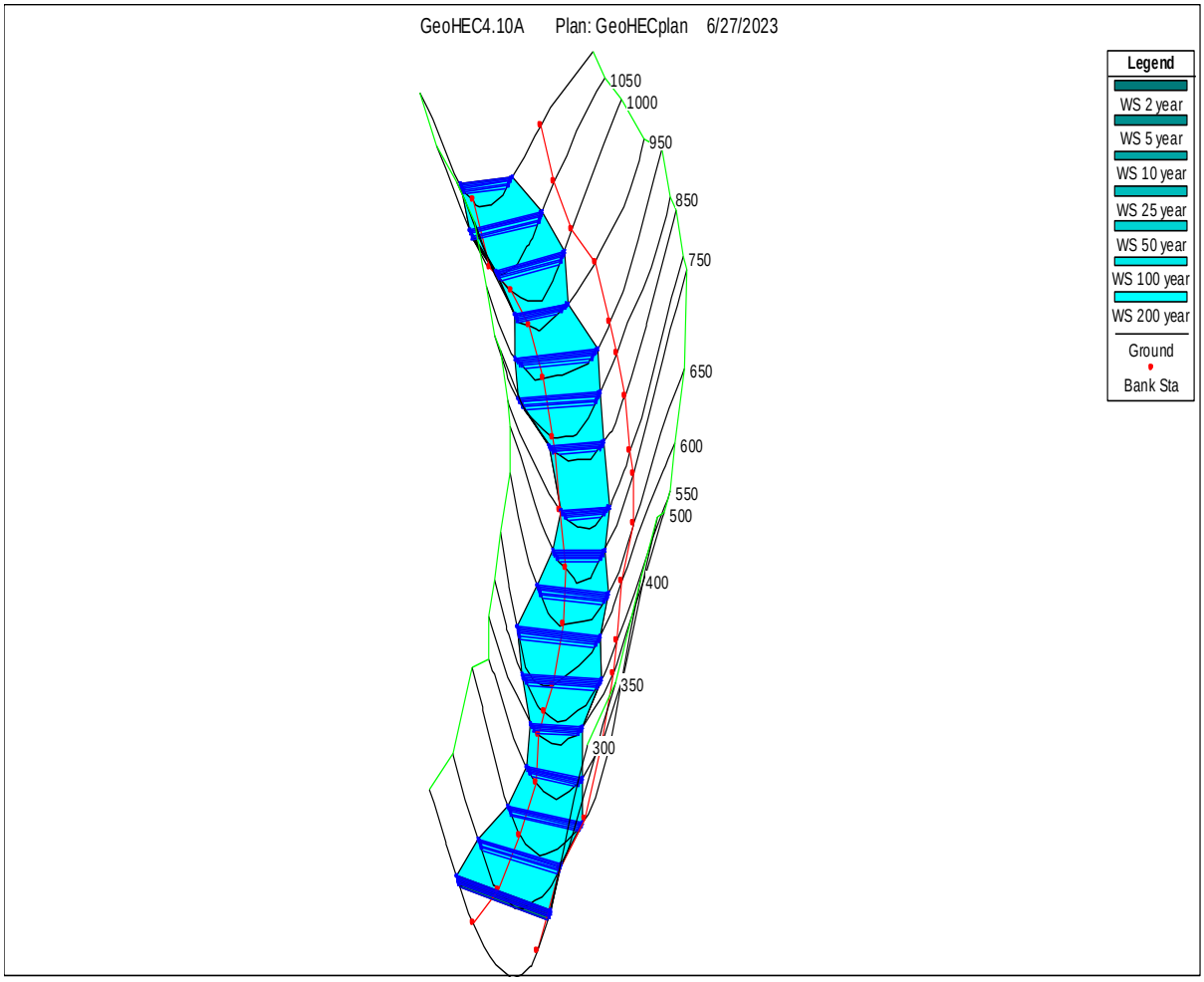

Figure 47: Perspective view of flood plain for different water surface profile

The xyz perspective view of the above figure starts at R.S. 1100 and ends at R.S. 300. The elevation difference of site one measured between these two points.

4.9. Calibration and validation of hydraulic model

4.9.1. Calibration of manning roughness coefficient

Manning's roughness-coefficient is the only one parameter used for model calibration and validation in the present analysis. Roughness coefficient is sensitive parameters used to reflect the resistance to flow at the channel bottom.

According to United State Department of transportation (1984) the study selects different roughness value for ROB, channel and LOB. To get the difference between simulated water depth and observed water depth within the allowable criteria, the study nominated the roughness value to be between 0.049-0.055 for ROB, 0.0373-0.0443 for channel and 0.039-0.046 for LOB after a number try and error. So the model was run between these ranges. Finally, after a number of trials the assessment finalize **0.046**, **0.0443** and **0.055** roughness coefficient for LOB, Channel and ROB dedicated to be the optimum values. The performance evaluation for maximum, minimum and optimum roughness coefficient (n) discussed in table 36, 37, 38 and 39 for R.S. 1100 and R.S.2050.

4.9.2. Model validation

Model suitability can be evaluated based on the difference between simulated water depth and observed water depth by performing the different statistical test. Model performance is necessary for the checking applicability of simulation. Forecasted water level (observed) for return period of 2, 5, 10, 25, 50, 100, 200years of profile used to compare the maximum simulated water depth from hydraulic modeling in Hec-RAS 6.3. Forecasting of water level made for 10 years maximum annual water depth (2012 to 2021) as follows.

4.9.2.1. Forecasting observed Water level

Hydraulic model in HEC-RAS 6.3 run for 2, 5, 10, 25, 50, 100 and 200year profiles. Thus, we need the observed flood level for these profiles for accuracy assessment. Therefore, the observed 10 year flow depth has to be forecasted for the predefined profiles.

Based on, statistical test, importance of the scheme and to be coherent with stream flow forecasts; the study forecasted water level using Log-pearson type III distribution using the procedure in method (page: 53). Annual maximum water depth is available at annex 25.

Using log-pearson type III distribution the following is computed: logarithm of skew (G): **0.5427**, logarithm of mean: **0.547** and logarithm of standard deviation (s): **0.078**. To get K factor for a given return period and logarithm of skew (G) interpolated using K values for log-pearson type III at annex.7.

Table 35: Forecasted water level for specified profile using Log-pearson type III distribution (observed water level)

Return period	K factor	$\log X_T = \overline{X} + K * S$	$X_T = \text{antilog}(\log X_T)$,(m)
2	-0.09	0.540	**3**
5	0.80	0.610	**4**
10	1.33	0.650	**4**
25	1.92	0.697	**5**
50	2.33	0.728	**5**
100	2.71	0.757	**6**
200	3.08	0.787	**6**

To validate the applicability of the model, the simulated flood depth at specified profile has to be compared with observed flood depth. To see to what extent they relate the study used the following statistical test for selected river stations (RS. 1100 and RS. 2050) in table 36 below.

The study made model performance evaluation for 25, 50, 100 and 200 return period. This is because of the purpose of the study is about potential assessment and it needs more care in designing and planning session of the scheme to use it for a longer period of time.

Table 36: The model performance evaluation of R.S. 1100 for maximum and minimum n values

Accuracy assessment for R.S.1100				Performance values					
				For min n values			For max n values		
Return period (yr)	Observed WL (m)	Simulated WL For min n values (m)	Simulated WL For max n values (m)	ENS	PBIAS	R	ENS	PBIAS	R
2	3	3.06	3.06						
5	4	3.64	3.65						
10	4	3.99	4.00						
25	5	4.39	4.41	0.02	-9.84	0.56	0.82	-4.37	0.96
50	5	4.67	4.69	0.78	-4.95	0.96	0.8	-4.67	0.97
100	6	4.93	4.96	0.68	-8.67	0.96	0.7	-8.29	0.97
200	6	5.19	5.22	0.67	-3.58	0.98	0.7	-3.39	0.98

According to (moriasi et al., 2007) the statistical test to check model predictability in R.S 1100 indicates that ENS values for maximum n values more predictor than for minimum n values, PBIAS shows very good to indicate accurate model simulation and R values indicates that there is strong linear relationship between observed and simulated water depth.

Table 37: The model performance evaluation of R.S. 2050 for maximum and minimum n values

Accuracy assessment for R.S.2050				Performance values					
				For min n values			For max n values		
Return period (yr)	Observed WL (m)	Simulated WL For min n values (m)	Simulated WL For max n values (m)	ENS	PBIAS	R	ENS	PBIAS	R
2	3	3.51	3.54						
5	4	4.14	4.19						
10	4	4.51	4.57						
25	5	4.95	5.01	0.78	7.8	0.96	0.74	8.84	0.96
50	5	5.26	5.32	0.78	7.52	0.96	0.74	8.48	0.97
100	6	5.55	5.62	0.86	5.13	0.97	0.83	5.92	0.96
200	6	5.83	5.90	0.89	4.09	0.97	0.88	5.09	0.97

According to (moriasi et al., 2007) the table result of R.S. 2050 to test model efficiency for maximum and minimum n values ENS shows very good predictability, PBIAS shows very good model simulation and R indicates that there is strong linear relationship between observed and simulated water depth.

Table 38: The model performance evaluation of R.S. 1100 for optimum n values

Accuracy assessment for RS.1100			Performance value		
			For optimum n value		
Return period (year)	Observed WL (m)	Simulated WL for optimum n values (m)	ENS	PBIAS	R
2	3	3.06			
5	4	3.65			
10	4	4.00			
25	5	4.41	0.82	-4.37	0.96
50	5	4.69	0.8	-4.67	0.97
100	6	4.96	**0.7**	**-8.29**	**0.97**
200	6	5.22	0.7	-3.39	0.97

The model performance evaluation for R.S. 1100 for optimum n values shows that ENS result indicates good match of the modeled values to the observed value for return period 100 and 200 year and a complete match for return period 50year. The PBIAS shows very good model

simulation. And the correlation coefficient (R) depicts that there is strong linear relationship between observed and simulated water depth.

Table 39: The model performance evaluation of R.S. 2050 for optimum n values

Accuracy assessment for RS.2050			Performance value For optimum n value		
Return period (yr)	Observed WL (m)	Simulated WL for optimum n values	ENS	PBIAS	R
2	3	3.54			
5	4	4.19			
10	4	4.57			
25	5	5.01	0.74	8.84	0.96
50	5	5.32	0.74	8.48	0.97
100	6	5.62	**0.83**	**5.92**	**0.96**
200	6	5.90	0.88	5.09	0.97

The performance of the model from table 39 for optimum n values shows that the ENS and PBIAS values very good model predictor and the correlation coefficient (R) depicts that there is strong linear relationship between observed and simulated water depth.

5. CONCLUSION AND RECOMMENDATION

5.1. Conclusion

A drastic increase of population, socio-economic development, urbanization, living standards with fast growing industry and agriculture has put a diversified pressure on energy demand. Therefore, to overcome the problem assessment of the available potential power at the targeted area is mandatory. The study used nearby available topography and stream flow to assess the potential site at 50km downstream of Koka dam. The study area covers 2,872km^2 and the assessment focuses on suitable type of hydropower that is not adversely affecting the surrounding environments.

The research has been selected three potential sites based on their available flow, head, accessibility, geology, soil, gorge and the distance from nearby town.

The assessment of Analytical hierarch process to select the most prioritized site indicates that, site one had 63%, site two had 26% and site three had 11% weight (importance). Based on the relative weight, qualitative and quantitative values of each criterion and alternatives, site one was selected as most suitable site.

The study developed flow duration curve to assess the variability of flow with time for each selected site. The flow duration at mostly prioritized site (site one) indicated by highest flow region with percent of time 10%-0% and flow equaled 59.67m3/s-238.54m3/s and relatively steep slope curve, the region of flow duration curve cover percent of time (10%-20%) of the year have comparatively moderate slope with flow of 46.32m^3/s to 59.67m^3/s. The shape of the curve from 20% to 85% of the year have almost flat slope occurring from 73 to 311 days of the year with constant flows (46.32m^3/s to 26.47m^3/s). And the flow ranges from 13.82m^3/s to 26.47m^3/s which occur with percent of time 85% to 100% available most of the year (311 to 365 days of the year). The average flow, which determine the plant capacity was 42.17m^3/s and dependable flow that would be occur 347 day of the year has quantified 19.71m^3/s.

The maximum theoretical, technical power and the annual energy potential for the mostly preferred site were assessed (8981kw, 6960kw and 61Gwh/year) for flow of 42.17m^3/s and the minimum power (4197kw, 3253kw and 28Gwh/year) for flow of 19.71m^3/s.

The study include flood level forecasting at site one to be more safe from the coming flood event at specified return period. The inundation area and the maximum flood depth at mostly

prioritized site one of river station 1100 were assessed (71.02m2, 3.06m), (92.48m2, 3.65m), (105.05m2, 4.00m), (122.5m2, 4.41m), (134.26m2,4.69m), (145.79m2, 4.96m) and (157.30m2, 5.22m) respectively for 2, 5, 10, 25, 50, 100 and 200 years return period.

The performance of spatial data in Arc-GIS to predict the elevation information checked using statistical result of RMSE and the result was 0.71.

The applicability of hydraulic modeling was assured by calibration of roughness (n). The allowable roughness values were 0.046, 0.0443 and 0.055 for LOB, Channel and ROB and following the calibration the graphical and statistical results during calibration and validation period showed adequate model performance with ENS, PBIAS and R values of 0.7, -8.29 and 0.97 for RS.1100 and 0.83, 5.92 and 0.96 for RS.2050, respectively for 100 year return period.

The successive cross sections in x, y and z perspective view indicates that at upstream and downstream of prioritized suitable site had the capacity to hold any of forecasted floods sufficiently within the total width of cross section (150m). So, the settlement and the land in the vicinity of the selected locations are not venerable to inundation.

5.2. Recommendation

Awash River at the downstream of koka dam, specifically 31.8km below Awash melkasa have the capacity to produce 60.09GWh/year annual energy with the head of 21.71m and stream flow 42.17m3/s. Consequently, it is possible to tackle the problem of highly increased and diversified electric demands at specific study area with locally available natural resources using environmentally friendly run-of river hydropower scheme. Hence, it is recommended that the government at national as well as local level or any other agency should look over it in detail and finding to implement thorough investigation of the area.

It is recommended that, to use run of the river hydropower scheme with storage according to extent of demand to get more reliable energy supply during driest season without difficulty to manage the negative effect on the surrounding environment.

It is recommended that, the assessment of sediment has to be included in the study. Since, it is one of the critical factors that alter the proper functioning of turbine-generator.

It is suggested that more hydrological data needs to be collected with successive network of gauging station over a period of time to get more reliable flow data.

6. REFERENCES

Aaron, C. C. 2008. Comparison of one-dimensional HEC-RAS with two-dimensional FESWMS model in flood inundation mapping.

ABEBE, H. M. 2001. Sedimentation in the Koka Reservoir, Ethiopia. In: B. Honningsvag, G. H. Midttomme, K. Repp, K. Vaskinn und T. Westeren (Hg.): Hydropower in the new Millenium. Proceedings of the 4th International Conference on Hydropower Development. International Conference on Hydropower Development. Bergen, Norway, 20-22 June 2001. Lisse, Netherlands: A.A. Balkema, p. 345–350.

Adedokun, G., J. A. Oladosu., and T. K. Ajiboye. 1979. Small Hydro Power Potential Capacity Estimation for Provision of Rural Electricity in Nigeria. 1,2. 3 (1):117– 20.

Afshari, A., Majid, Mojahed dan, R.,and Mohd, Y. 2010. Simple Additive Weighting approach to Personnel Selection problem. International Journal of Innovation, Management and Technology, Vol. 1, No. 5, December 2010.

Alemgna, K. J. 2019. Regional Flood Frequency Analysis for Upper Wabi-Shebelle River Basin, Ethiopia. (Jimma University).

Anderson, J. H. 1976. A Land Use and Land Cover Classification System for use with Remote Sensor Data. Geological Survey Professional Paper 964.

Asirat, T., Yonas, T., and Endalkachew, A. 2020. Assessment of Hydropower Potential Using Geospatial Technology. Case Study of GunaTana Landscape Upper Abay Basin, Ethiopia. Debre Tabor University.

Bates, P.D., Horritt, M.S., Hunter, N.M., Mason, D., and Cobby, D. 2005. Numerical modelling of floodplain flow. Computational Fluid Dynamics: Applications in Environmental Hydraulics, 2005 John Wiley & Sons, Ltd. 271 – 297.

Biswadeep, B., and Utpal, K. M. 2022. Numerical Approach for Channel Flood Routing in an Ungauged Basin: a Case Study in Kulsi River Basin, India.

Botes, ZA., and Smith. 2010. A New Spatial Planning Tool for the Delineation of Flood Risk Areas. Planning Africa 2010 Conference. South African Planning Institute.

Brandt, S.A. 2005. Resolution issues of elevation data during inundation modeling of river floods. Proc. XXXI Int. Association of Hydraulic Engineering and Research Congress, Water Engineering for the Future: Choices and Challenges, September 11 – 16, Seoul, Korea: 3572 – 3581.

Brunner, P. 2013. Advance in hydrological engineering, unsteady flow hydraulics model of lower Columbia River system.

Buehring, W., Huber, C., Marques de Souza, J. 1984. Power system expansion planning for electrical generating systems -A Guidebook, Technical Report Series No. 241, IAEA, Vienna, Austria.

Casas, A., Benito V.R., Thorndy craft, V.R., and Rico M. 2006. The topographic data source of digital

Chow, V.T., Maidment, D.R., and Mays, L.W. 1988. Applied Hydrology. McGrow-Hill Book, Inc.

Cobb, B. R., and Sharp, K. V. 2013. Impulse (Turgo and Pelton) turbine performance characteristics and their impact on pico-hydro installations. Renewable Energy, 50, 959-964.

Condie, R. 1997. The log Pearson type 3 distribution: The T-year event and its asymptotic standard e"or by maximum likelihood theory, Water Resources Research, 13(6), 987-991.

Copestake, P., and Young, A. 2002. How Much Water Can a River Give? Uncertainty and the Flow Duration Curve . British Hydrological Society (BHS), 10th National Hydrology Symposium, Exeter, United Kingdom.

Cowan, W.L. 1956. Estimating hydraulic roughness coefficients. Agricultural Engineering, v. 37, no. 7, p. 473-475.

David, R. M. 1998. Hand Book of Hydrology, published by McGraw-Hill Incorporation, New York.

Davis. 1992. Design and construction of urban storm water management systems. Institute for Water Resources Hydrologic Engineering Centre. Urban Water Resources Research Council. Reston: American Society of Civil Engineers and the Water Environment Federation.

Dragan, S., and Slobodan, P. 2009. Vulnerability of Infrastructure to Climate Change. Water Resources Research Report City of London: Background Report 2 Hydraulic Modeling and Floodplain Mapping, London.

Edossa, D. C., Babel, M. S., and Gupta, A. D. 2010. Drought analysis in the Awash river basin, Ethiopia. Water resources management, 24(7), 1441-1460.

EELPA. 1964. The Ethiopian Electric Light and Power Authority Project Ethiopia.

Eliyas, B. T. 2018. Floodplain Mapping and Modeling for Geray River," FHWA-RD-03-053.

FESWMS FST2DH User's Manual. 2002. Federal Highway Administration. Publication number FHWA-RD-03-053.

Fread, D.L. 1993. Flow routing. In: (ed.) Maidment, DR, Hand Book ofHydrology. Ch. 10.

Gary, B. W. 2016. HEC-RAS River Analysis System Hydraulic Reference Manual. Washington DC.: US Army Corps of Engineers, Hydrologic Engineerig Center.

GEORGE, J., ARCEMENT, JR., and VERNE, R. 1989. Guide for Selecting Manning's Roughness Coefficients for Natural Channels and Flood Plains.

Gerald, C.C. 2016. Micro Hydro Potential Modelling - Integrating GIS into Energy Alternatives for Climate Change Mitigation. (University of Nairobi).

Getenet, W. 2019. Assessment of micro to small hydropower potential site. (A case study on Chemoga River, Upper Blue Nile, Ethiopia).

Hall, G. 2009. School of Graduate Studies Calendar Earth.

Hamisi, J. 2013. Study of Rainfall Trends and Variability Over Tanzania a Research Project Submitted in Partial Fulfilment of the Requirements for the Postgraduate Diploma in Meteorology University of Nairobi. Research Project (August).

HEC-RAS. 2010. Hydraulic Reference Manual (version: 4.1), U.S. Army Corps of Engineering, Davis.

Hortness, J. E. 2006. Estimating low flow frequency statistics for unregulated streams in Idaho. US Geol. Survey. Sci. Invest. Report 2006-5035.

Hudson, J., Inácio, F., José, R., Juliana, A., Sebastião, C., and Guimarães, J. 2016. Assessment of the Potential of Small Hydropower Development in Brazil. Renewable and Sustainable Energy Reviews 56:380–87.

Ian, H. 2010. An Introduction to Geographical Information Systems. Pearson Education India.

Imru, M. 1992. Sedimentation in the Koka reservoir, Ethiopia; possibilities of prediction and control. MSc thesis, Int. Inst, for Hydraul. & Environ. Engng, Delft, the Netherlands.

Ismail and Ibrahim. 2017. Estimation of rainfall and stream flow missing data for Terengganu, Malaysia by using interpolation technique methods.

Kemal, A. 2020. Evaluating the impact of land use land cover change on stream flow of birr watershed.

Kerim, T., Abebe, A, and Hussen, B. 2016. Study of Water Allocation for Existing and Future Demands under Changing Climate Condition: Case of Upper Awash Sub River Basin. Environ. Earth Science, 6, 14.

Kong, F. Z., and Wang, X. Z. 2008. Method estimating Muskingum model parameters based on physical characteristics of a river reach. Journal of China University of Mining and Technology, 37(4), 494-497. (in Chinese)

Kshitij, U. 2015. Application of Analytical Hierarchy Process in Evaluation of Best Sewage Treatment Plant.

Kumar, A., and Tormod, S. 2009. Special Report Renewable Energy Sources: Hydropower. Intergovernmental Panel on Climate Change 70.

Kusre, B., Baruah, D., Bordoloi, P., Patra, S. 2010. Assessment of hydropower potential using GIS and hydrological modeling technique in Kopili River basin in Assam (India). Applied Energy, 87, 298-309.

Macavoy, S. 2012. Alternative Energy Solutions . Hydro-Electric and Tidal Energy 1–24.

Marcus, O., Thomas, Ö., and Niklas L. P. L. 2021. Management strategies for run-of-river hydropower plants: an optimal switching approach.

Matalas, N.C.,and Wallis, J.R Eureka. 1973. It Fits a Pearson Type 3 Distribution. Water Resources Research, 9(2), 281-289.

Matjaž, G., and Marina, P. 2012. Strengths, Weaknesses, Opportunities and Threats of Catchment Modeling with Soil and Water Assessment Tool (SWAT) Model. Water Resources Management and Modeling, Dr. Purna Nayak (Ed.), ISBN: 978-953-51-0246-5, InTech.

Mbaka., John, G and., Mercy M. 2016. Small Hydro-Power Plants in Kenya : A Review of Status, Challenges and Journal of Renewable. (September 2017):19– 26. McGraw-Hill, New York, USA, 1-36.

Mehari K. 2017. GIS based assessment of hydropower potential. (A case study on Gumara River Basin).

Melo, I., Tomasik, B., Torrieri, G., Vogel, S., Bleicher, M., Korony, S., and Gintner, M., 2009. Kolmogorov-Smirnov test and its use for the identification of fireball fragmentation. Phys Rev C, 80(2), Artn 024904.

MH Tewolde. 2005. Flood Routing in ungauged catchments using Muskingum methods.

Millington, N., Das, S., and Simonovic, S.P. 2011. The comparison of GEV, Log-Pearsontype 3 and Gumbel distributions in the Upper Thames river watershed under global climate models. Water Resources Research Report No. 077, 1913-3200.

Ministry of Water Irrigation and Electricity FDRE. 2017. A Renewable Future. The Ethiopian Power Sector:. Berlin Energy Transition Dialogue (March):18.

Mohammed, T.A., Said, S., Bardaie, M.Z., and Basri, S. 2006. One-Dimensional Simulation of Flood Levels in a Tropical River System Using HEC-2 Model. Joint International Conference on Computing and Decision Making in Civil and Building Engineering, June 14 – 16 : Montreal, Canada.

Moriasi, D.N., Arnold, J.G., Van Liew, M.W., Bingner, R.L., Harmel, R.D., and Veith, T.L. 2007. Model Evaluation Guidelines for Systematic Quantification of Accuracy in Watershed Simulations. ASABE, 50, 885–900

Moura.Z.,Bias,E.d.S.,andBrites,R.2014.Avaliaçãodaacuráciaverticaldemodelosdigitaisdeelevação(MDEs)nasbaciasdoParanoáe São Bartolomeu. Rev. Bras. Cartogr, 66, 1–14.

Mulugeta, S., Fedler, C., and Ayana, M. 2019. Analysis of Long-Term Trends of Annual and Seasonal Rainfall in the Awash River Basin, Ethiopia. Water, 11(7), 1498.

Najim. 2013. Application of the HEC-HMS model for runoff simulation in a tropical catchment. Environ. Model vol (46), pp.155–162.

Okot, D. K. 2013. Review of small hydropower technology. Renewable and Sustainable Energy Reviews, 26, 515-520.

Omer C.R., Nelson E.J., and Zundel A.K. 2003. Impact of varied data resolution on Hydraulic Modeling and Floodplain Delineation. Journal of the American Water Resources Association 39 (2), 467- 475.

OWWDSE. 2014. Upper Awash Sub Basin Integrated Land Use Planning Study. Addis Ababa.

Pakgohar, A. 2014. Using Easy Fit Software for Goodness-of-Fit Test and Data Generation. International Journal of Mathematical Archive-5(1), 7(118-124).

Phien, H.N.,and Ajirajah, T.J. 1984. Application of the log-pearson type-3 distribution in hydrology. Journal of hydrology 73 (3-4), 359-372.doi: 10.101610022-1694(84) 90008-8.

Polidori, L., El Hage, M., and Valeriano, M.D.M. 2014. Digital elevation model validation with no ground control: Application to the topodata DEM in Brazil. Bol. Ciências Geodésicas, 20, 467–479. [CrossRef]

Rajnish, K., and Dr. Jayant, N. 2014. Consistency in the Analytic Hierarchy Process.

Rajput, R. K. 2008. A textbook of Power Plant Engineering. New Delhi: Laxmi Publications Limited.

Rizzoli, P., Martone, M., Gonzalez, C., Wecklich, C., Borla Tridon, D.. Bräutigam, B.,Bachmann, M., Schulze, D., Fritz, T.,and Huber, M. 2017. Generation and performance of DEM.

Rotilio, M., Chiara, M., and Pierluigi De Berardinis. 2017. The Small Scale Hydropower Plants in Sites of Environmental Value. An Italian Case Study Sustainability (Switzerland) 9(12).

Saaty, T.L. 1980. The Analytic hierarchy process: Planning, priority setting, resource allocation. ISBN 007-054371-2. New York McGraw-Hill.

Sanoj, S. 2014-2015. Small Hydropower: Feasible Location, Potential and Installation in Odisha.

SHAHIN, M. M. A. 1993. An overview of reservoir sedimentation in some African river basins. In Proceedings of the Yokohama Symposium, July 1993. Sediment Problems: Strategies for Monitoring, Prediction and Control, July 1993. IAHS. Pub. no. 217: IAHS, p. 93–100.

Singh, D. 2009. Micro-hydro-power: Resource Assessment Handbook. New Delhi, Renewable Energy Cooperation-Network for Asia Pacif

Sinnakaudan, S., Ab Ghani A.,and Chang C.K. 2002. Flood inundation analysis using HEC-6 and ArcView GIS 3.2a. In Proceeding, 5th International Conference on Hydro-Science & Engineering, September 18–21, Warsaw University of Technology, Poland.

Stol, Ph.Th. 1965. On Quantative Methods for Analysing Hydrologic Data. In: Proceedings ofihe Seminar of ECAFE Regions 1965166 on the Use and Inierpretation of Hydrologic Daia. United Nations' Water Resources Series 34. United Nations, New York.

Tallaksen, L., and Van Lanen, H. 2004. Hydrological Drought: Processes and Estimation Methods for Stream Flow and Groundwater. 1st Ed. Amsterdam: Elsevier Press.

Tayefi, V., Lane, S.N., Hardy, R.J., and Yu, D. 2007. A comparison of one- and two-dimensional approaches to modeling flood inundation over complex upland floodplains. Hydrologic Processes 21 : 3190 – 3202.

Tefera, B. S. 2015. Flood mitigation alternatives for selected reachs of awash river from logiya to dubti. (Student thesis in ADDIS ABABA UNIVERSITY).

Tewolde, M. H., and Smithers, J. C. 2006. Flood routing in ungauged catchments using Muskingum methods. Water SA, 32(3), 379-388.

Thomas L. Saaty. 1990. How to make a decision: The Analytic Hierarchy Process. European Journal of Operational Research 48 ,9-26.

Todini, E. 2007. A mass conservative and water storage consistent variable parameter Muskingum-Cunge approach. Hydrology and Earth System Sciences Discussions, 11(4), 1549-1592. [doi:10.5194/hessd-4- 1549-2007]

Trade, Uk-ethiopia and Investment Forum. 2015. Ethiopian Electric Power the Ethiopian Energy Sector – Investment Opportunities.

US Army Corps of Engineers. 2002. HEC-RAS, River Analysis System User's Manual.

US Army Corps of Engineers. 2008. HEC-RAS, River Analysis System User's Manual. Version4,

Uysal, M., Toprak, A.S., and Polat, N. 2015. DEM generation with UAV Photogrammetry and accuracy analysis in Sahitler hill. Measurement 73, 539–543. [CrossRef]

Wang, F.G., and Wang, X.D. 2010. Fast and Robust Modulation Classification via Kolmogorov-Smirnov Test. Ieee T Commun, 58(8), 2324-2332.

Wein. 2015. Assessment of Run-Of-River Hydropower Potential and Power Supply Planning in Nepal using Hydro Resources.

Wilson, B. N., and Ruffini, J. R. 1988. Comparison of physically-based Muskingum methods. Transactions of the American Society of Agricultural Engineers, 31(1), 91-97.

WMO/GWP. 2003. Integrated Flood Management case study Ethiopia.

Xiao-meng, S., Fan-zhe, K., and Zhao-xia ZHU. 2011. Application of Muskingum routing method with variable parameters in ungauged basin.

Yang, J. 2010. Underwater tunnel piercing in refurbishment of Akkats power station. ICOLD Annual Meeting and Symposium, May 2010, Hanoi, Vietnam

Yang, J., Andreasson, P., Högström, C-M., and Teng, P. 2018. The tale of an intake vortex and its mitigation countermeasure: a case study from akkats hydropower station. Water 10(7):881

Yaynshet, W. 2020. Regional Flood Frequency Analysis. for zeway – shala sub basin, rift valley basin, ethiopia. (addis ababa university).

Yevjevich, V. M., and Jeng, Raymond Ing-song. 1969. Properties of non-homogeneous hydrologic time series. Hydrology papers (Colorado State University); no. 32.

Yildiz, V. 2015. Numerical simulation model of run of river hydropower plants: Concepts, Numerical modeling, Turbine system and selection, and design optimization.

Yohannis, B. T., and Peter, F. 2022. Modelling of Flood Inundation due to Levee Breaches: Sensitivity of Flood Inundation against Breach Process Parameters. (Hamburg University of Technology).

Yuksel, I. 2008. Hydropower in Turkey for a clean and sustainable energy future. Renew Sustain Energy Rev, 12:1622–1640.

Zemade, A. 2011. Assessing pathways, synergies and tradeoffs in alleviating poverty through sustainable ecosystem services in Sub-Saharan Africa. Situational Analysis 3 Ethiopia and the River Awash Basin. Ripple Office Addis Ababa (Ethiopia).

Zuleid, A., Ferreira., and Pedro, C. 2022. A Comparative study about Vertical Accuracy of Four Freely Available Digital Elevation Models. A Case Study in the Balsas River Watershed, Brazil.

Zuo, Q., and Shikui, L. 2015. Effects of Dams on River Flow Regime Based on IHA / RVA. (August 2014):275–80.

7. APPENDEX

Annex 1: Longitudinal profile of site two

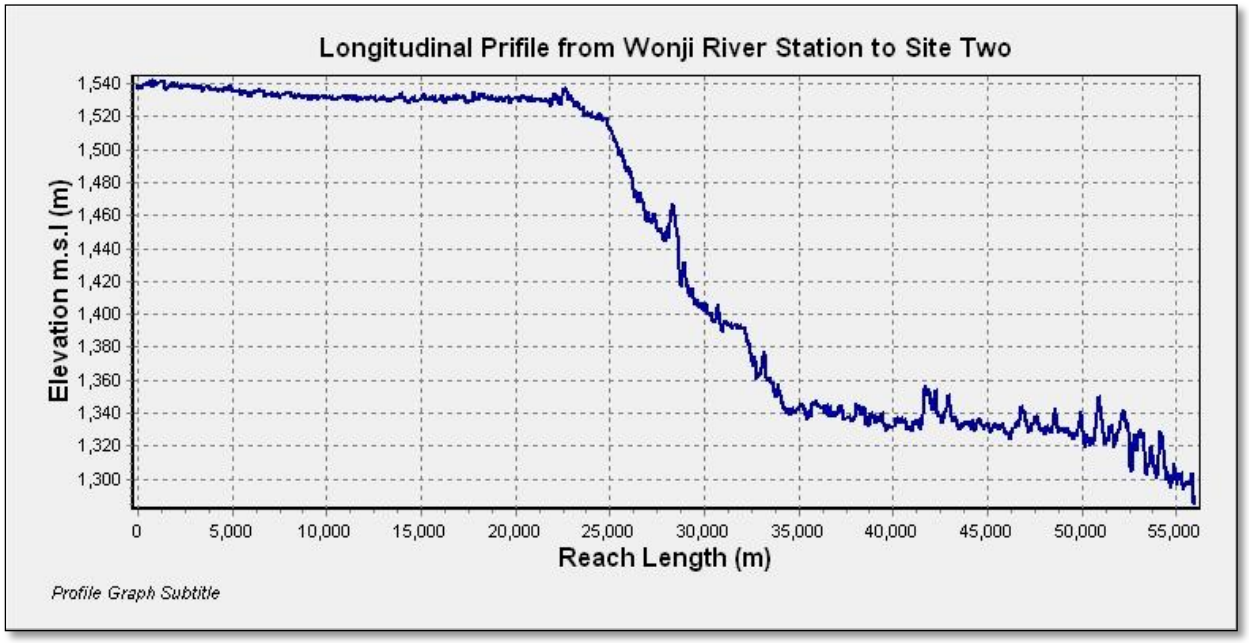

Annex 2: Longitudinal profile of site three

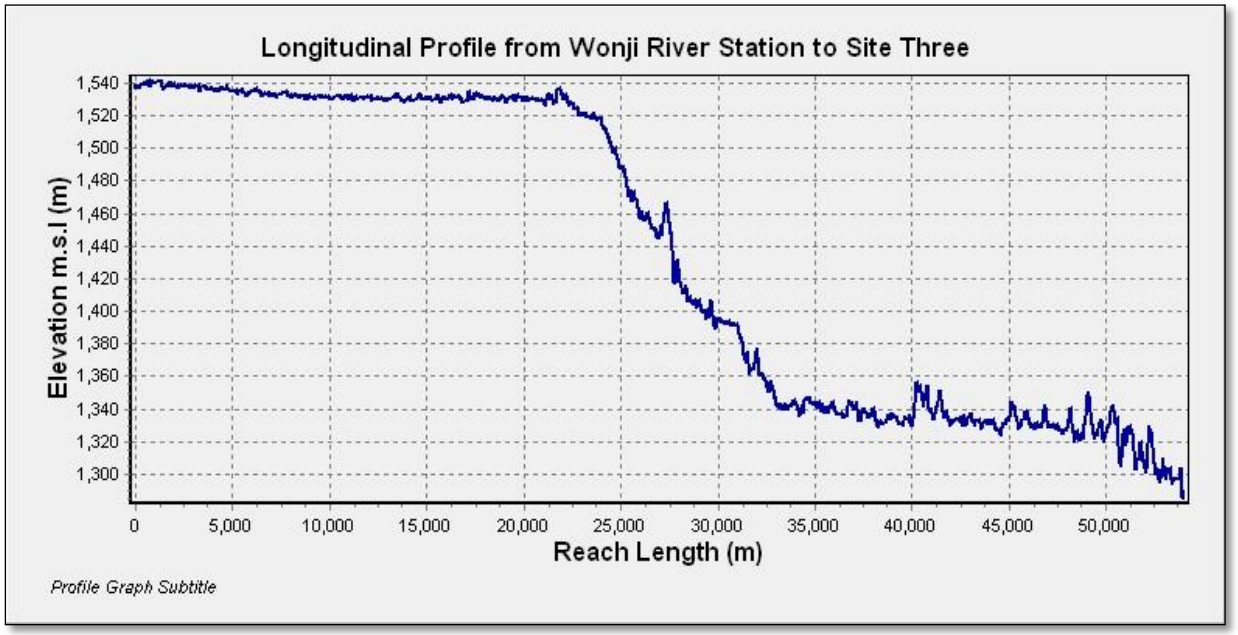

Annex 3: Long term (1991-2016) mean monthly stream flow of Wonji station (m^3/s)

Year	Mean monyhly stream flow Monthes of the year											
	Jan	Feb	Mar	Apr	May	Jun	Jul	Aug	Sep	Oct	Nov	Dec
1991	29.58	35.01	43.69	34.68	42.87	29.74	44.42	45.51	123.60	55.62	57.51	45.16
1992	69.67	55.69	28.60	29.32	34.23	28.19	18.88	21.33	68.53	32.36	30.53	31.12
1993	32.14	36.35	29.58	32.90	34.23	45.51	42.67	138.83	237.86	67.29	37.85	35.54
1994	33.93	33.98	36.88	35.48	29.86	36.92	42.36	46.09	49.11	42.08	49.66	43.62
1995	37.37	33.71	32.79	30.52	33.31	37.15	42.47	50.19	40.82	39.04	38.11	31.67
1996	33.55	33.64	36.56	36.40	36.25	38.19	42.08	188.37	112.02	36.53	30.92	33.81
1997	34.69	36.71	40.07	34.79	31.88	32.33	29.81	24.78	22.04	23.56	19.78	14.56
1998	14.61	13.95	13.83	15.23	14.83	17.36	19.47	155.57	107.13	45.98	31.37	31.30
1999	31.78	27.07	36.96	36.62	44.21	57.72	55.88	105.46	58.56	40.85	37.24	38.75
2000	34.73	29.32	28.94	29.21	46.37	40.98	29.26	46.33	44.80	42.15	25.56	19.73
2001	33.22	34.98	31.15	26.48	40.08	34.75	42.09	49.00	64.98	40.73	39.82	38.23
2002	37.57	37.13	37.43	37.76	38.95	40.31	44.41	48.53	45.07	36.93	17.77	18.43
2003	17.49	20.80	17.63	18.84	18.56	23.84	34.68	42.41	84.08	44.55	38.40	46.82
2004	40.34	37.92	36.77	40.60	36.75	41.84	44.93	41.05	32.83	30.22	25.58	26.02
2005	31.93	39.02	43.86	38.90	31.72	36.94	34.54	36.83	67.71	31.51	31.00	29.37
2006	27.60	33.97	35.79	47.41	46.27	48.18	32.34	98.02	157.07	38.79	28.25	29.61
2007	25.51	28.49	32.39	32.32	35.87	40.06	57.92	123.02	188.38	42.57	37.12	36.81
2008	36.17	37.14	37.32	44.93	46.13	30.89	36.62	59.61	139.05	54.65	34.79	38.72
2009	45.91	35.94	36.89	39.65	43.09	35.87	31.11	29.04	30.07	37.42	34.88	44.68
2010	36.67	30.71	31.16	32.82	38.23	36.36	50.53	84.07	129.27	43.50	37.13	39.73
2011	35.50	34.41	36.69	38.14	48.17	39.52	35.20	33.13	37.95	35.50	37.47	40.14
2012	38.11	34.41	32.94	33.76	34.12	38.96	53.07	99.10	148.80	42.37	39.82	52.82
2013	49.90	43.65	41.00	55.23	56.42	54.67	68.68	63.12	86.62	61.57	42.01	40.28
2014	23.55	22.55	22.47	22.90	24.75	29.48	51.76	105.20	59.28	36.80	34.63	26.44
2015	23.75	22.63	22.50	22.96	25.21	30.51	55.76	115.13	61.93	36.19	35.19	26.19
2016	23.41	22.21	22.29	22.73	25.29	30.53	56.66	115.81	58.55	32.64	33.45	24.95

Annex 4: Routed (Muskingum routing in HEC-HMS 4.10) mean monthly stream flow for site one ($m^{3/}s$)

Year	Mean monthly stream flow Monthes of the year											
	Jan	Feb	Mar	Apr	May	Jun	Jul	Aug	Sep	Oct	Nov	Dec
1991	29.552	35.132	43.474	34.793	42.916	29.583	44.481	45.355	123.743	55.597	57.413	45.306
1992	69.365	56.038	28.590	29.347	34.155	28.273	18.894	21.316	68.483	32.342	30.557	31.081
1993	32.158	36.350	29.577	32.870	34.252	45.503	42.542	138.161	238.543	67.426	37.873	35.500
1994	33.932	33.993	36.868	35.467	29.910	36.903	42.426	45.968	49.113	42.103	49.617	43.729
1995	37.371	33.661	32.842	30.507	33.294	37.300	42.310	50.135	41.083	38.855	38.107	31.697
1996	33.503	33.645	36.548	36.430	36.223	38.213	42.016	188.055	112.257	36.655	30.923	33.839
1997	34.661	36.714	40.045	34.823	31.881	32.363	29.810	24.803	22.033	23.539	19.820	14.558
1998	14.587	13.968	13.823	15.233	14.852	17.323	19.387	155.113	107.557	46.039	31.370	31.300
1999	31.771	27.079	36.948	36.547	44.277	57.560	56.010	105.100	58.920	40.874	37.227	38.739
2000	34.765	29.310	28.968	29.170	46.326	41.097	29.165	46.294	44.820	42.168	25.630	19.706
2001	33.206	34.957	31.165	26.470	40.061	34.770	42.110	48.874	65.067	40.726	39.830	38.223
2002	37.600	37.086	37.452	37.767	38.942	40.293	44.445	48.471	45.083	36.981	17.773	18.458
2003	17.500	20.907	17.523	18.837	18.535	23.873	34.674	42.358	84.083	44.565	38.253	46.923
2004	40.365	37.928	36.768	40.610	36.771	41.830	44.939	41.039	32.847	30.223	25.597	26.010
2005	31.845	39.068	43.832	38.973	31.719	36.807	34.684	36.781	67.640	31.623	31.023	29.326
2006	27.610	33.946	35.710	47.417	46.339	48.187	32.277	97.571	157.450	38.903	28.290	29.603
2007	25.516	28.493	32.358	32.310	35.868	40.037	57.839	122.626	188.710	42.752	37.063	36.845
2008	36.126	37.169	37.335	44.897	46.145	30.930	36.677	59.339	139.000	54.919	34.700	38.723
2009	45.955	35.936	36.874	39.613	43.152	35.857	31.126	29.026	30.093	37.406	34.820	44.826
2010	36.548	30.761	31.152	32.837	38.168	36.360	50.423	84.113	129.173	43.713	37.097	39.852
2011	35.387	34.429	36.648	38.133	48.148	39.520	35.235	33.155	37.940	35.494	37.487	40.123
2012	38.123	34.400	32.932	33.790	34.097	38.973	53.055	98.542	149.253	42.503	39.800	52.784
2013	49.929	43.679	40.971	55.190	56.448	54.633	68.761	63.058	86.607	61.568	42.070	40.303
2014	23.610	22.532	22.481	22.897	24.723	29.453	51.358	105.216	59.673	36.774	34.647	26.471
2015	23.748	22.614	22.506	22.957	25.184	30.473	55.335	115.197	62.317	36.171	35.220	26.229
2016	23.419	22.207	22.284	22.730	25.268	30.497	56.277	115.958	58.813	32.623	33.507	24.955

Annex 5: Routed (Muskingum routing in HEC-HMS 4.10) mean monthly stream flow for site two ($m^{3/}s$)

Year	Mean monthly stream flow Monthes of the year											
	Jan	Feb	Mar	Apr	May	Jun	Jul	Aug	Sep	Oct	Nov	Dec
1991	29.555	35.139	43.474	34.777	42.916	29.577	44.474	45.358	123.743	55.597	57.417	45.306
1992	69.377	56.031	28.603	29.347	34.158	28.273	18.897	21.306	68.497	32.352	30.553	31.084
1993	32.165	36.350	29.584	32.887	34.261	45.493	42.539	138.174	238.527	67.439	37.867	35.506
1994	33.942	33.989	36.865	35.477	29.910	36.890	42.429	45.961	49.097	42.113	49.617	43.710
1995	37.374	33.664	32.852	30.503	33.300	37.307	42.316	50.129	41.070	38.855	38.110	31.697
1996	33.497	33.648	36.552	36.433	36.219	38.210	42.029	188.058	112.250	36.648	30.930	33.848
1997	34.665	36.711	40.042	34.823	31.887	32.370	29.806	24.794	22.030	23.542	19.830	14.552
1998	14.597	13.971	13.823	15.230	14.848	17.323	19.397	155.135	107.567	46.039	31.373	31.303
1999	31.774	27.082	36.945	36.547	44.274	57.570	56.000	105.106	58.910	40.874	37.233	38.735
2000	34.771	29.317	28.965	29.180	46.313	41.090	29.171	46.300	44.817	42.168	25.627	19.713
2001	33.206	34.946	31.161	26.477	40.068	34.770	42.113	48.881	65.063	40.719	39.823	38.219
2002	37.594	37.089	37.452	37.757	38.952	40.293	44.445	48.481	45.083	36.974	17.770	18.458
2003	17.497	20.900	17.523	18.833	18.539	23.870	34.677	42.345	84.083	44.558	38.247	46.910
2004	40.371	37.928	36.768	40.610	36.768	41.833	44.945	41.045	32.837	30.223	25.587	26.010
2005	31.845	39.068	43.839	38.980	31.729	36.803	34.684	36.784	67.650	31.626	31.023	29.329
2006	27.606	33.950	35.710	47.417	46.339	48.180	32.290	97.590	157.437	38.913	28.290	29.606
2007	25.523	28.486	32.352	32.317	35.855	40.033	57.855	122.632	188.707	42.755	37.070	36.845
2008	36.145	37.155	37.335	44.897	46.145	30.937	36.668	59.342	139.007	54.913	34.697	38.716
2009	45.955	35.939	36.871	39.627	43.142	35.843	31.126	29.016	30.093	37.413	34.820	44.829
2010	36.555	30.761	31.152	32.840	38.174	36.353	50.416	84.103	129.167	43.713	37.110	39.839
2011	35.387	34.421	36.655	38.140	48.139	39.520	35.245	33.152	37.937	35.497	37.480	40.126
2012	38.119	34.417	32.932	33.793	34.094	38.977	53.058	98.558	149.247	42.497	39.800	52.784
2013	49.932	43.679	40.971	55.187	56.448	54.640	68.742	63.045	86.593	61.577	42.073	40.300
2014	23.613	22.532	22.477	22.903	24.726	29.440	51.377	105.229	59.667	36.784	34.640	26.474
2015	23.765	22.604	22.506	22.953	25.190	30.470	55.339	115.203	62.313	36.165	35.210	26.223
2016	23.416	22.210	22.287	22.730	25.271	30.490	56.284	115.958	58.807	32.616	33.493	24.965

Annex 6: Routed (Muskingum routing in HEC-HMS 4.10) mean monthly stream flow for site three ($m^{3/}s$)

Year	Mean monthly stream flow Monthes of the year											
	Jan	Feb	Mar	Apr	May	Jun	Jul	Aug	Sep	Oct	Nov	Dec
1991	29.56	35.13	43.48	34.78	42.91	29.59	44.47	45.37	123.74	55.60	57.42	45.30
1992	69.39	56.02	28.58	29.34	34.15	28.27	18.90	21.31	68.50	32.35	30.56	31.08
1993	32.17	36.35	29.56	32.89	34.25	45.50	42.55	138.20	238.49	67.44	37.87	35.51
1994	33.95	33.99	36.87	35.47	29.91	36.90	42.42	45.99	49.11	42.11	49.63	43.71
1995	37.37	33.68	32.84	30.51	33.29	37.29	42.31	50.14	41.06	38.87	38.11	31.71
1996	33.51	33.65	36.54	36.44	36.22	38.22	42.02	188.08	112.23	36.65	30.93	33.85
1997	34.67	36.72	40.05	34.82	31.89	32.37	29.80	24.80	22.04	23.54	19.83	14.56
1998	14.59	13.97	13.82	15.23	14.85	17.32	19.40	155.15	107.54	46.04	31.37	31.31
1999	31.78	27.08	36.95	36.55	44.27	57.57	56.00	105.12	58.91	40.87	37.23	38.73
2000	34.76	29.31	28.95	29.18	46.32	41.08	29.17	46.30	44.81	42.17	25.62	19.71
2001	33.21	34.94	31.16	26.47	40.07	34.76	42.11	48.89	65.06	40.73	39.82	38.21
2002	37.59	37.09	37.45	37.77	38.95	40.29	44.44	48.47	45.09	36.97	17.77	18.44
2003	17.49	20.90	17.52	18.84	18.54	23.87	34.67	42.35	84.09	44.55	38.27	46.91
2004	40.36	37.93	36.77	40.62	36.77	41.83	44.94	41.05	32.85	30.22	25.59	26.01
2005	31.85	39.06	43.83	38.97	31.72	36.80	34.68	36.79	67.64	31.63	31.02	29.34
2006	27.60	33.95	35.70	47.41	46.34	48.20	32.28	97.61	157.43	38.91	28.28	29.59
2007	25.52	28.49	32.36	32.32	35.86	40.04	57.85	122.64	188.69	42.75	37.07	36.85
2008	36.14	37.16	37.33	44.90	46.15	30.93	36.67	59.36	139.01	54.89	34.71	38.71
2009	45.95	35.93	36.87	39.62	43.15	35.85	31.12	29.03	30.10	37.41	34.82	44.82
2010	36.55	30.76	31.15	32.83	38.17	36.37	50.43	84.10	129.18	43.71	37.11	39.84
2011	35.40	34.42	36.66	38.15	48.15	39.51	35.24	33.14	37.93	35.49	37.47	40.12
2012	38.12	34.41	32.93	33.79	34.09	38.97	53.05	98.57	149.24	42.49	39.80	52.78
2013	49.93	43.68	40.97	55.18	56.45	54.63	68.74	63.06	86.59	61.57	42.07	40.30
2014	23.61	22.54	22.48	22.91	24.73	29.45	51.39	105.23	59.66	36.78	34.65	26.46
2015	23.74	22.61	22.51	22.97	25.19	30.46	55.35	115.19	62.29	36.16	35.21	26.23
2016	23.42	22.21	22.28	22.73	25.28	30.50	56.30	115.95	58.79	32.61	33.50	24.96

Annex 7: K values for log-pearson type III distribution

Skew coefficient G	Recurrence interval (T-yr)						
	2	5	10	25	50	100	200
	Percent of chance (annual probability of occurrence P (%))						
	50	20	10	4	2	1	0.5
3.3	-0.396	0.42	1.18	2.276	3.152	4.051	4.97
2.3	-0.36	0.518	1.25	2.162	3.048	3.845	4.652
2	-0.307	0.609	1.302	2.219	2.912	3.603	4.298
1.8	-0.282	0.643	1.318	2.193	2.848	3.499	4.147
1.6	-0.254	0.675	1.329	2.163	2.75	3.355	3.99
1.4	-0.225	0.705	1.337	2.128	2.706	3.271	3.828
1.2	-0.193	0.732	1.34	2.087	2.626	3.149	3.661
1	-0.164	0.758	1.34	2.043	2.542	3.022	3.489
0.9	-0.148	0.769	1.339	2.018	2.498	2.937	3.401
0.8	-0.132	0.78	1.336	1.993	2.453	2.891	3.312
0.7	-0.113	0.79	1.333	1.967	2.407	2.824	3.223
0.6	-0.099	0.8	1.328	1.939	2.359	2.755	3.132
0.5	-0.083	0.805	1.323	1.91	2.311	2.686	3.041
0.4	-0.066	0.816	1.317	1.88	2.261	2.615	2.949
0.3	-0.05	0.823	1.309	1.849	2.211	2.544	2.856
0.2	-0.033	0.83	1.301	1.818	2.159	2.472	2.763
0.1	-0.017	0.836	1.292	1.785	2.107	2.4	2.67
0	0	0.841	1.282	1.751	2.054	2.326	2.576
-0.1	0.017	0.846	1.27	1.716	2	2.252	2.482
-0.2	0.033	0.85	1.258	1.68	1.945	2.178	2.388
-0.3	0.05	0.853	1.245	1.643	1.89	2.104	2.294
-0.4	0.066	0.855	1.231	1.606	1.834	2.029	2.201
-0.5	0.083	0.86	1.216	1.567	1.777	1.955	2.108
-0.6	0.099	0.857	1.2	1.528	1.72	1.88	2.016
-0.7	0.113	0.857	1.183	1.488	1.663	1.806	1.926
-0.8	0.132	0.856	1.166	1.448	1.606	1.733	1.837
-0.9	0.148	0.854	1.147	1.407	1.549	1.66	1.749
-1	0.164	0.852	1.128	1.366	1.492	1.588	1.664
-1.2	0.193	0.843	1.056	1.282	1.379	1.449	1.501
-1.4	0.225	0.832	1.041	1.198	1.27	1.315	1.351
-1.6	0.254	0.817	0.994	1.116	1.166	1.197	1.216
-1.8	0.282	0.799	0.945	1.035	1.069	1.087	1.097
-2	0.307	0.777	0.895	0.959	0.98	0.99	0.995
-2.3	0.36	0.71	0.771	0.793	0.795	0.799	0.5
-3	0.396	0.636	0.66	0.666	0.666	0.667	0.667

Annex 8: Reduced standard Deviation S_n in Gumbel Extreme value Distribution

N	0	1	2	3	4	5	6	7	8	9
10	0.9496	0.9676	0.9833	0.9971	1.0095	1.0206	1.0316	1.0411	1.0493	1.0565
20	1.0628	1.0696	1.0754	1.0811	1.0864	1.0915	1.0961	1.1004	1.1047	1.1086
30	1.1124	1.1159	1.1193	1.1226	1.1255	1.1285	1.1313	1.1339	1.1363	1.1388
40	1.1413	1.1436	1.1458	1.148	1.1499	1.1519	1.1538	1.1557	1.1574	1.159
50	1.1607	1.1623	1.1638	1.1658	1.1667	1.1681	1.1696	1.1708	1.1721	1.1734
60	1.1747	1.1759	1.177	1.1782	1.1793	1.1803	1.1814	1.1824	1.1834	1.1844
70	1.1854	1.1863	1.1873	1.1881	1.189	1.1898	1.1905	1.1915	1.1923	1.193
80	1.1938	1.1945	1.1953	1.1959	1.1967	1.1973	1.198	1.1987	1.1994	1.2001
90	1.2007	1.2013	1.202	1.2026	1.2032	1.2038	1.2044	1.2049	1.2055	1.206
100	1.2065									

Sn = 1.2825 at N = ∞

Source: SK Garg: Irrigation engineering and hydraulic structure

Annex 9: Reduced mean, Y_n in Gumbel Extreme value Distribution

N	0	1	2	3	4	5	6	7	8	9
10	0.4952	0.4996	0.5035	0.507	0.51	0.5128	0.5157	0.5181	0.5502	0.552
20	0.5236	0.5252	0.5268	0.5283	0.5296	0.5309	0.532	0.5332	0.5343	0.5353
30	0.5362	0.5371	0.538	0.5388	0.5396	0.5402	0.541	0.5418	0.5424	0.543
40	0.5436	0.5442	0.5448	0.5453	0.5458	0.5463	0.5468	0.5473	0.5477	0.5481
50	0.5485	0.5489	0.5493	0.5497	0.5501	0.5504	0.5508	0.5511	0.5515	0.5518
60	0.5521	0.5524	0.5527	0.553	0.5533	0.5535	0.5538	0.554	0.5543	0.5545
70	0.5548	0.555	0.5552	0.5555	0.5557	0.5559	0.5561	0.5563	0.5565	0.5567
80	0.5569	0.557	0.5572	0.5574	0.5576	0.5578	0.558	0.5581	0.5583	0.5585
90	0.5586	0.5587	0.5589	0.5591	0.5592	0.5593	0.5595	0.5596	0.5598	0.5599
100	0.56									
Yn = 0.5770 at N = ∞										

Source: SK Garg: Irrigation engineering and hydraulic structure

Annex 10: Base values of roughness coefficient for different bed material

Base values of Manning's n [Modified from Aldridge and Garrett, 1973] Stable channels and flood plains(nb)			
Bed material	Median size of bed material (mm)	Straight uniform channel	Smooth channel
Concrete		(0.012-0.018)	0.011
Rock cut			0.025
Firm soil		(0.025-0.032)	0.02
Coarse sand	1-2	(0.026-0.035)	
Fine gravel			0.024
Gravel	2-64	(0.028-0.035)	
Coarse gravel			0.026
Cobble	64-256	(0.030-0.050)	
Boulder	>256	(0.040-0.070)	

Annex 11: Adjustment values for factors that affect the roughness of a channel

Adjustment values for factors that affect the roughness of a channel [Modified from Aldridge and Garrett, 1973,.		
Channel Conditions	Adjustment(n) values	Examples
Degree of Irregularity(n1)	Moderate (0.006-0.010)	Compares to dredged channels having moderate to considerable bed roughness and moderately sloughed or eroded side slopes
Variation in channel cross section(n2)	Gradual 0	Size and shape of channel cross sections change gradually
Effect of obstruction(n3)	Minor (0.005-0.015)	Obstructions occupy less than 15 percent of the cross-sectional area, and the spacing between obstructions is such that the sphere of influence around one obstruction does not extend to the sphere of influence around another obstruction. Smaller adjustments are used for curved smooth-surfaced objects than are used for sharp-edged angular objects.
Amount of vegetation(n4)	Small (0.002-0.010)	Dense growths of flexible turf grass, such as Bermuda, or weeds growing where the average depth of flow is at least two times the height of the vegetation; supple tree seedlings such as willow cottonwood, arrow weed, or saltcedar growing where the average depth of flow is at least three times the height of the vegetation.
Degree of meandering (m)	Minor 1	Ratio of the channel length to valley length is 1.0 to 1.2

Annex 12: Annual stream flow of surrounding stations

year	Annual stream flow of surruonding station (m3/s)				
	Downstream of koka Dam	Awash Wonji	Awash Metahara	Awash Melka seddi	Awash 7 Kilo
1991	17585.70	17858.40	14624.72	17976.75	18500.50
1992	14705.37	13633.24	12691.97	19526.20	19569.83
1993	22176.19	23429.91	21213.68	19331.64	28831.87
1994	13999.70	14606.45	10448.07	16433.70	24084.63
1995	13891.21	13614.11	11326.96	14091.97	16892.05
1996	22776.61	20122.73	15482.28	26025.08	29303.33
1997	17572.14	10475.83	8967.31	18305.15	21103.73
1998	21917.06	14687.10	14035.08	25076.27	32715.77
1999	25656.06	17432.75	17129.11	25499.62	30340.27
2000	20784.24	12739.43	15573.70	18918.73	21712.32
2001	18815.14	14469.86	13372.18	11461.78	20341.24
2002	18892.92	13396.69	10326.91	7655.93	11437.19
2003	15207.34	12423.28	10271.10	16267.94	28844.38
2004	14793.21	13263.55	11603.22	18114.47	18410.19
2005	13321.80	13761.78	9968.57	22086.22	18769.03
2006	20171.43	18939.11	19205.03	31246.18	33689.89
2007	17875.49	20710.42	17672.85	24074.62	26125.53
2008	15082.85	18152.53	15662.50	21502.90	27366.30
2009	7885.45	13532.31	10226.93	21105.53	19083.50
2010	13644.25	17967.77	12130.98	33917.35	21262.53
2011	15754.39	13749.90	2020.53	19514.44	20494.30
2012	13682.66	19766.17	14513.28	18548.18	18801.73
2013	15013.76	20188.57	18242.58	22718.40	23127.71
2014	14055.10	14039.93	9572.55	24219.32	23260.28
2015	14620.96	14597.49	12720.51	13312.43	13309.75
2016	14337.61	14312.16	12277.10	12918.87	12915.97

Annex 13: Annual maximum and annual stream flow of selected sites

year	Annual maximum flow (m3/s)			Annual flow (m3/s)		
	Site one	Site two	Site three	Site one	Site two	Site three
1991	202.30	202.10	201.80	17856.80	17289.50	**17290.70**
1992	131.30	131.20	131.00	13632.90	13184.60	**30475.20**
1993	372.40	372.00	371.20	23429.60	22629.30	**53103.60**
1994	96.40	96.20	95.90	14607.80	14120.90	**67226.30**
1995	82.70	82.70	83.10	13614.00	13197.20	**80423.10**
1996	262.40	262.30	262.40	20122.40	19523.10	**99946.80**
1997	58.20	58.30	58.50	10477.40	10113.00	**110060.30**
1998	227.80	227.50	227.20	14683.70	14241.80	**124301.80**
1999	166.50	166.50	166.50	17431.10	16816.80	**141119.20**
2000	57.20	57.20	57.20	12740.60	12321.00	**153439.60**
2001	82.10	82.10	82.00	14468.20	14017.30	**167456.90**
2002	81.10	81.30	81.50	13398.70	12951.20	**180407.90**
2003	105.20	105.10	105.00	12421.20	12044.20	**192452.40**
2004	75.50	75.50	75.70	13265.90	12831.50	**205284.50**
2005	107.40	107.40	107.40	13761.30	13245.30	**218529.40**
2006	225.80	225.70	225.80	18939.20	18293.00	**236822.20**
2007	262.30	262.30	262.30	20709.30	20038.80	**256861.50**
2008	261.60	261.80	262.10	18150.90	17609.10	**274471.00**
2009	65.40	65.40	65.30	13537.00	13086.60	**287556.90**
2010	194.00	193.90	193.90	17968.30	17415.80	**304973.30**
2011	61.80	61.80	61.70	13746.30	13289.80	**318262.20**
2012	229.30	229.30	229.30	19765.20	19109.50	**337370.10**
2013	135.50	135.50	135.60	20190.20	19557.80	**356927.50**
2014	176.40	176.30	176.60	14040.60	13561.30	**370490.10**
2015	199.10	198.90	199.10	14597.70	14105.10	**384595.50**
2016	210.30	210.10	210.10	14334.70	13864.40	**398461.20**

Annex 14: Mean monthly stream flow of mojo station (m^3/s)

Year	Mean monthly stream flow Monthes of the year											
	Jan	Feb	Mar	Apr	May	Jun	Jul	Aug	Sep	Oct	Nov	Dec
1991	0.576	0.372	0.522	70.985	1.192	3.600	15.448	17.074	5.160	0.936	0.817	1.348
1992	0.570	0.359	0.538	74.038	1.117	3.675	15.583	17.586	5.137	0.904	0.817	1.375
1993	0.566	0.351	0.555	77.229	1.077	3.776	15.833	18.190	5.189	0.889	0.817	1.404
1994	0.562	0.343	0.573	80.560	1.064	3.869	15.595	18.420	5.164	0.877	0.815	1.434
1995	0.559	0.338	0.588	84.035	1.069	3.955	15.807	18.507	5.096	0.866	0.813	1.466
1996	0.556	0.333	0.603	87.651	1.081	4.027	16.416	19.127	4.906	0.862	0.812	1.499
1997	0.553	0.330	0.616	91.428	1.099	4.102	17.025	19.634	4.106	0.857	0.810	1.534
1998	0.551	0.326	0.628	95.376	1.118	4.206	17.639	19.864	3.518	0.857	0.809	1.571
1999	0.549	0.325	0.636	99.502	1.143	4.237	18.162	18.589	3.503	0.860	0.807	1.611
2000	0.548	0.327	0.648	103.808	1.170	4.325	18.867	18.865	3.526	0.855	0.805	1.652
2001	0.546	0.328	0.662	108.305	1.200	4.417	19.277	18.552	3.570	0.855	0.802	1.696
2002	0.543	0.330	0.677	112.994	1.231	4.538	19.246	18.447	3.652	0.855	0.800	1.742
2003	0.541	0.333	0.692	117.892	1.264	4.674	19.957	18.386	3.728	0.855	0.801	1.792
2004	0.540	0.338	0.710	123.004	1.294	4.773	20.253	18.597	3.824	0.857	0.802	1.843
2005	0.538	0.344	0.724	128.337	1.324	4.557	20.319	18.796	3.776	0.859	0.802	1.808
2006	0.536	0.345	0.721	133.901	1.155	4.588	18.381	19.272	3.871	0.860	0.802	1.771
2007	0.535	0.343	0.657	139.706	1.129	4.615	18.987	19.753	3.945	0.863	0.802	1.734
2008	0.538	0.343	0.622	145.762	1.124	4.445	19.646	18.678	3.933	0.867	0.804	1.694
2009	0.541	0.346	0.617	152.084	1.129	4.076	19.282	17.160	4.038	0.870	0.805	1.651
2010	0.545	0.346	0.619	158.680	1.140	4.190	18.105	17.483	4.149	0.873	0.806	1.603
2011	0.549	0.346	0.622	165.564	1.154	4.167	18.590	17.921	4.276	0.877	0.807	1.548
2012	0.553	0.346	0.621	165.564	1.173	4.167	18.000	18.465	4.276	0.882	0.807	1.588
2013	0.550	0.341	0.630	172.442	1.157	4.226	18.019	18.517	4.197	0.870	0.807	1.607
2014	0.550	0.341	0.630	172.442	1.157	4.226	18.019	18.517	4.197	0.870	0.807	1.607
2015	0.550	0.341	0.630	176.519	1.157	4.226	18.019	18.517	4.197	0.870	0.807	1.607
2016	0.550	0.341	0.630	121.512	1.157	4.226	18.019	18.517	4.197	0.870	0.807	1.607

Annex 14: Mean monthly stream flow of Hombole station

Year	Mean monthly stream flow Monthes of the year											
	Jan	Feb	Mar	Apr	May	Jun	Jul	Aug	Sep	Oct	Nov	Dec
1991	3.974	3.751	5.484	643.938	9.922	25.552	81.517	192.626	94.715	21.626	7.406	4.560
1992	3.956	3.717	5.590	671.587	9.716	25.993	83.262	193.503	91.618	20.339	7.266	4.544
1993	3.941	3.695	5.700	700.477	9.562	26.456	84.563	194.748	89.397	19.652	7.136	4.532
1994	3.926	3.685	5.816	730.662	9.478	27.020	86.257	194.756	86.423	19.151	7.027	4.515
1995	3.909	3.682	5.917	762.196	9.417	27.732	88.240	196.527	84.660	18.806	6.911	4.505
1996	3.895	3.678	6.008	795.102	9.439	28.526	89.100	198.518	83.262	18.540	6.788	4.498
1997	3.887	3.679	6.080	829.444	9.497	29.140	89.148	200.965	81.865	18.356	6.694	4.492
1998	3.888	3.683	6.185	865.287	9.628	29.981	90.335	201.454	76.992	18.207	6.629	4.490
1999	3.889	3.686	6.300	902.678	9.789	29.732	91.021	200.956	73.802	18.108	6.572	4.491
2000	3.892	3.692	6.384	941.574	9.973	30.055	92.024	201.252	73.250	18.046	6.533	4.474
2001	3.892	3.694	6.426	982.181	10.173	30.225	93.698	198.658	72.877	18.031	6.505	4.473
2002	3.888	3.680	6.474	1024.562	10.397	30.659	92.443	196.619	72.252	18.042	6.486	4.475
2003	3.884	3.670	6.457	1068.789	10.639	30.154	93.659	195.187	72.086	18.070	6.485	4.473
2004	3.880	3.667	6.429	1114.925	10.837	30.187	93.981	195.306	72.589	18.103	6.509	4.472
2005	3.881	3.671	6.193	1163.037	10.999	30.145	94.418	192.864	73.003	18.159	6.539	4.472
2006	3.881	3.672	6.160	1213.262	10.694	29.775	94.268	192.406	73.099	18.234	6.576	4.473
2007	3.882	3.673	6.071	1265.643	10.522	29.742	93.673	192.456	74.059	18.330	6.619	4.476
2008	3.884	3.676	6.021	1320.347	10.333	29.752	94.391	192.484	75.515	18.442	6.669	4.478
2009	3.886	3.688	5.994	1377.466	10.106	29.322	93.237	192.521	77.074	18.578	6.724	4.487
2010	3.891	3.688	5.981	1437.091	10.066	28.807	91.986	191.489	79.116	18.716	6.782	4.497
2011	3.898	3.688	6.033	1499.302	10.023	28.547	91.078	192.714	81.380	18.874	6.846	4.502
2012	3.908	3.688	6.022	1499.302	10.055	28.547	89.755	194.659	81.380	19.067	6.846	4.504
2013	3.901	3.686	6.078	1561.413	10.057	28.911	90.548	195.576	79.110	18.703	6.752	4.495
2014	3.901	3.686	6.078	1561.413	10.057	28.911	90.548	195.576	79.110	18.703	6.752	4.495
2015	3.901	3.686	6.078	1613.537	10.057	28.911	90.548	195.576	79.110	18.703	6.752	4.495
2016	3.901	3.686	6.078	1101.809	10.057	28.911	90.548	195.576	79.110	18.703	6.752	4.495

Annex 15: Routed (HEC-HMS 4.10) mean monthly stream flow of hombole station

Year	Mean monthly stream flow Monthes of the year											
	Jan	Feb	Mar	Apr	May	Jun	Jul	Aug	Sep	Oct	Nov	Dec
1991	3.980	3.740	5.472	6.992	620.004	25.426	81.196	192.773	95.342	21.769	7.411	4.559
1992	3.966	3.712	5.575	6.849	645.262	25.903	82.945	193.517	92.135	20.504	7.269	4.544
1993	3.951	3.683	5.683	6.909	671.573	26.327	84.297	194.827	89.898	19.713	7.139	4.532
1994	3.939	3.677	5.801	6.876	699.097	26.900	85.875	194.983	87.079	19.273	7.026	4.515
1995	3.923	3.671	5.905	6.994	727.759	27.576	87.896	196.377	85.031	18.853	6.913	4.502
1996	3.910	3.669	5.997	7.031	757.712	28.379	88.882	198.663	83.842	18.637	6.790	4.493
1997	3.902	3.668	6.069	7.147	788.937	29.002	88.936	200.811	82.301	18.403	6.694	4.489
1998	3.902	3.671	6.168	7.221	821.530	29.793	89.929	201.866	78.110	18.294	6.627	4.488
1999	3.902	3.670	6.289	7.336	855.507	29.745	90.835	201.064	74.130	18.157	6.571	4.488
2000	3.907	3.673	6.375	7.300	890.911	29.804	91.586	201.508	73.869	18.123	6.527	4.473
2001	3.907	3.672	6.424	7.281	927.803	30.209	93.345	199.249	73.263	18.079	6.500	4.468
2002	3.903	3.660	6.466	7.275	966.241	30.400	92.442	196.865	72.909	18.114	6.481	4.475
2003	3.898	3.648	6.464	7.269	1006.293	30.229	92.962	195.650	72.490	18.124	6.480	4.470
2004	3.894	3.646	6.426	7.253	1047.967	29.887	93.974	195.375	73.147	18.175	6.503	4.468
2005	3.893	3.648	6.232	7.203	1091.333	30.158	93.796	193.674	73.492	18.215	6.536	4.467
2006	3.893	3.651	6.133	7.166	1136.134	29.570	94.223	192.318	73.744	18.307	6.571	4.470
2007	3.893	3.648	6.108	7.112	1182.794	29.654	93.187	193.060	74.494	18.393	6.618	4.468
2008	3.897	3.651	5.999	7.079	1231.531	29.548	94.041	192.540	76.103	18.516	6.666	4.471
2009	3.897	3.658	6.017	7.106	1282.157	29.269	93.030	193.055	77.574	18.644	6.721	4.479
2010	3.901	3.671	5.963	7.145	1335.135	28.629	91.645	191.813	79.673	18.791	6.780	4.492
2011	3.910	3.671	6.039	7.199	1390.294	28.421	90.765	192.895	81.920	18.941	6.845	4.496
2012	3.920	3.671	6.018	7.199	1447.832	28.421	89.449	194.877	81.920	19.143	6.845	4.501
2013	3.913	3.670	6.074	7.134	1507.742	28.784	90.238	195.807	79.657	18.780	6.751	4.491
2014	3.913	3.670	6.074	7.134	1507.742	28.784	90.238	195.807	79.657	18.780	6.751	4.491
2015	3.913	3.670	6.074	7.134	1557.984	28.784	90.238	195.807	79.657	18.780	6.751	4.491
2016	3.913	3.670	6.074	7.134	1043.891	28.784	90.238	195.807	79.657	18.780	6.751	4.491

Annex 16: Flow duration curve of site two

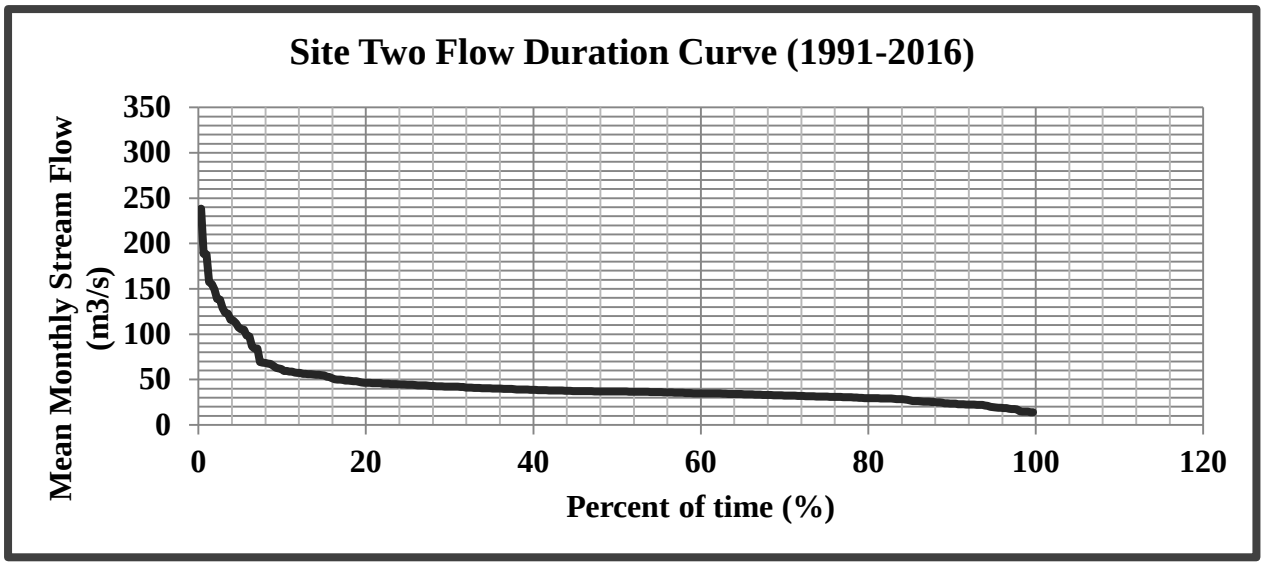

Annex 17: Flow duration curve of site three

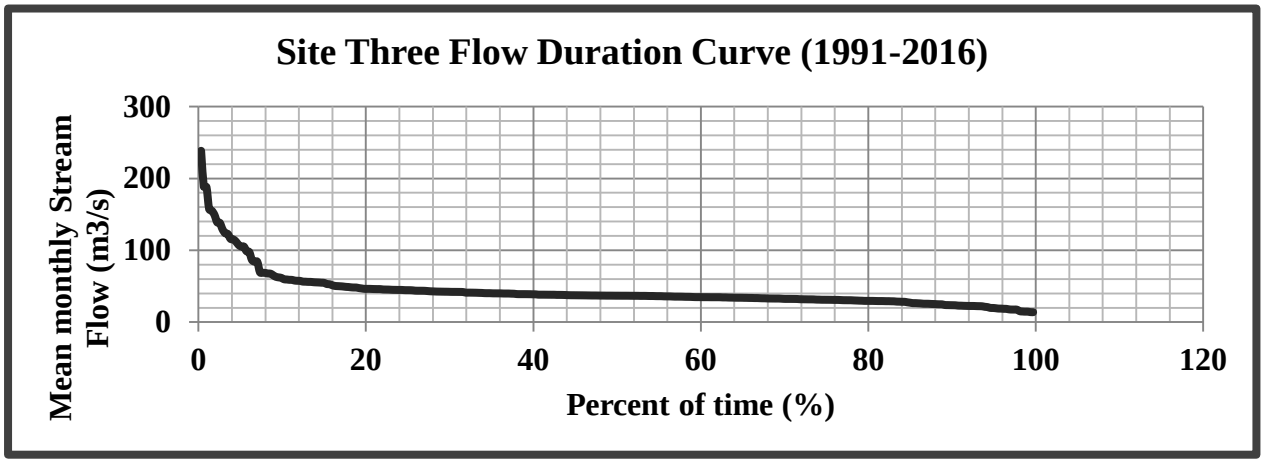

Annex 18: Theoretical power of site two

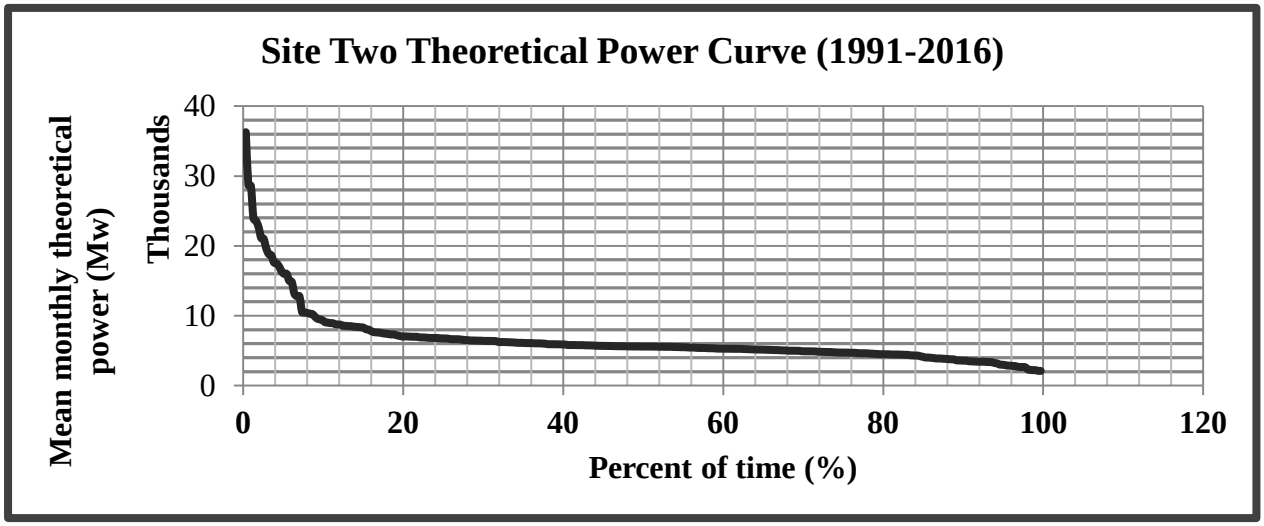

Annex 19: Theoretical power curve of site three

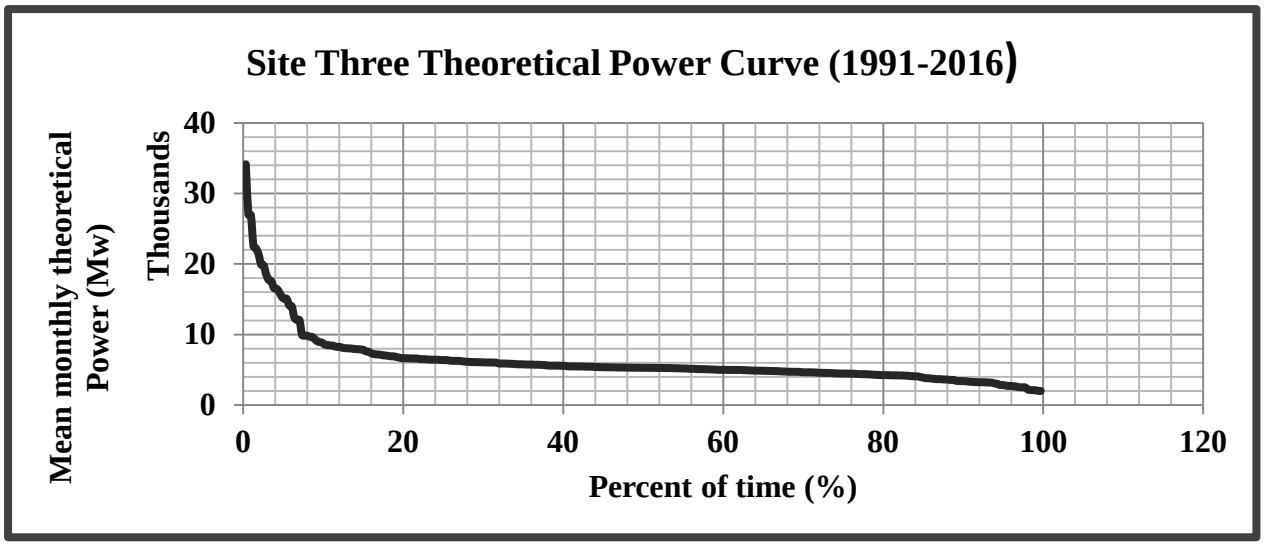

Annex 20: Technical power curve of site two

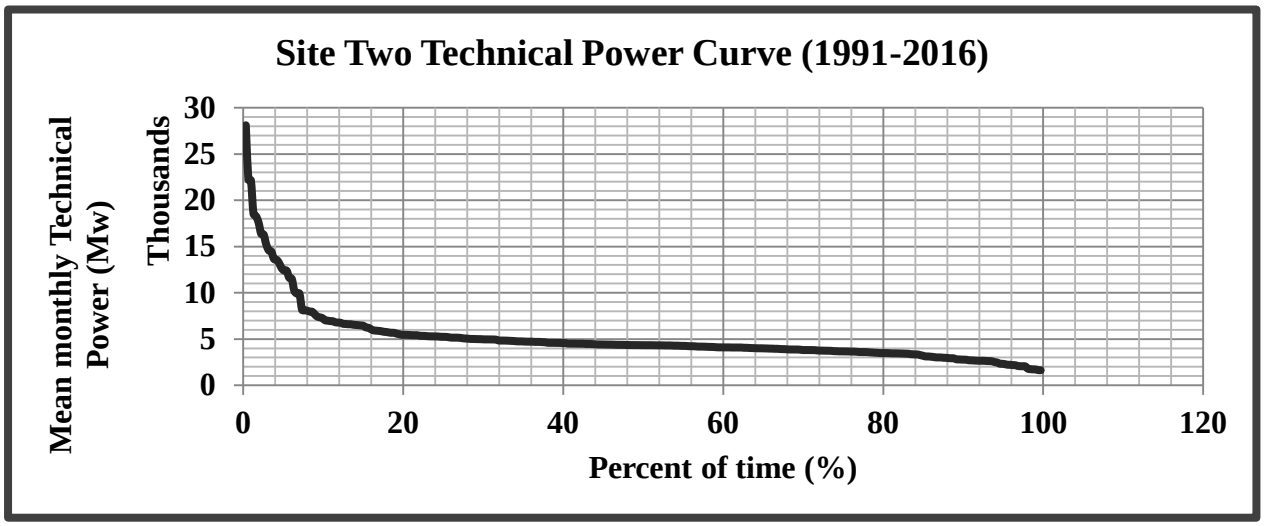

Annex 21: Technical power curve of site three

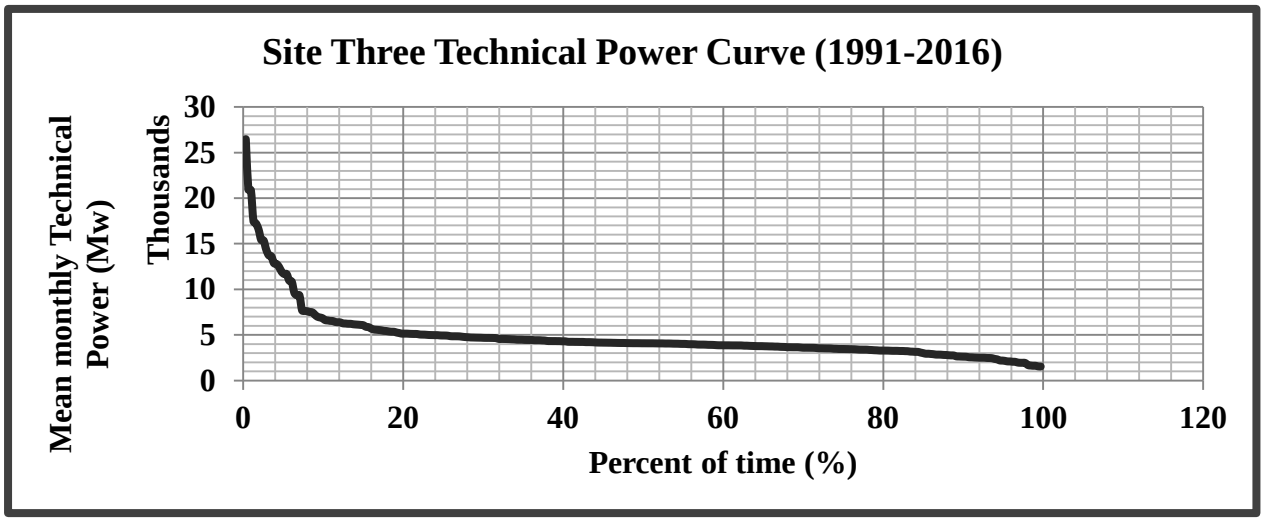

Annex 22: Annual energy curve of site two

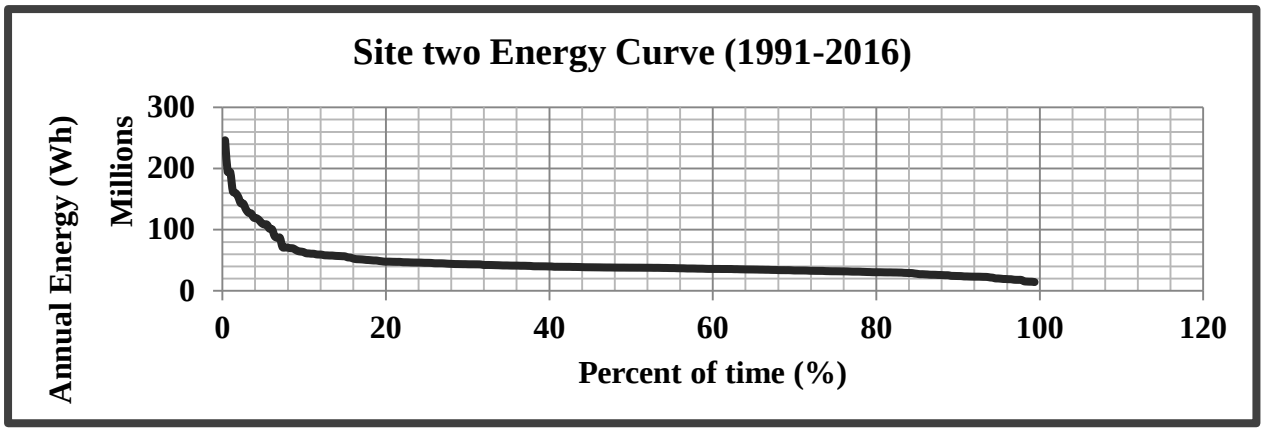

Annex 23: Annual energy curve of site three

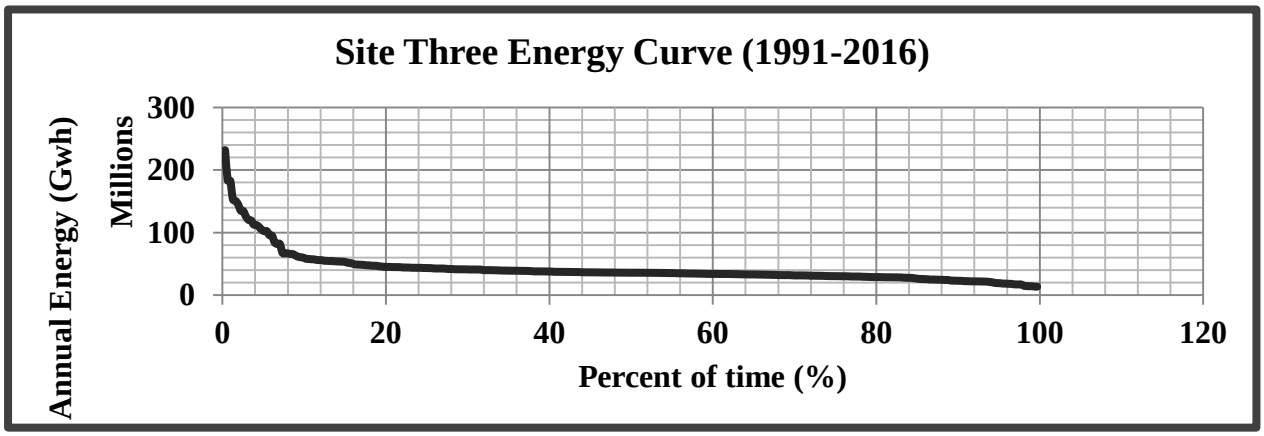

Annex 24: Long term mean monthly flow to koka reservior

Year	Mean monthly stream flow Monthes of the year											
	Jan	Feb	Mar	Apr	May	Jun	Jul	Aug	Sep	Oct	Nov	Dec
1991	5.364	4.509	6.592	10.119	7.417	36.415	193.346	385.234	130.846	39.833	9.907	5.854
1992	5.153	3.938	6.912	9.765	8.202	24.689	121.231	260.196	97.817	24.007	9.663	5.510
1993	5.170	4.293	7.207	6.606	8.036	30.455	150.511	294.955	98.717	29.013	10.134	6.059
1994	4.974	3.988	7.346	10.711	12.765	31.278	139.042	299.758	127.129	30.142	10.453	6.006
1995	3.804	3.032	4.188	5.651	5.923	18.519	81.970	178.241	65.006	24.181	8.050	4.717
1996	5.282	4.183	6.131	9.959	9.231	25.233	104.118	206.843	103.804	21.289	10.001	6.234
1997	4.440	3.786	3.590	14.270	4.509	33.478	158.846	335.779	113.837	36.550	11.218	6.588
1998	5.424	4.258	11.800	17.606	12.844	42.471	237.375	583.802	242.627	68.353	9.621	5.946
1999	5.462	4.515	5.129	3.839	3.965	36.133	221.748	441.621	88.993	52.109	9.030	5.430
2000	4.499	4.062	2.208	3.392	6.169	21.472	144.744	269.328	108.109	31.612	12.895	6.422
2001	6.098	5.562	13.398	8.024	13.075	50.597	157.902	223.542	87.424	12.216	8.662	6.558
2002	6.251	4.591	5.362	6.088	5.603	13.708	71.567	157.334	52.054	10.033	7.950	4.277
2003	4.173	3.649	5.565	11.467	7.263	26.063	146.148	234.178	112.625	16.378	9.260	6.445
2004	4.100	3.062	4.487	16.632	5.573	21.639	95.953	193.524	90.201	17.360	9.735	4.909
2005	5.582	4.002	12.193	10.388	35.584	28.391	137.796	213.445	102.703	18.896	11.685	6.097
2006	4.728	4.597	10.397	19.638	17.023	28.406	175.478	289.438	151.818	19.292	12.332	6.476
2007	5.317	5.977	5.590	9.270	14.852	46.969	141.575	288.139	178.197	26.231	11.724	8.151
2008	5.267	4.376	3.437	4.356	6.322	18.824	129.933	245.512	166.606	19.157	23.497	6.578
2009	10.218	4.477	3.601	10.398	5.744	7.824	51.516	203.032	120.218	27.328	6.575	7.221
2010	4.877	12.847	11.643	23.745	22.560	38.725	176.814	193.100	167.782	19.181	10.424	5.721
2011	5.066	4.391	7.068	5.540	12.357	30.551	76.251	216.511	162.313	34.956	10.712	6.297
2012	4.728	4.005	3.381	11.342	8.751	13.915	102.016	282.415	245.650	19.717	8.216	5.596
2013	4.519	3.612	7.038	14.215	12.498	35.761	106.584	174.971	144.727	42.289	13.222	5.760
2014	4.500	5.366	5.255	6.965	11.782	15.494	76.631	162.919	94.643	34.388	11.074	7.525
2015	5.003	3.797	5.200	3.961	13.063	28.016	50.913	132.879	65.781	17.269	6.439	4.567
2016	4.687	4.160	5.210	9.133	11.513	23.295	89.684	191.736	137.700	28.262	9.735	5.858

Annex 25: Annual maximum water depth of selected sites and Wonji station

Annual maximum water depth(Observed) (m)			
year	Downstream of koka dam	Wonji station	Site one
2012	3.058	2.876	3.056
2013	3.412	3.202	3.410
2014	2.997	2.835	2.995
2015	3.200	3.010	3.198
2016	2.820	2.716	2.764
2017	4.530	4.241	4.351
2018	3.800	3.585	3.682
2019	4.240	3.969	4.089
2020	5.000	4.719	4.849
2021	3.495	3.287	3.383